Design of a ratiometric reporter to improve the dynamic range and sensitivity of a bacterial biosensor

Gareth Edward Davies

Pembroke College

University of Oxford

Thesis submitted for the

Degree of Doctor of Philosophy

Trinity Term 2014

Abstract

Design of a ratiometric reporter to improve the dynamic range and sensitivity of a bacterial biosensor

Gareth Edward Davies
Pembroke College
University of Oxford

Submitted for the Degree of
Doctor of Philosophy
Trinity Term 2014

For applications from biosensor generation to synthetic biology, the ability to accurately and quantitatively generate input-output data from biological systems over a wide dynamic range is becoming increasingly important. This study has demonstrated that a simple approach utilising multiple promoters, recognising the same transcriptional activator but with differing affinities, linked to compatible reporter genes can achieve this goal. This simple system highlights that even for complex promoters with multiple binding sites we can use the ratio of two reporters to obtain accurate and reproducible input-output data for reporters contained on a high copy number plasmid without the need for any background subtraction or accurate determination of cell number. It has also demonstrated that the precise promoter strengths are not too crucial to the design, provided they are significantly different, as taking the ratio of either the high affinity/low affinity or medium affinity/low affinity channels give similar improvements over any single channel alone.

The modularity of this system means that it should be possible to exchange the IPTG inducible promoter and hence place the *ntrC** gene under the regulation of any environmentally important promoter.

It should also be possible to simply construct different strength promoters for the same transcriptional activator by standard DNA synthesis techniques, therefore allowing direct ratiometric detection of specific active transcription factors. Finally, there is considerable interest in the biosensor field in the use of immobilised cells for field based applications. In these cases, determining the exact number of viable cells present at the time of use may be problematic and obtaining high signal levels may also be essential. In this regard, the use of ratiometric reporters from constructs on high copy number plasmids could alleviate many of these potential problems and significantly simplify the required biosensor detection equipment.

Declaration

The work in this thesis was carried out in the Department of Biochemistry, University of Oxford from September 2008 to September 2011, under the supervision of Dr. George H. Wadhams and Dr. Phil. C. Biggin. All of the work is my own unless otherwise stated and has not been submitted for a degree at this or any other university.

Acknowledgements

I would like to my supervisors Dr George H. Wadhams and Dr Phil C. Biggin for their continued support and advice throughout my D. Phil. I would also like to help all of the members of the lab for their continued assistance in my day to day research, especially Dr Sonja Pawelczyk for her assistance in generating some of the data in Chapter 5.7. I would like to say a special thanks to my parents and sister for their continued support and encouragement. Finally, I would especially like to thank my beautiful wife, Heidi for all her love and support throughout my long educational career.

Abbreviations

All abbreviations used in this thesis are listed below (Table 1).

Ap	Ampicillin
ADP	Adenosine diphosphate
ATP	Adenosine triphosphate
bp	Base pairs
CAP	Catabolite activator protein
CFP	Cyan fluorescent protein
CIP	Calf intestinal alkaline phosphatase
Cm	Chloramphenicol
DMSO	Dimethyl sulfoxide
DIC	Differential interference contrast
DNA	Deoxyribonucleic acid
dNTP	Deoxynucleoside 5’-triphosphate
FACS	Fluorescence-activated cell sorting
GFP	Green fluorescent protein
HK	Histidine kinase
Hrs	Hours

IPTG	Isopropyl β-D-1-thiogalactopyranoside
kb	Kilobase
Km	Kanamycin
lac	Lactose
L-ara	L-arabinose
LB	Luria Bertani
Min	Minutes
Nal	Nalidixic acid
NEB	New England Biolabs
NH_3	Ammonium
Ntr	Nitrogen sensing system
OD	Optical density
ORF	Open reading frame
Ori	Origin of replication
P	Phosphate group
PCR	Polymerase chain reaction
^{R}	Resistance
RR	Response regulator

RFP	Red fluorescent protein
RNA	Ribonucleic acid
RPM	Revolutions per minute
SDS	Sodium dodecyl sulphate
σ	Sigma factor
Sm	Streptomycin
Tet	Tetracycline
TFBI	Transformation buffer 1
TFBII	Transformation buffer 2
UV	Ultraviolet
YFP	Yellow fluorescent protein

Table 1: List of abbreviations used in this thesis.

Table of Contents

List of Figures

List of Tables

1. Introduction

1.1 Advantages of biosensors over traditional measurement techniques

The advantage of using bacterial based biosensors to detect pollutants in the environment over the current chemical tests is that biological based biosensors can report the level of bio-available pollutants rather than having to analyse the entire composition of the sample, which is both costly and time consuming, often requiring expensive equipment and dedicated laboratory space. The bioavailability of a chemical in the environment refers to the portion of that chemical that is available or can be made available for uptake by biological organisms, either from the direct surroundings or by the ingestion of food (Peijnenburg and Jager, 2003). This differs from the total amount of a chemical in the environment because not all forms of the chemical present in the environment are available for uptake by biological organisms (Figure 1).

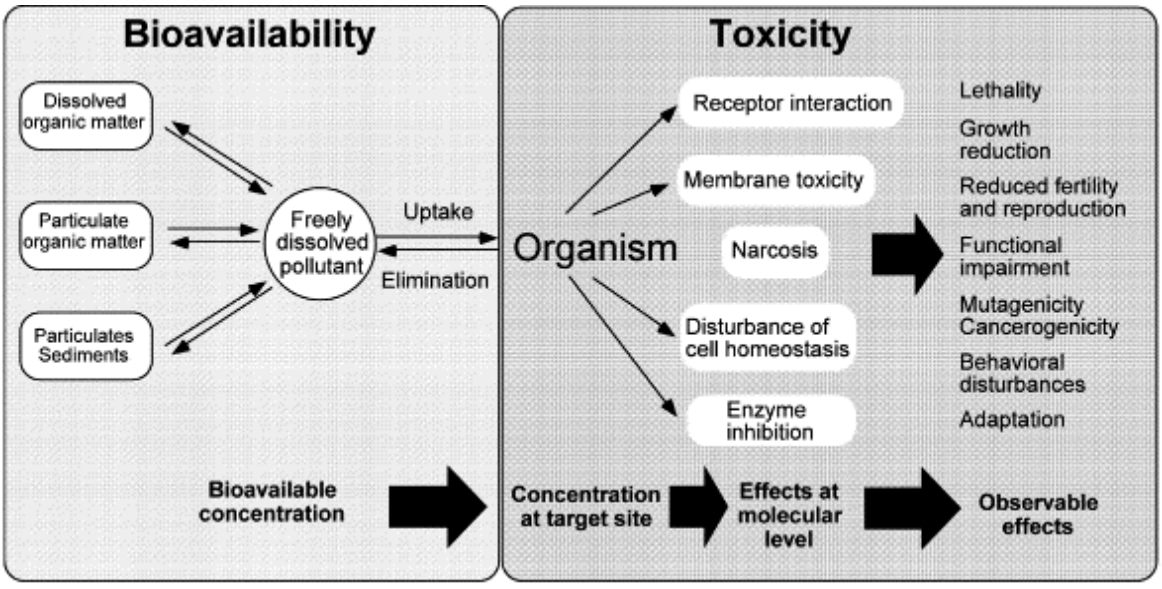

Figure 1: The relationship between bioavailability of pollutants and their toxicity to organisms (Fent, 2003).

Examples of chemical tests that can be performed quicker and more efficiently by biosensors are the biochemical oxygen demand (BOD) and chemical oxygen demand (COD) tests that are used to measure organic pollutants in treated waste water (Olaniran *et al.*, 2011). The non-biosensor BOD test requires a 5 day incubation period and requires a skilled and experienced operator to carry out the test in order to get reproducible measurements (Eaton *et al.*, 2005), this is both costly and time consuming to get results (Nomura *et al.*, 1998). The aforementioned non-biosensor COD test is unable to distinguish between the biodegradable and biologically inert organic matter present in the water sample which can overestimate the pollution going back into the environment (Bourgeois *et al.*, 2001). In contrast, bacterial biosensor alternatives have been developed and tested giving a good correlation between levels of pollutants in waste water and biosensor luminescence production using *E. coli* and *S. sonnei* bioluminescence biosensors (Olaniran *et al.*, 2011). These give good linear responses between increasing pollutants including cadmium, lead, mercury, arsenic, ammonium, nitrite, nitrate and phosphate with r^2 values of up to 0.997, but with some variability over the whole range of pollutants measured. Toxicity levels were calculated using the percentage inhibition of bioluminescence compared to an untreated control measurement. A fluorescence biosensor has also been developed to measure BOD that has a BOD detection range of 0.2-40 mg/L, has a shorter response time and better shelf life than the chemical alternative, this is possible as the bacteria are immobilised in a matrix (Lin *et al.*, 2006a). Electronic biosensor alternatives have also been developed by using a porous polymer entrapped *Pseudomonas syringae* coupled with a dissolved oxygen (DO) electrode *(Kara et al., 2009)*, this gave a response in 3-5 minutes and measured

soluble BOD through changes in dissolved oxygen as metabolisable organic compounds in the water sample was passed through the flow cell.

The SOS Chromotest biosensor is based on an *E. coli* K12 derivative containing a genomic *P-gal* gene (LacZ) fusion to the *sulA* gene that regulates the SOS cell division inhibitor response (Huisman and D'Ari, 1981a;Quillardet *et al.*, 1982). The substrate supplied in the SOS Chromotest kits, 5-bromo-4-chloro-2-indolyl-β-D-galactopyranoside (X-gal), is converted to a blue compound by P-gal which can then be read in a spectrophotometer at 620 nm (McDaniels *et al.*, 1990). Alkaline phosphatase is also assayed at the same time as a means to take into account any protein inhibition or cell death caused by the compounds tested. The Umu test biosensor was prepared in a similar way by a fusion of the SOS response *umuC* gene from *E. coli* and the *lacZ* gene on the multiple copy plasmid pSK1002 (Shinagawa *et al.*, 1983). The plasmid was then later used in *S. typhimurium* TA1535 in the Umu test (Oda *et al.*, 1985). The output of the Umu test is measured differently to the SOS chromotest as the substrate for P-Gal is o-nitrophenyl P-D-galactoside (ONPG) instead of X-Gal, ONPG is converted to ONP on cleavage by P-Gal which produces a yellow colour that is measured at 420 nm in a spectrophotometer. Both of these tests offer cheaper and simpler screens for carcinogenicity testing than using rat models or mammalian cells (Su *et al.*, 2011).

With so many different biosensors present in the literature (See section 1.4), it is surprising that so few are available for commercial use. These commercially available tests include the Ames test (Ames *et al.*, 1973), the SOS chromotest

(Quillardet *et al.*, 1982), and the Umu test (Oda *et al.*, 1985); which use the host stress responses to evaluate the carcinogenicity of chemicals. Tests against mutagenic compounds correlate well between the three tests and correlate well with rodent screens, thus offering a quicker and cheaper way of testing carcinogenicity (McDaniels *et al.*, 1990). Of these tests, only the Umu test is internationally accredited. It is thought that one of the main reasons preventing commercialisation of more recent biosensors is the national and international legislation controlling the application of genetically modified bacteria, in addition to concerns over biosensor shelf life, scalability and reliability in the field (van der Meer and Belkin, 2010).

1.2 Limitations of biosensors

When creating a biosensor the output needs to be fine tuned in order to give a measurable response over a useful concentration range of the chemical being detected. The main problem when using a single output for a biosensor is the range of detection. If your reporter is very sensitive to low concentrations of a chemical, then it is likely that the output will quickly become saturated and you will not be able to measure higher concentrations. Alternatively, if the reporter is tuned to measure higher concentrations, then it is likely that at low concentrations the signal from the reporter will be too low to measure above the background noise.

The toxicity of the chemical being detected must also be taken into account when designing biosensors, as well as the effect of high levels of protein expression on cells when producing large amounts of a reporter protein. These are particularly

important as toxic chemicals in a sample may alter the expected output of the biosensor.

Testing of complex mixtures such as waste water effluent pose a particular challenge to biosensors as synergistic and antagonistic interactions between different pollutants in the sample can greatly alter the overall toxicity of a sample. The combined toxic effect of a sample cannot simply be inferred from the total amounts of individual components. It has been shown that mixtures of pollutants can product a toxic effect 3-10 times that of the individual components (Hernando *et al.*, 2005). This highlights the importance of using of a battery of toxicity assays to provide a real assessment of the environmental risk of wastewater as no single organism responds appropriately to all pollutants when analysing a complex mixture (Olaniran *et al.*, 2011).

Availability of the analyte to the detection system can be a factor when considering extracellular vs intracellular detection due to potential problems of analyte permeability of the cell membrane (Melamed *et al.*, 2014). Binding of analyte to cytoplasmic sensing proteins of the bacteria require the analyte to cross the membrane either by diffusion or by facilitated or active transport.

The absolute response of a biosensor depends on the number of live bacteria present for detection in the sample detection well. Therefore additional measurements often need to be taken to account for the number of cells present

and this does not always give accurate results as dead cells may not produce a signal but may still scatter light in an OD measurement.

1.3 Aims of this study

This project aims to investigate methods to improve the range of detection and sensitivity of an input that can be reported on by a bacterial biosensor. This will be achieved by generating a multi-fluorescent reporter plasmid, capable of generating three different coloured fluorescent reporter proteins at different levels in response to a single input. This will be possible as the promoters controlling the expression of the fluorescent protein will be of high, medium and low affinity for the same transcriptional activator, generating sequential expression of the different reporter proteins as the level of the input increases. This will allow an increased range of signal detection as at low levels of signal the high affinity promoter will respond, as signal levels increase and this reporter becomes saturated, the medium affinity promoter will respond, and lastly the low affinity promoter will respond giving a wider range of signal detection than any of the individual reporters alone. Promoters of the Ntr system were selected to drive expression of the reporter proteins as these are well characterised in the literature and have been shown to respond sequentially to a single transcriptional regulator, NtrC.

The reporter plasmid will be initially tested using the host Ntr system to drive expression as a proof of concept that differential levels of expression from the different affinity promoters can be achieved.

In order to overcome issues of titrating out the transcriptional activator, NtrC, a constitutively active form of the activator (NtrC*) will also be generated and expressed from an inducible plasmid. This should produce sufficient transcriptional activator to generate a response from all three of the reporters on the reporter plasmid. Additionally, this will also allow detection of a wider range of chemicals as the production of NtrC* from the inducer plasmid can be put under the control of different promoters, thus allowing whatever controls the expression of NtrC* to be measured via production of fluorescence from the reporter plasmid.

In addition to generating a wider range of detection, the multi-fluorescent reporter plasmid will also be able to give a more precise measurement of a signal molecule, due to the fact that when more than one fluorescent protein is expressed a ratio of the two measurements can be used instead of a direct measurement. This ratio removes the error associated with different copy numbers of plasmids and regulator/transcriptional proteins in the host cells and the reduction in error should allow better resolution between two different concentrations of a chemical and thus a more accurate biosensor than would be possible with an individual output. It also removes changes in absolute values of an analyte due to differences in numbers of live bacteria present.

The major aims of this study are therefore to:

1. Construct multi-fluorescent output (MFO) plasmid
2. Test MFO responses to nitrogen limitation in *E. coli*
3. Test MFO responses to nitrogen limitation in other species
4. Decouple MFO response from nitrogen limitation by creation of constitutively active transcriptional activator (NtrC*)
5. Determine if ratiometric output from MFO provides enhanced detection of analyte output for a biosensor

1.4 Current biosensors

Biosensors can be broadly split into two categories; optical biosensors and electrochemical biosensors. Optical biosensors rely on an optically detectable output such as fluorescence, luminescence or a colorimetric response in proportion to the presence of an analyte in the sample. Electrochemical biosensors are used to detect analytes using a number of different techniques; voltammetry, conductometry, amperometry, potentiometry and microbial fuel cells.

1.4.1 Optical biosensors

Optical biosensors tend to be based on genetically engineered microorganisms to create living whole-cell biosensors. These biosensors generally consist of a sensor element, a transducer and a reporter protein (Figure 2) (Daunert *et al.*, 2000) functioning inside a living bacterial host cell to provide a measurable and

quantifiable signal in response to the presence of a particular chemical in the environment either by activating or suppressing production of a reporter protein.

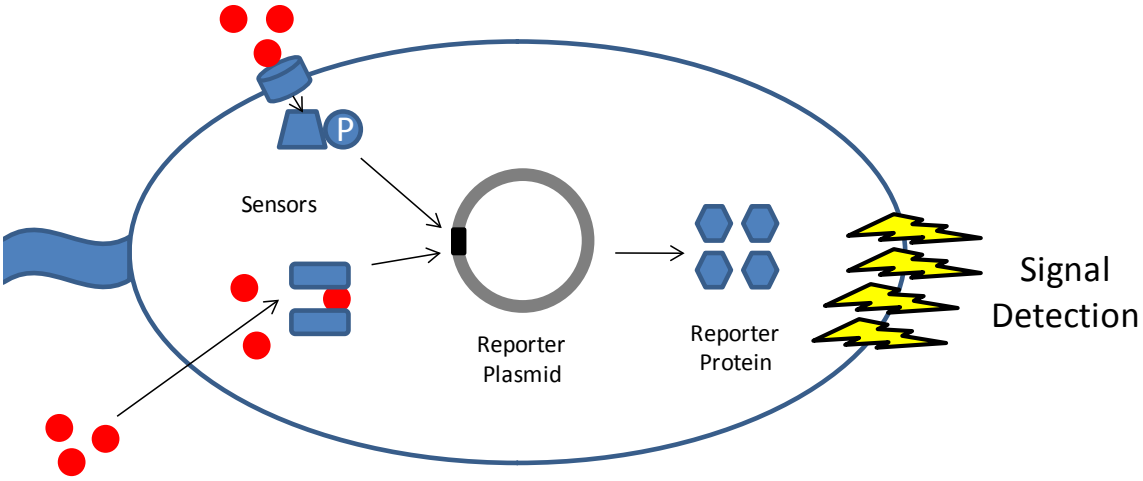

Figure 2: A typical bacterial biosensor. The sensing proteins can detect a chemical either intracellularly, if the chemical can cross the cell membrane, or in the periplasm if it cannot. The amount of chemical present regulates the production of a reporter protein from a reporter plasmid.

The current repertoire of compound-specific biosensors spans a wide range of compounds, different host cells, and various outputs (Table 2) (D'Souza, 2001;Harms *et al.*, 2006;Leveau and Lindow, 2002;van der Meer and Belkin, 2010).

Sensor proteins	Host chassis	Promoter–reporter fusion	Chemical targets
XylR of *Pseudomonas putida*	*Escherichia coli*	*Pu*–lucFF*	Benzene, toluene and xylene
DmpR of *P. putida*	*P. putida*	*Po[‡]–luxAB*	Phenol
TbuT of *Ralstonia pickettii*	*E. coli*	*tbuA1p–luxAB*	Benzene, toluene and xylene
HbpR of *Pseudomonas nitroreducens*	*E. coli*	*hbpCp–luxAB*	Hydroxylated biphenyls
PhnR of *Burkholderia sartisoli*	*B. sartisoli*	*phnSp–luxAB*	Naphthalene and phenanthrene
IbpR of *P. putida*	*E. coli*	*ibpAp–luxCDABE*	Various aromatics
NahR of *P. putida*	*P. putida*	*nahGp–luxAB*	Naphthalene and salicylate
AlkS of *Pseudomonas oleovorans*	*E. coli*	*alkBp–luxAB*	C_6–C_{10} alkanes
TodST of *P. putida*	*P. putida* str. F1	*todXp–luxCDABE*	Toluene, benzene, phenol, *p*-xylene, *m*-xylene and trichloroethene
SepR of *P. putida*	*P. putida* str. F1	*sepAp–luxCDABE*	Solvents
FruR of *Erwinia herbicola*	*E. herbicola*	*fruBp–gfp*[AAV][§]	Fructose and sucrose
AraC of *E. coli*	*E. coli*	*pBAD–gfpuv*[‖]	L-Arabinose
ArsR of *E. coli*	*E. coli*	*arsRp–luxAB*	Arsenite and antimonite
MerR of *E. coli*	*E. coli*	*merTp–luxCDABE*	Hg^{2+}
CadC of *Staphylococcus aureus*	*Bacillus subtilis*	*cadCp–lucFF*	Cd^{2+}, Pb, Sn and Zn
ZntR of *E. coli*	*E. coli*	*zntAp–luxCDABE*	Zn, Pb and Cd
TetR of *E. coli*	*E. coli*	*tetAp–luxCDABE*	Tetracyclines
MphR of *E. coli*	*E. coli*	*mphAp–lacZ*	Macrolides (such as erythromycin)
SOS response proteins of *B. subtilis*	*B. subtilis*	*yorBp–lucFF*	Various antibiotics (for example, ciprofloxacin)
SpoIIID and σ^L of *B. subtilis*	*B. subtilis*	*yhel–lucFF*	Various antibiotics (for example, linezolid)
NisRK of *Lactococcus lactis*	*L. lactis*	*nisAp–gfpuv*[‖]	Nisin
LuxR of *Aliivibrio fischeri*	*E. coli*	*luxIp–gfp*[ASV][§]	*N*-Acyl homoserine lactones

Table 2: Some examples of current biosensors (van der Meer and Belkin, 2010)

Fluorescent biosensors produce fluorescent proteins in response to the presence of an analyte. The fluorescence intensity measured is monotonic to the amount of

analyte present. The majority of fluorescent proteins used are derivatives of green fluorescent protein (GFP) from the jellyfish *Aequorea victoria,* however there are now a number of alternatives available from other species to allow a full colour spectrum of reporters from fluorescent biosensors (See section 1.9). These fluorescent protein reporters are particularly useful for biosensors as they can be readily inserted into existing bacterial genetic switches in place of the normal response gene using molecular biology techniques to create *in vivo* bacterial biosensors.

There are numerous examples of *in vivo* fluorescent biosensors in the literature; one key example is biosensors that fluoresce in the presence of toxic levels of Uranium. This biosensor contains GFPuv under the transcriptional regulation of the *urcA* promoter, which is up-regulated by the uranyl cation (Hillson *et al.*, 2007). The output of the biosensor, when the analyte concentration reached 0.5 µM could be detected using a handheld UV lamp allowing it to be applied in the field without any specialist monitoring equipment. The monitoring of environmental pollutants is an area of keen interest in the development of biosensors, a system has also been developed for the monitoring of biochemical oxygen demand BOD (Lin *et al.*, 2006a;Lin *et al.*, 2006b;Zhao *et al.*, 2005). This can be used to test water samples as an alternative to the traditional 5 day chemical test. The fluorescence biosensor has a BOD detection range of 0.2-40 mg/L and has a shorter response time and better shelf life than the chemical alternative, partially because the bacteria are immobilised in a matrix (Lin *et al.*, 2006a).

Förster resonance energy transfer (FRET) biosensors are another type of fluorescent protein biosensors, but work by the proximity of a FRET donor and FRET receiver such as YFP and CPF that give a response when the FRET pair are close enough for energy transfer to occur. This energy transfer is possible because the emission spectrum of the FRET donor overlaps with the excitation spectrum of the FRET receiver. As a result the detectable output of the biosensor changes from the emission wavelength of the donor to the emission wavelength of the receiver when the two fluorescent proteins are in close enough proximity to each other for the energy transfer to happen. This has been applied in CFP/YFP fusions to bacterial periplasmic solute binding proteins, so that when a solute is bound by the binding protein the conformational change brings the two fluorescent proteins together allowing FRET to occur (See Figure 3). The CFP and YFP are brought close enough together for FRET to occur, giving a change in fluorescence signal from the biosensor (Takanaga and Frommer, 2010). This technique of using genetically encoded nanosensors for measuring intracellular compounds has been applied to identify novel glucose transporters (SWEETs) in *Arabidopsis (Chen et al., 2010)* and take non-invasive measurements of metabolite levels inside cells (Fehr *et al.*, 2003b;Hou *et al.*, 2011) including targeted localisation to sub cellular compartments to directly monitor flux across the endoplasmic reticulum (ER) membrane (Fehr *et al.*, 2004). The FRET energy transfer efficiency is proportional to the sixth power of the distance and therefore falls off rapidly the further the donor and acceptor are from each other (Harris, 2010). Another challenge in this type of biosensor is measurement of the signal, as the biosensors only have one of each fluorescent protein attached to them, very sensitive and expensive equipment is needed to record measurements.

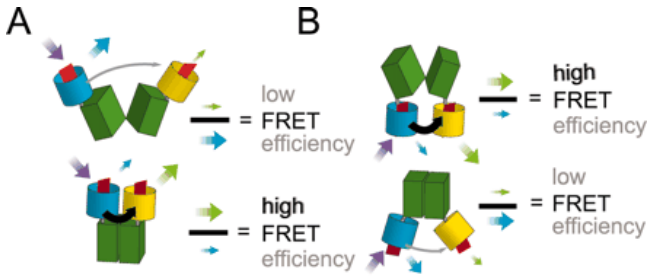

Figure 3: Substrate-induced FRET changes. A, CFP and YFP were fused to N and C termini of periplasmic binding proteins (PBPs). In maltose binding protein (MBP), the termini are located on the distal ends of the lobes relative to the hinge region. Upon the binding of maltose, chromophores come closer together and FRET increases. B, glucose-galactose binding protein (GGBP) termini are positioned on the proximal ends. Thus, glucose binding moves chromophores further apart; hence, FRET decreases. Adapted from (Fehr *et al.*, 2003a)

Bioluminescent biosensors use a change in luminescence output proportional to the presence of an analyte to measure its concentration. The original compound-specific biosensor was a naphthalene biosensor in *Pseudomonas fluorescens;* this was developed by inserting the *lux* cassette, encoding luciferase, from *Vibrio fisheri* into the naphthalene catabolic plasmid of *P. fluorescens* (King *et al.*, 1990). Since then, the use of the *lux* cassette has been a popular option for bioluminescent biosensors (Borisov and Wolfbeis, 2008) as the cassette can be put under the control of a constitutive or inducible promoter that responds to an analyte and the change in bioluminescence measured as the output using a lumenometer. Biosensors that constitutively express the *lux* cassette are generally applied as toxicity biosensors, as compounds that are toxic to the host bacteria will reduce the level of bioluminescence produced by the bacteria. For inducible systems, the *lux* cassette has been put under the transcriptional control of the benzene, toluene, ethylbenzene and xylene (BTEX) specific *tod* promoter (Dawson *et al.*, 2008). It was also shown in a separate study that bioluminescence

gives faster and more sensitive detection of BTEX compounds than fluorescence detection of the same compound, by comparison of the *Pseudomonas putida Pu* gene fused to the *gfp* and *luxCDABE* genes and expressed on plasmids in *E. coli* (Li *et al.*, 2008c). The dose-response curves for the fluorescent and bioluminescent sensors were similar. However, the bioluminescent sensor strain appeared to be more sensitive to toluene, and displayed a dose-dependent response at toluene concentrations of as low as 7.5 μmol L^{-1}. In contrast, the detection threshold for the fluorescent biosensor was 25 μmol L^{-1}(Li *et al.*, 2008a). They concluded that the bioluminescence biosensor was more suitable for rapid and sensitive detection of toluene and related compounds, while the green fluorescence biosensor was more applicable for long-term exposure and cumulative signal detection.

Colorimetric biosensors use a change in a chromogenic substrate into a coloured compound; this is controlled by a metabolic activity of the microbial sensor. The colour change can be observed by eye or measured more accurately using a spectrophotometer making it a simple and cost-effective way of monitoring the output. The SOS Chromotest is an example of a colormetric output. The biosensor is based in an *E. coli* K12 derivative containing a genomic *P-gal* gene (LacZ) fusion to the *sulA* gene that regulates the SOS cell division inhibitor response (Huisman and D'Ari, 1981b;Quillardet *et al.*, 1982). The substrate supplied in the SOS Chromotest kits, 5-bromo-4-chloro-2-indolyl-β-D-galactopyranoside (X-gal), is converted to a blue compound by P-gal which can then be read in a spectrophotometer at 620 nm (McDaniels *et al.*, 1990). Alkaline phosphatase is also assayed at the same time as a means to take into account any protein

inhibition or cell death caused by the compounds tested. This highlights the importance of knowing how many of the biosensor cells are functioning normally in the test well when quantifying an analyte.

The Umu test biosensor was prepared in a similar way by a fusion of the SOS response *umuC* gene from *E. coli* and the *lacZ* gene on the multiple copy plasmid pSK1002 (Shinagawa *et al.*, 1983). The plasmid was then later used in *S. typhimurium* TA1535 in the Umu test (Oda *et al.*, 1985). The output of the Umu test is measured differently to the SOS chromotest as the substrate for P-Gal is o-nitrophenyl P-D-galactoside (ONPG) instead of X-Gal, which forms ONP on cleavage by P-Gal which produces a yellow colour that is measured at 420 nm in a spectrophotometer.

1.4.2 Electrochemical biosensors

There are a wide range of electrochemical approaches used in microbial biosensors. These can be segregated by the type of measurement that is used by the biosensor to quantify changes in analyte. The categories are; amperometry, conductometry, microbial fuel cell (MFC), potentiometry and voltammetry.

Amperometry measures the change in current between a working electrode and a reference electrode. The change in current is generated by the oxidation or reduction of a metabolite on the surface of the working electrode (Ding *et al.*, 2008). It is possible to make highly sensitive amperometry biosensors due to the highly sensitive measurement methods available to measure current. This is one

of the most extensively used methods of monitoring for electrochemical biosensors and has been applied in medical, military and environmental fields (D'Souza, 2001;Yagi, 2007). Examples from medical/health applications include glucose monitoring (Kirgoz *et al.*, 2007); which is of particular interest for monitoring blood glucose in diabetics and also in the food industry for quality control of food and fermentation products. Glucose metabolism is a very common process in microbes, and many biosensors have been developed utilising oxygen consumption as a measure of glucose metabolism and availability in a sample (Kirgoz et al., 2007). Common microbial hosts for this type of biosensor are *Pseudomonas fluorescens and Gluconobacter oxydans.*

Conductometry measures conductivity changes in a solution that can arise from production and uptake of charged species by the metabolism of bacteria (Lei *et al.*, 2006). This is an extremely fast technique and as it requires no reference electrode like amperometry it can be miniaturised for applications, however they are very non-selective as anything that changes the levels of charged species in the solution will register a response (Shul'ga *et al.*, 1994). This technique has been applied to detection of heavy metal ions in water samples by immobilising the algae, *Chlorella vulgaris* in bovine serum albumin membranes and depositing them on a platinum electrode (Chouteau *et al.*, 2005). This sensor was able to detect Cd^{2+} and Zn^{2+} after 30 minutes exposure with a detection limit as low as 10 ppb.

Voltammetry is able to measure both the current and potential giving information on the analyte present and its concentration. It is also able to perform scans that allow multiple analytes with different peak potentials to be detected. This makes it a very versatile technique and due to its very low noise levels in the measurements, a very sensitive method (Wang, 2007). A novel Cu^{2+} biosensor has been developed to monitor biosorption of copper from contaminated water during bioremediation (Alpat *et al.*, 2008). This was based on the fungus C*ircinella sp*. mixed into a carbon paste electrode and gave a detection limit of 54 nM.

Potentiometry measures an analyte by detecting the difference between the potential difference of a working electrode and a reference electrode which are separated by a selectively permeable membrane. The selectivity and sensitivity of the gas sensing and ion selective electrodes are excellent (Bobacka *et al.*, 2008), but the need for a stable reference electrode is often limiting for bacterial applications (Lei *et al.*, 2006). A potentiometric oxygen electrode has been used to produce an ethanol biosensor based on immobilized yeast, *Saccharomyces ellipsoideus* (Rotariu *et al.*, 2004). The response to ethanol is achieved in about 7 minutes for the steady-state method and 2 minutes for kinetic measurements and shows close correlation with spectroscopic methods.

Microbial fuel cells (MFC) are used to convert chemical energy into electrical energy (Figure 4). As a result metabolism of target analytes can be monitored by an increase in electrical output and inhibition of the microbial metabolism by toxins would result in a decrease in electrical output (Rabaey and Verstraete, 2005).

MFC technology has been combined with cyclic voltammetry to measure volatile fatty acid (VFA) concentration in the monitoring of bio-processes such as anaerobic digestion in microbial fuel cells (Kaur *et al.*, 2013). Using cyclic voltammetry to measure the oxidation peak at a consistent scan rate gave a linear correlation to VFA concentration and peak current produced, up to 40 mg l^{-1} in a rapid response time of 1–2 min. A MFC based biosensor array was produced capable of measuring individual acetate, propionate and butyrate concentrations with sensitivity down to 5 mg l^{-1} and up to 40 mg l^{-1} (Kaur *et al.*, 2013).

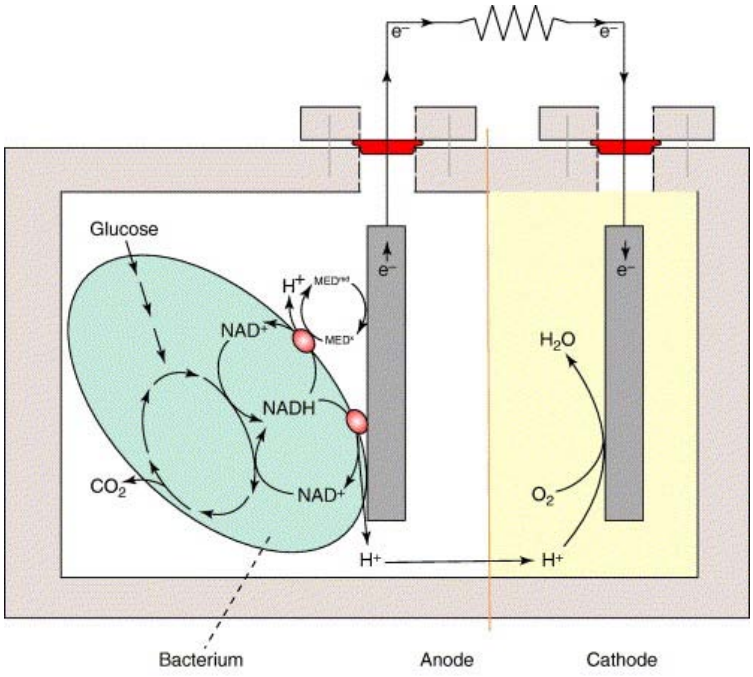

Figure 4: The working principle of a microbial fuel cell. Substrate is metabolized by bacteria, which transfer the gained electrons to the anode. This can occur either directly through the membrane or via mobile redox shuttles. MED, redox mediator; Red oval, terminal electron shuttle in or on the bacterium. Taken from (Rabaey and Verstraete, 2005).

Protein hinge-bending motions can also be used for bioelectric interfaces (Benson *et al.*, 2001a;Willner, 2001). This technology is based upon the hinge type motion that many periplasmic binding proteins undergo when a solute binds to them (Gerstein *et al.*, 1994). Maltose binding protein (MBP) was used as the sensor part of the biosensor by attaching MBP to an electrode surface using a His tag-Ni complex. A Ru(II) redox active reporter links the binding of maltose to a change in electrical signal (Figure 5).

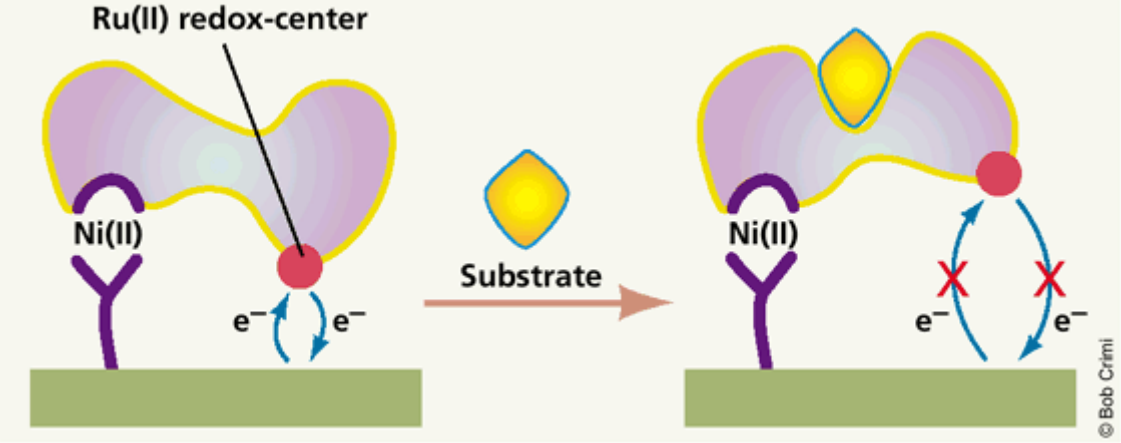

Figure 5: The maltose-binding protein is affixed to the electrode surface via a His tag–Ni(ii) complex. The Ru(ii) complex redox-active reporter unit (red circle) linked to the maltose-binding protein communicates with the electrode in the absence of maltose, resulting in a current response. The interaction of maltose (yellow unit) with the maltose-binding protein induces bending of the protein and allosteric displacement of the reporter unit. This perturbs the electrical contact between the reporter and the electrode and diminishes the system's current response. Taken from (Willner, 2001).

The detection range of non-enzymatic sensors is dictated by the ligand binding constants. The lower limit of detection is determined in large part by the tightest binding constant that can be obtained, which is ~1 nM for this class of protein

(Tam and Saier, Jr., 1993). The affinity of the sensor could be altered by creating point mutations in the recognition domain of MBP so that an appropriate response range could be selected depending on the expected levels of maltose in a sample. The maltose concentration from the biosensor was shown to be within 5% error of the concentration measured by enzymatic assay even when sampling a complex mixture such as beer (Benson *et al.*, 2001b).

1.5 Design of a biosensor

When designing a biosensor a number of aspects need to be taken into consideration to ensure that the final biosensor functions over the desired range of analyte concentrations. The design of a biosensor can be separated into three different areas; analyte detection (Section 1.6), signal transduction (Section 1.7) and output (Section 1.9). Some examples of current reporter pathways are shown in Figure 6.

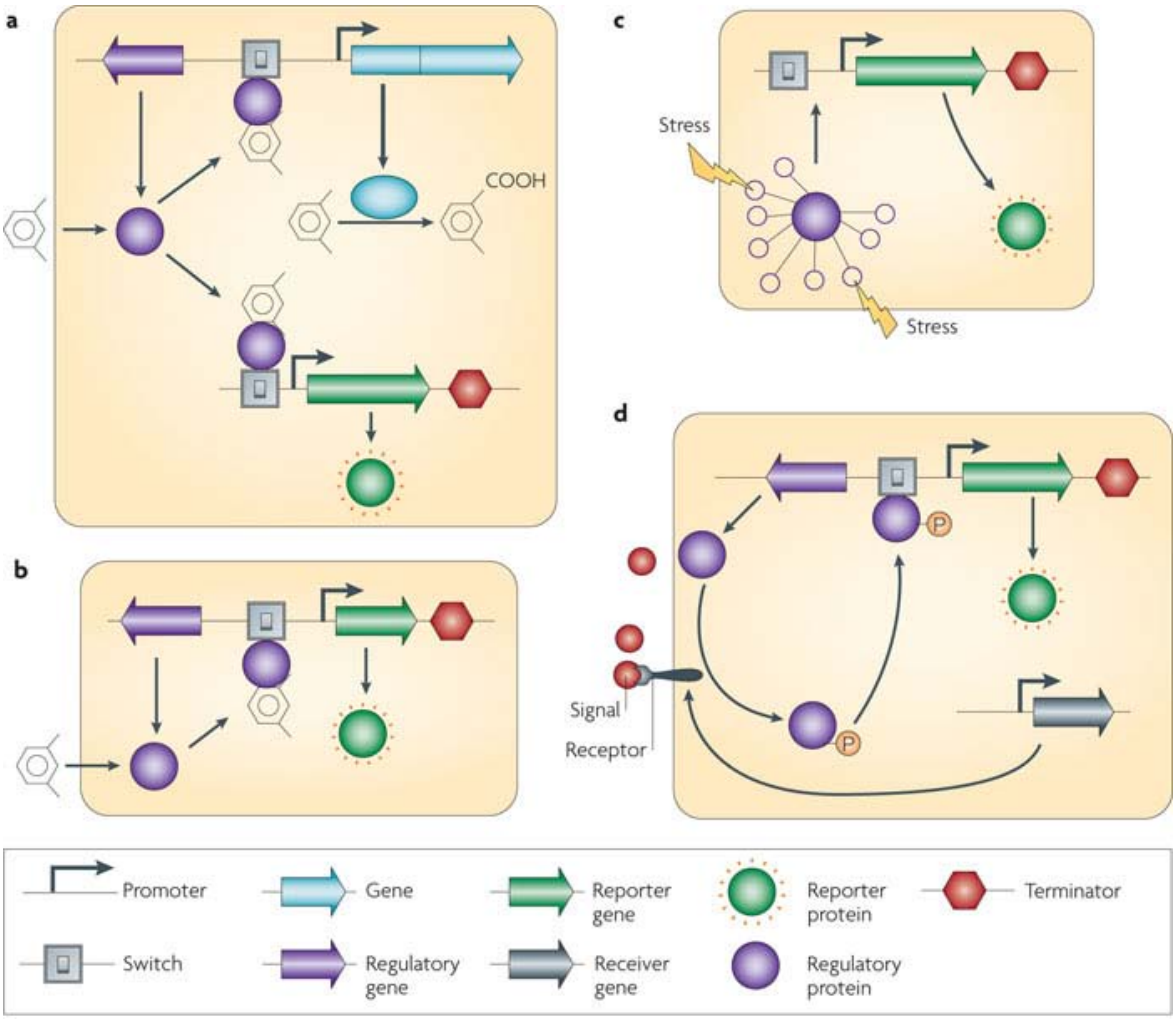

Figure 6: Typical methods for engineering a reporter system. a) A design for a bacterial reporter responding to a metabolisable organic compound. b) The same compound-activated regulatory circuit as shown in part a, but in a heterologous host than cannot metabolise the detected compound. c) The design principle of toxicity- or stress-responsive reporter cells. d) An example of a more elaborate design in which a target compound (signal) is detected in the periplasm by means of a receptor protein. Receptor binding triggers an intracellular phosphorelay that is transmitted to the switch and promoter, leading to the expression of the reporter gene. (van der Meer and Belkin, 2010)

1.6 Analyte detection

An understanding of the analyte is important when designing a biosensor as the sensing system must be able to be linked to the output. The availability of the

analyte must also be considered as it needs to interact with the sensor in order to trigger an output from the biosensor. For example, if the sensor protein is inside the cell then the analyte must be able to cross the membrane. Bacteria have a wide range of sensing proteins that can be used to create biosensors and generally fall into the categories of one-component or two-component sensors. Another consideration with the analyte is whether or not it is metabolisable by the host cell as this could affect the total concentration reported by the biosensor.

1.7 Signal transduction

1.7.1 One-component systems

Transcription in prokaryotes is normally regulated by single molecule repressors and activators that have a ligand-binding domain and a DNA-binding domain. One-component systems are the simplest form of signal transduction proteins found in prokaryotes, involving a direct fusion of an input domain and an output domain in a single protein (Ulrich *et al.*, 2005) (Figure 7). These usually function in the cytoplasm and hence the analyte has to cross the membrane either passively or actively.

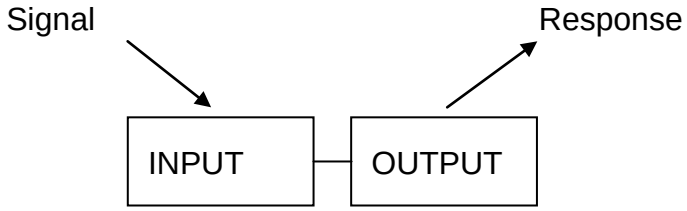

Figure 7: The domains of a one-component response regulator. The input domain detects the signal and the output domain regulates transcriptional activity (Ulrich *et al.*, 2005).

The classical examples of one-component sensing systems are the LacI repressor (Lewis *et al.*, 1996) and the catabolite activator protein (CAP) (Kolb *et al.*, 1993) of *E. coli*. Both of these systems bind a ligand and then regulate transcription of the *lac* operon among other promoters. CAP binds cyclic AMP (cAMP) and dimerises to allow DNA binding and induction of transcription from the *lac* promoter. This is an example of an inducible system and senses glucose availability to the cell as cAMP levels increase when glucose transport levels are low. The LacI repressor binds to the operator region of the *lac* promoter, looping the DNA and preventing transcription of the *lac* operon. The binding of allolactose, or an artificial analogue, IPTG, alters the conformation of the LacI repressor and decreases its affinity for DNA resulting in dissociation and relief of the repression on the promoter. Allolactose is a metabolic product of lactose metabolism and indicates the presence of lactose as a food source. The highest level of transcriptional activation of the *lac* operon occurs when lactose is available and glucose levels are low (Kuo *et al.*, 2003). This highlights the complexity of transcriptional

regulation from a promoter, even where simple one component systems are involved.

1.7.2 Two-component systems

Two-component systems share similar input and output domains with one-component systems (Ulrich *et al.*, 2005), however the activity is split between two proteins and normally consists of a sensory histidine kinase (HK) and a response regulator (RR). The basic mechanism of the two-component system involves the sensor domain of the histidine kinase detecting an input signal resulting in conformational changes in the linker domain and subsequent changes in the auto-phosphorylation or the phosphatase activity of the kinase domain (Ulrich *et al.*, 2005). If ATP is present to donate a phosphoryl group, a highly conserved histidine residue on the kinase domain will be phosphorylated. The response regulator then binds to the phosphorylated kinase domain and the phosphoryl group is transferred to a highly conserved aspartate residue on the response regulator (Figure 8). The phosphorylated response regulator then dissociates from the histidine kinase and binds to DNA, either to alter the transcriptional activity at a particular promoter or to participate in further protein-protein interactions.

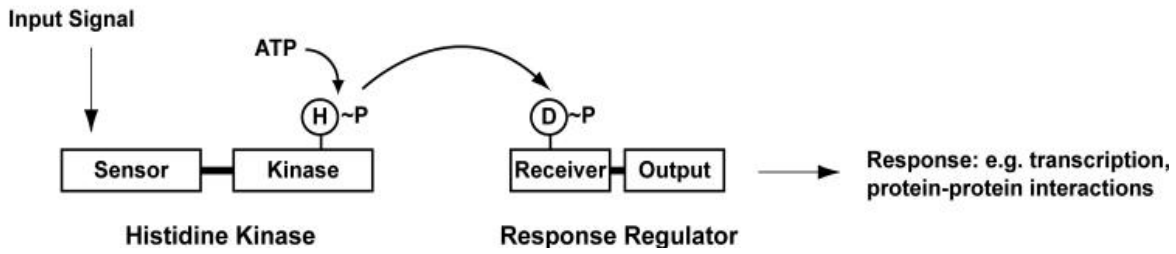

Figure 8: The basic mechanism of a two-component system (Skerker *et al.*, 2005).

This is the type of sensing system found in the nitrogen sensing (Ntr) system (Section 1.7.3), however there are more complex two-component and phosphorelay systems (Laub and Goulian, 2007;Stock *et al.*, 2000;Wadhams and Armitage, 2004). The *E. coli* oxygen sensing system (Arc) has multiple phosphoryl group receiving domains in the histidine kinase, the *E. coli* chemotaxis system has a single kinase and multiple response regulators and the sporulation system of *B. subtilis* has multiple histidine kinases and one response regulator. Thus there is vast diversity in the inputs that can be sensed and also diversity in the output responses generated (Figure 9).

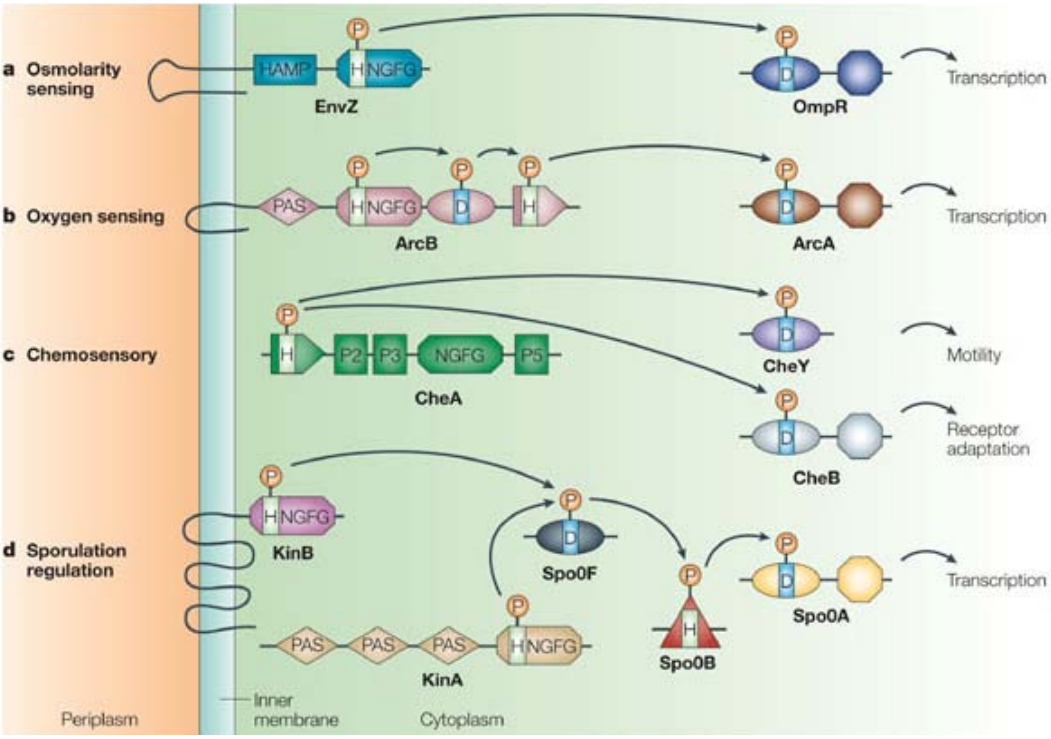

Figure 9: Some of the different combinations of histidine protein kinase (HPK) and aspartate response regulator (RR) domains in histidine–aspartate phosphorelay (HAP) systems. a | The EnvZ/OmpR pathway of *Escherichia coli*, which is involved in regulating the expression of the two outer-membrane porins OmpF and OmpC. A membrane-bound HPK (EnvZ) controls the activity of the RR OmpR in response to changes in osmolarity. b | The complex ArcB–ArcA HAP system of E. coli. The membrane-bound HPK ArcB senses changes in the redox state of components of the respiratory electron-transport chain through its PAS (PER, ARNT, SIM) domain. The phosphoryl group is then passed from the conserved His in the ArcB kinase domain to a fused RR domain, then to a fused histidine-containing phosphotransfer (HPt) domain and finally to a DNA-binding RR ArcA. ArcA regulates microaerophilic gene expression. c | The chemosensory pathway of E. coli. The soluble HPK chemotaxis protein CheA has five domains per monomer that are designated P1–P5 from the N terminus to the C terminus. CheA senses changes through transmembrane chemoreceptors, which induce the trans-autophosphorylation of dimeric CheA on a His residue of the HPt domain. Two RRs compete for this phosphoryl group: CheY, a single-domain, motor-binding protein, which controls flagellar motor switching, and CheB, which controls the adaptation of the chemoreceptors. d | Part of the complex system that regulates sporulation in *Bacillus subtilis*. A single-domain RR, Spo0F, is regulated by two HPKs, one of which has numerous transmembrane domains (KinB), the other of which is soluble with numerous PAS domains (KinA). Spo0F indirectly phosphorylates a DNA-binding RR, Spo0A, by way of a His residue in Spo0B. Throughout this figure, light-green rectangles highlight conserved, phosphorylatable His residues, light-blue rectangles highlight conserved, phosphorylatable Asp residues, and orange circles highlight phosphoryl (P) groups. NGFG represents the kinase domain and, with the exception of CheA, the conserved His residue that precedes the kinase domain is contained within the dimerization domain. Despite being dimeric in nature, HPKs are shown here as

monomers for simplicity, and the HAMP domain ('histidine kinases, adenylyl cyclases, methyl-binding proteins and phosphatases' domain) is a linker domain. (Wadhams and Armitage, 2004)

The advantage of two-component systems over one-component systems as a detector in a biosensor is that they can often detect chemicals outside the bacterial cell or in the periplasm (Figure 10). One-component sensors function in the cytoplasm of the cell, so the compound sensed must be able to cross the cell membrane in order to interact with the sensor protein (Melamed *et al.*, 2014). This is particularly relevant when using a sensory protein from one species in a different host, as there may be other proteins required to transport the chemical into the cell before detection can occur. Alternatively toxic chemicals may be kept at a low concentration within the cell by transport proteins, despite an increase in concentration outside the cell, preventing the increase in signal from being seen by a biosensor (Krell *et al.*, 2010). Two-component systems use signal transduction domains to transmit signals across the membrane and are therefore able to detect compounds in the periplasm of the cell.

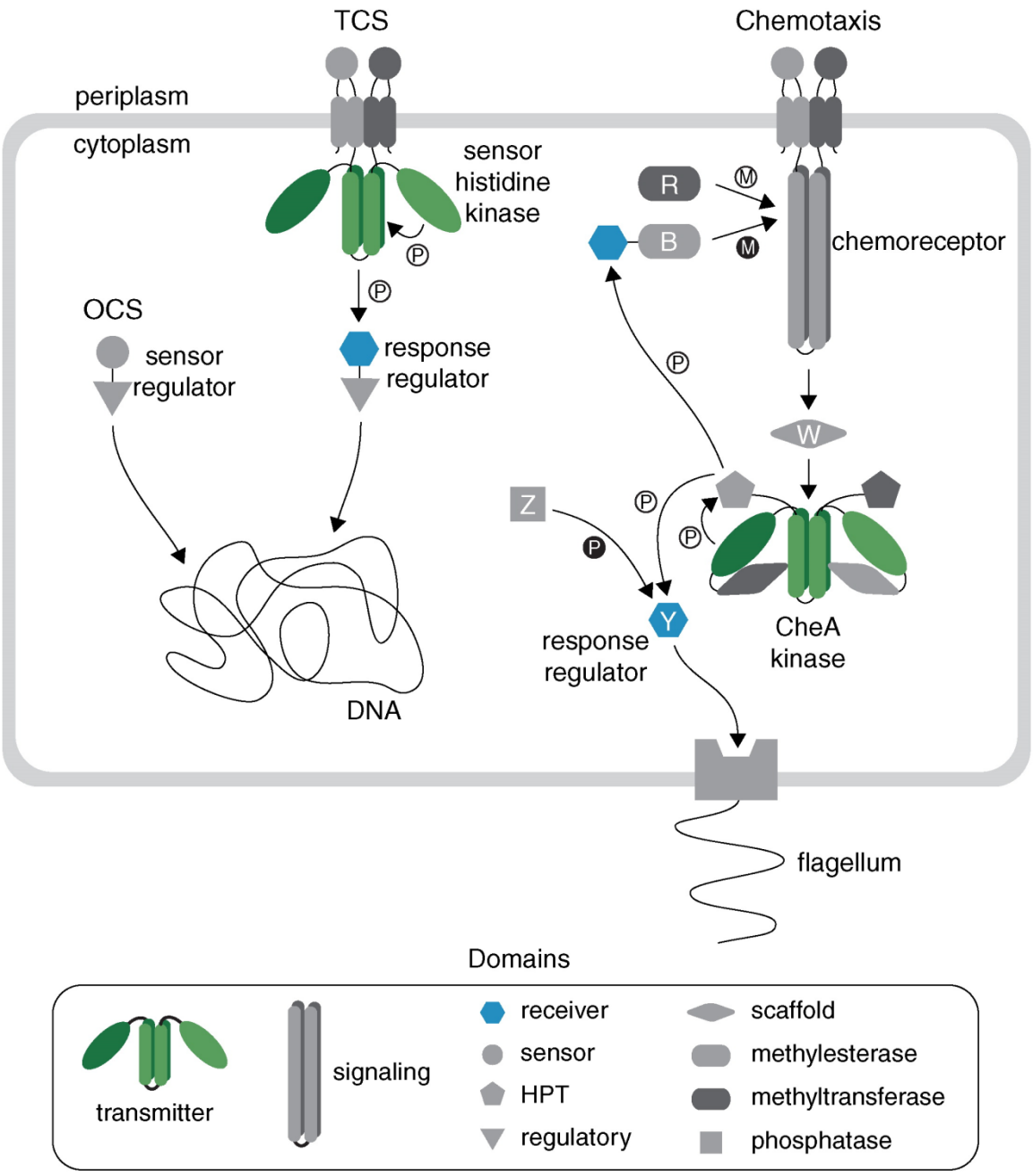

Figure 10: Comparison of one-component (OCS), two-component (TCS) and Chemotaxis signaling pathways. The chemotaxis system (represented by the canonical *E. coli* system) employs a number of additional components not reported in other TCSs that regulate methylation (M) (CheB and CheR), dephosphorylation (CheZ), and scaffolding (CheW). (Wuichet *et al.*, 2010).

The most extensively studied two-component chemical detection system in bacteria, the chemotaxis system, does not regulate transcription as a natural output, but rather alters the swimming behaviour of the bacterium. Therefore, the presence of the chemicals it can detect cannot be directly linked to a measurable output such as fluorescence by the standard method of putting a reporter gene under the control of the regulated promoter to produce a measurable output. Instead, chimeric proteins have been engineered, such as the Taz receptor (Figure 11) (Utsumi *et al.*, 1989) which combines the sensing and signal transduction domain of the *E. coli* Tar receptor with the histidine kinase domain of the EnvZ osmosensor (Yoshida *et al.*, 2007a) in order to regulate production of a reporter protein via the response regulator OmpR in response to changes in aspartate concentration in the growth media (Yoshida *et al.*, 2007b). Therefore there is potential to utilise this diverse chemical sensing system in a genetic switch biosensor.

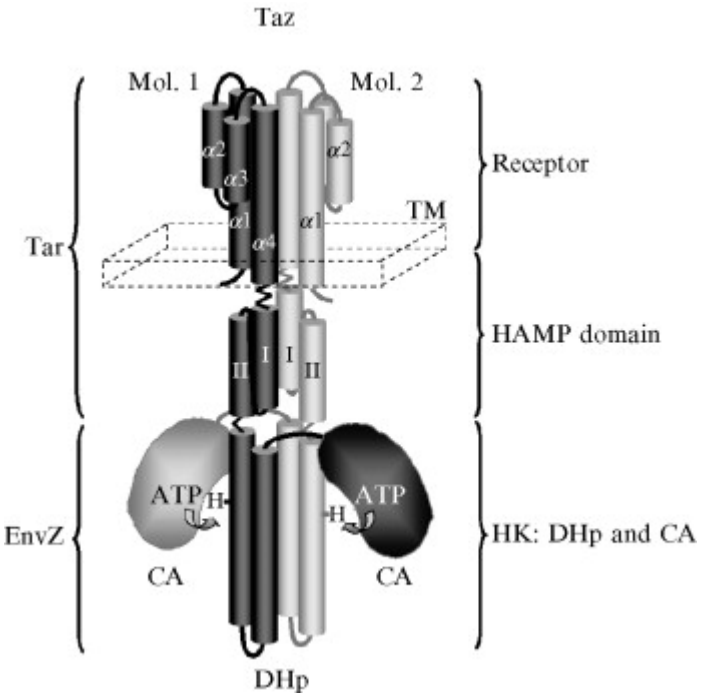

Figure 11: The schematic model of a Tar-EnvZ chimeric protein, Taz. Taz consists of Tar receptor, Tar HAMP domain, and EnvZ histidine kinase domain. Taz undergoes ATP-dependent trans-autophosphorylation in which the ATP-binding pocket of Mol. 1 (dark gray) phosphorylates the phosphorylation site, H243, of Mol. 2 (light gray). TM, transmembrane; DHp. a dimerization histidine phosphotransfer domain; CA, a catalytic ATP-binding domain (Yoshida *et al.*, 2007c).

1.7.3 The *E. coli* nitrogen sensing (Ntr) system

The Ntr system is a complex two-component system. We will look at this in more detail as it will be used in the production of our biosensor, not for its ability to indirectly respond to nitrogen availability in the environment but for its variable strength output mechanism. This will be manipulated to give a multi-level response to an individual input to improve the range and sensitivity of the final biosensor.

Bacteria such as *E. coli* are able to use many different nitrogen sources from the environment, both organic and inorganic. However, these different sources of nitrogen come with different energetic costs to the cell as they are all converted to the preferred source of nitrogen, ammonium. Ammonium is preferred over other nitrogen sources as is can be incorporated into proteins with the lowest energetic cost to the cell (White *et al.*, 2012). The role of the Ntr system is to control the expression of nitrogen assimilating genes so that the use of more energetically expensive sources is limited when more energetically favourable options are available to the cell. This results in inhibition of genes for utilising other ammonium sources, such as glutamine uptake proteins and amino acid uptake and catabolism proteins, when ammonium is plentiful. These are then activated in a sequential manner depending on the severity of nitrogen starvation that the cell is experiencing. This reduces the utilisation of more energetically costly sources when ammonium is present, although low levels of utilisation will occur.

Ammonium is referred to as the preferred source of nitrogen as it is assimilated using the following reactions, which produce the building blocks for all of the nitrogen containing molecules in the cell with the minimum energetic cost to the cell:

$$\alpha\text{-Ketoglutarate} + NADPH + H^+ + NH_3 \xrightarrow{\text{Glutamate dehydrogenase}} \text{L-glutamate} + NADP^+ + H_2O$$

$$\text{L-Glutamate} + ATP + NH_3 \xrightarrow{\text{Glutamine synthetase}} \text{L-glutamine} + ADP + P_i$$

$$\alpha\text{-Ketoglutarate} + \text{glutamine} + NADPH + H^+ \xrightarrow{\text{Glutamate synthase}} 2\ \text{L-glutamate} + NADP^+$$

When ammonium levels are high in the environment, the glutamate dehydrogenise reaction is the main reaction for ammonium uptake as it does not consume ATP in the reaction. However, this enzyme has a high K_m (~1 mM) for ammonium (White *et al.*, 2012). Therefore, if ammonium levels fall below 1 mM, this reaction becomes unfavourable and the glutamine synthetase reaction becomes the dominant reaction for uptake of ammonium as it has a much lower K_m for ammonium (White *et al.*, 2012). The glutamine synthetase enzyme is only produced at very low levels when ammonium is plentiful, so when ammonium levels drop in the environment its production must be increased in order to assimilate the lower concentrations of ammonium. This is the first stage where regulation by the Ntr system is required.

The ammonium levels in the environment are indirectly sensed via the intracellular concentrations of glutamine (Jiang *et al.*, 1998) and α-ketoglutarate (Ninfa and Jiang, 2005) by the sensory protein P_{II}, this connects nitrogen availability with

carbon availability in the environment. The level of glutamine in the cell affects the uridylylation state of the P_{II} protein (Figure 12), and the P_{II} protein controls the balance between the kinase and phosphatase activity of the histidine kinase NtrB. In turn, NtrB regulates the activity of the response regulator NtrC by altering its phosphorylation state. This two-component system is responsible for the regulation of transcription from promoters containing NtrC-P binding sites.

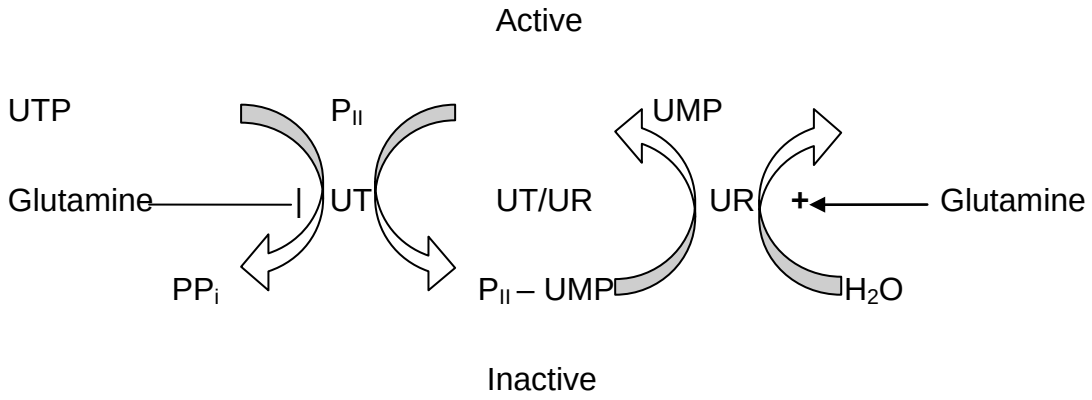

Figure 12: The regulation of the bi-functional enzyme UT/UR by glutamine levels in the cell and the subsequent effects on the activation state of the P_{II} protein (adapted from (White *et al.*, 2012).

When ammonium levels are high in the environment, the intracellular level of glutamine is high and the level of α-ketoglutarate is low. The P_{II} protein is in its active form as glutamine inhibits the uridylyltransferase activity and promotes the uridylyl removal activity of the UT/UR enzyme (Figure 12). The active P_{II} protein interacts with NtrB and promotes its phosphatase activity, resulting in the de-phosphorylation of NtrC-P to its inactive from. This results in repression of the σ^{54}-dependent *gln-Ap2* promoter and basal level transcription from the σ^{70}-dependent *gln-Ap1* promoter (Figure 13).

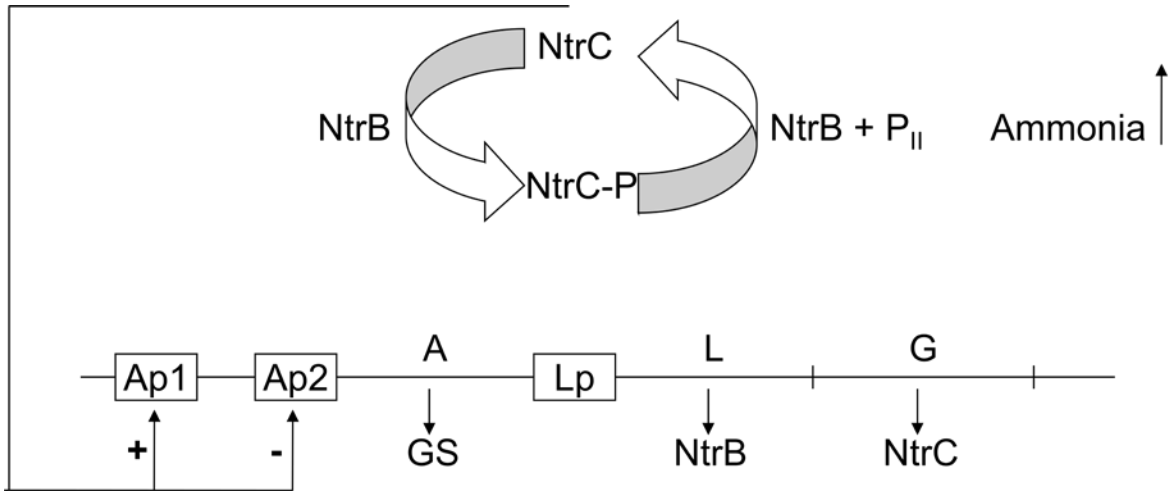

Figure 13: The Ntr system in high ammonium. When ammonium levels are high NtrB interacts with P_{II} and de-phosphorylates NtrC into its inactive form. This results in a low level of basal transcription from the σ^{70}-dependent Ap1 promoter producing only low levels of glutamine synthetase, NtrB and NtrC. (Adapted from (White *et al.*, 2012).

When ammonium levels drop in the environment, the intracellular level of glutamine falls because when the cells have been growing in high ammonium concentrations there is very little glutamine synthetase present. The level of α-ketoglutarate rises because the conversion of α-ketoglutarate to glutamate requires glutamine or ammonium. The P_{II} protein is now deactivated by uridylylation as the inhibition of the uridylyltransferase is relieved and the uridylyl removal activity is inhibited on the UT/UR enzyme (Figure 12). P_{II}-UMP is not able to interact with NtrB and the rising levels of α-ketoglutarate speed de-repression of the kinase activity by interacting directly with active P_{II} and preventing its interaction with NtrB. This results in the kinase activity of NtrB becoming dominant over its phosphatase activity. NtrB phosphorylates the response regulator NtrC, which results in repression of the σ^{70}-dependent *gln-Ap1* promoter and a high level transcription from the σ^{54}-dependent *gln-Ap2* promoter. The main reason for this

increase in transcription is to produce more glutamine synthetase to be able to use the lower concentrations of ammonium in the environment (Figure 14).

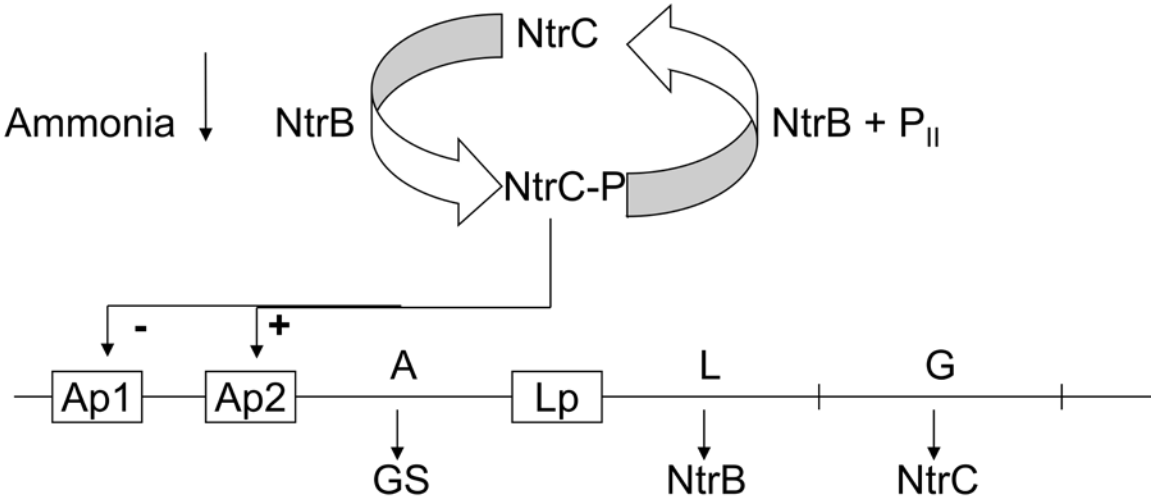

Figure 14: The Ntr system in low ammonium. When ammonium levels drop, the P_{II} protein no longer inhibits the kinase activity of NtrB. As a result NtrC is now phosphorylated into its active form and can activate transcription from the σ^{54}-dependent Ap2 promoter, thus increasing production of glutamine synthetase and creating a feed-forward loop by up regulating its own production**.**

The genes encoding NtrB and NtrC are also present in this operon and the activation of NtrC by NtrB in response to low ammonium creates a feed-forward loop as NtrC-P regulates its own operon, increasing the amount of NtrB and NtrC in the cell. The basal level of NtrC in the cell in an ammonium rich environment is ~5 dimers per cell (Reitzer and Magasanik, 1983). This is only sufficient to activate transcription of the *gln-ALG* operon to increase production of glutamine synthetase and the NtrB/C proteins (Rothstein *et al.*, 1980). During prolonged ammonium starvation, the level of NtrC in the cell increases to ~70 dimers per cell as a result of the feed-forward loop (Reitzer and Magasanik, 1983). When these are

phosphorylated by NtrB, there are a sufficient numbers of NtrC-P dimers in the cell to activate lower-affinity Ntr promoters in a sequential manner (Atkinson *et al.*, 2002). This allows the cell to have a hierarchy of responses to starvation depending on how severe the level of starvation is.

This sequential activation of different *ntr* promoters is a result of the different affinity NtrC-P binding sites found in these promoters. The highest affinity binding site for NtrC-P is an inverted repeat with the sequence (TGCACCn5GGTGCA) (Ninfa *et al.*, 1987). This is found in the Ap2 promoter of *glnALG* and controls the production of glutamine synthetase, NtrB and NtrC. Any deviation from this optimal binding site will result in a weaker interaction between the NtrC-P and the DNA; these weaker sites are therefore less likely to be bound by NtrC-P when there are low levels of NtrC-P in the cell as the interaction is less energetically favorable. However, as the level of NtrC-P in the cell increases the high affinity sites will already be occupied and there will be free NtrC-P available to bind to the weaker sites in a sequential manner depending on how far each binding site deviates from the optimal sequence.

In addition to activating binding sites, the promoters also contain lower affinity NtrC-P binding sites that act to reduce expression from *glnALG* when the levels of NtrC-P in the cell become very high. This prevents the feed-forward loop from getting out of control by limiting the amount of NtrB and NtrC that is produced in the cell.

There is also a possibility the levels of σ^{54} in the cell will limit the amount of transcription possible from the Ntr promoters. The levels of σ^{54} in *E. coli* cells is constant throughout different growth phases but is only present at up to 30 copies per cell (Jishage *et al.*, 1996).

For our biosensor the promoters of *glnALG* (Magasanik, 1989;Reitzer *et al.*, 1989), *glnHPQ* (Claverie-Martin and Magasanik, 1991) and *nac* (Atkinson *et al.*, 2002) were chosen; these are high, medium and low affinity respectively and are all bound by NtrC-P with varying affinities (Figure 15).

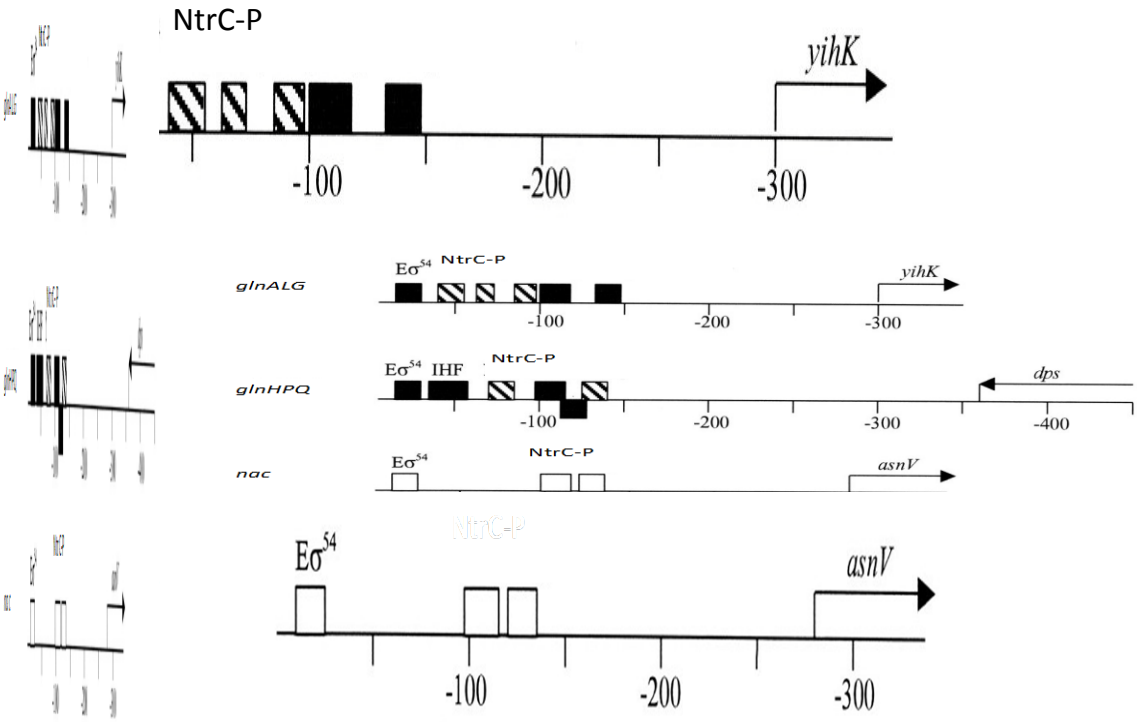

Figure 15: The NtrC-P binding sites in the promoter regions of the *glnALG*, *glnHPQ* and *nac* operons of *E. coli*. High affinity NtrC-P binding sites are shown as filled boxes, medium affinity as striped boxes and low affinity as clear boxes. (Reitzer and Schneider, 2001).

The promoters of *glnALG*, *glnHPQ* and *nac* were chosen as they were the best characterised of the Ntr promoters in the literature (Atkinson *et al.*, 2002;Leigh and Dodsworth, 2007;Reitzer and Schneider, 2001) and the most likely to give the improved range of fluorescence output by allowing activation of the high affinity promoter at low concentrations of NtrC-P and when the concentration of NtrC-P increases and becomes saturating for this promoter the medium and low affinity promoters will become activated.

1.8 Location of biosensor parts

For biosensors based in living cells the reporter can either be inserted into the chromosome which would give a single copy per cell or on a plasmid which could give a number of copies per cell. The advantage of having a single copy is that there is reduced variability coming from variation of plasmid copy number between different cells, however due to there only being a single copy of the reporter there is a lower signal generated and thus a low signal to noise ratio for the biosensor. The reverse is true for the plasmid based systems in that a high signal to noise ratio is possible for the biosensor, but cell to cell variation in plasmid copy number can introduce additional variation in the output measured from the biosensor (Knudsen *et al.*, 2014). If multiple plasmids are used in the same cell then the compatibility groups of their origins of replication (1.8.1) must be considered to ensure all parts of the biosensor are passed on during cell division.

Another consideration with high copy number plasmids in biosensors is the number of binding sites on the plasmid titrating out all of the transcriptional

activators which are present in a limited number in the cell. For example *E. coli* RpoN has been shown to be present at about 110 copies per cell (Jishage *et al.*, 1996). This sigma factor is required to initiate transcription from Ntr regulated promoters (Reitzer and Schneider, 2001).

1.8.1 Origins of replication

The origin of replication on a plasmid is the site where replication of the plasmid DNA is initiated from. The origin of replication site that a particular plasmid has also determines the copy number of that plasmid within the cell. Origins of replication are split into different incompatibility groups (Sambrook and Russell, 2001). Two plasmids that replicate by the same mechanism cannot co-exist in the same cell as one plasmid will become dominant and the other may be lost from the cell during division. A summary of these incompatibility groups is shown below (Table 3). If two plasmids are required to co-exist in the same cell for a biosensor then they must belong to different incompatibility groups and have different antibiotic resistances for selection.

Incompatibility groups	Mechanism of replication control
pMB1, ColE1	RNAi
IncFII, pT181	RNA
P1, F, R6K, pSC101, p15A	Iterons

Table 3**:** Plasmid incompatibility groups (Sambrook and Russell, 2001)

1.8.2 Terminators

Transcriptional terminators are regions of DNA found after a gene that form secondary structures to destabilise the RNA polymerase/DNA interaction and terminate transcription. A commonly used and highly effective transcriptional terminator is the *E. coli rrnB* terminator (Orosz *et al.*, 1991). The *rrnB* acts as a double terminator consisting of two large stems, T1 and T2 and two small inverted repeats, IR1 and IR2 (Figure 16). These four secondary structures make up the terminator and do not require any proteins to terminate transcription. It has been shown that the T2 stem loop provides most of the termination efficiency, but the inclusion of T1, IR1 and IR2 provide an even stronger terminator which gives almost 100% termination efficiency in both forward and reverse directions (Orosz *et al.*, 1991).

Figure 16: The *rrnB* terminator of *E. coli*. Showing the T1, IR1, IR2 and T2 terminator regions (Orosz *et al.*, 1991).

The efficiency of the *rrnB* terminator is close to 100% in both directions and is thought to be the result of gene duplication and a further transposition event as other ribosomal RNA genes, such as *rrnG* and *rrnD,* only contain single termination loops (Orosz *et al.*, 1991). It has been shown that the termination efficiencies of the *E. coli rrnB* T1 terminator (on its own), the phage lambda

terminator site R2, and the *E. coli* tryptophan attenuator ware 89%, 79% and 24% respectively (Nojima *et al.*, 2005). This makes the *rrnB* dual terminator the ideal choice to prevent any unwanted read-through in a reporter plasmid as it has a higher termination efficiency than other transcriptional terminators that have been studied.

1.9 Output

There are a number of choices when selecting an appropriate output for a biosensor. These include fluorescent proteins, bioluminescence and enzymatic reactions, catalysed by enzymes such as UidA (de Ruijter *et al.*, 2003), PhoA (Beaulieu *et al.*, 2013) and LacZ (see section 1.4.1) (Table 4).

Gene	Protein	Advantages	Defects
lux	Bacterial luciferase	Ease of measurement	Heat lability
		Rapid response	Oxygen requirement
luc	Firefly luciferase	High sensitivity	Exogenous substrate requirement
		No heat lability	Oxygen requirement
gfp	Green fluorescent protein (jelly fish)	Autofluorescence	Low sensitivity
		No substrate requirement	Lag time before expression
lacZ	β-gal (*E. coli*)	Detection by naked eye	Exogenous substrate requirement
		Wide variety of detection methods	Complicated colorimetric operation
GUS	UidA (β-glucuronidase) (*E. coli*)	Localisation of promoter activity in plants	Needs oxygen
		Fluorogenic or visible output	Time to generate protein
PhoA	Alkaline phosphatase	Fluorogenic or visible output	Exogenous substrate requirement

Table 4: Advantages and disadvantages of different reporter outputs (Yagi, 2007).

Green fluorescent protein (GFP) has a molecular weight of about 27 kDa, and was originally isolated from the jellyfish *Aequorea victoria*. It has since become a major

tool for investigating a broad range of biological questions, as it is easily measured using ultraviolet (UV) light, fluorescence microscopy or fluorescence-activated cell sorting (FACS) and is applicable to many systems. Its crystal structure (Yang *et al*., 1996) revealed a highly stable β-barrel protecting the chromophore inside the cylinder (Figure 17).

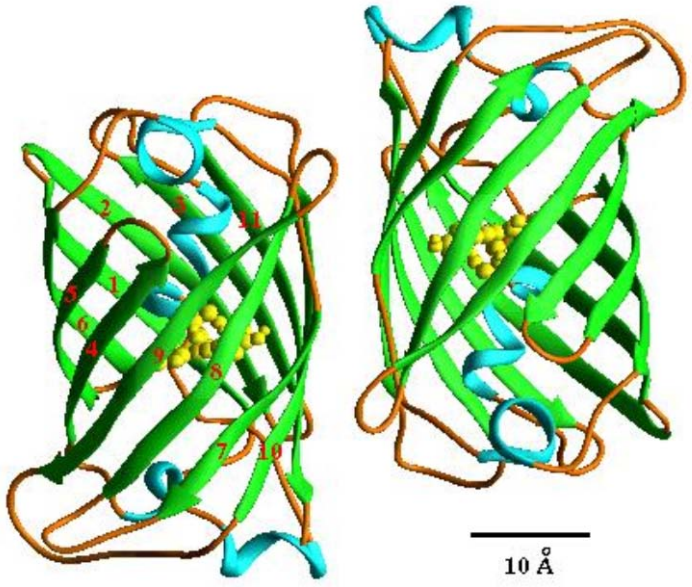

Figure 17: The structure of green fluorescent protein. The β-barrel structure, made of 11 β-sheets, protects the chromophore located near the geometric centre of the barrel. Adapted from (Yang *et al.*, 1996).

Before fluorescent proteins are able to fluoresce, they must undergo maturation. This involves the folding of the protein into a β-barrel structure and then the formation of the chromophore inside the β-barrel. The chromophore formation in GFP is a self-catalytic process involving the catalytic residues Arg96 and Glu222. The chromophore is made up of the residues Ser65, Tyr66 and Gly67, which are

cyclised in a process requiring the presence of molecular oxygen (Reid and Flynn, 1997) shown below (Figure 18).

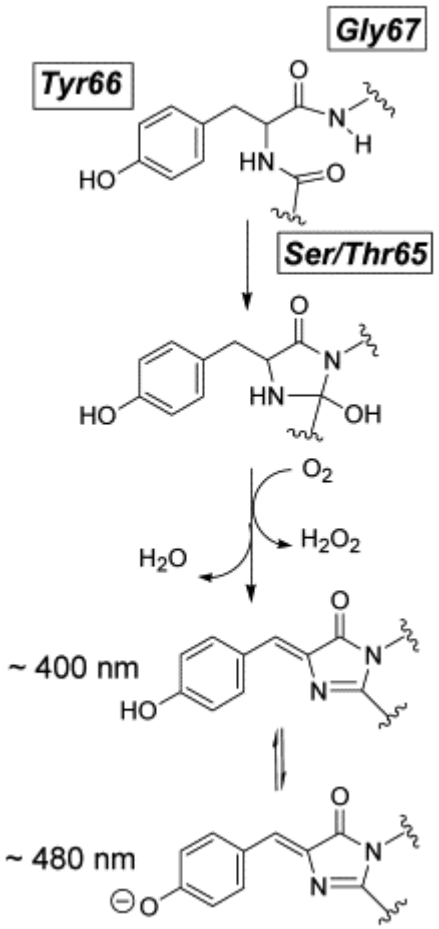

Figure 18: The formation of the chromophore in wild-type GFP. The product is in equilibrium between the protonated state, which absorbs light at ~400 nm, and the unprotonated state, which absorbs light at ~480 nm (Sniegowski *et al.*, 2005b).

The time required for fluorescent proteins to mature and become fluorescent must be taken into account when using them as an output for a biosensor. The optimum temperature for maturation is 28°C and wild-type GFP can take ~4 hrs to mature (Sniegowski *et al.*, 2005a). However, since GFP was first used as a molecular

tool, there have been mutational experiments to alter its characteristics and today we have an extremely wide selection of different coloured fluorescent proteins with different properties to choose from (Day and Davidson, 2009;Muller-Taubenberger and Anderson, 2007). The properties that are altered in these mutant GFP proteins include a shift in the excitation and emission spectra of the chromophore, a brighter fluorescence output and faster maturation rates.

Wild-type GFP has two different absorbance peaks, a major one at 395 nm and a minor one at 470 nm, and a single emission peak at 509 nm. A mutation in the chromophore, Y66W, results in ECFP (Patterson *et al.*, 2001) which shifts the excitation and emission spectra towards the blue end (Figure 20). A mutation in the structural part of the protein, T203Y, results in EYFP (Patterson *et al.*, 2001) with a spectrum shift 20 nm towards the red end (Figure 20). Other mutations in these proteins have resulted in faster maturing variants that can produce fluorescence after 30 min – 1 hr. While no GFP variant has been produced with an emission maxima any longer than 529 nm (Miyawaki *et al.*, 2003), a GFP-like protein was discovered in *Anthozoa* (corals) which has filled in this gap at the red end of the spectrum (Figure 19). This protein family has undergone similar mutational studies as the GFP derivatives had in the past to try to optimise the performance of the fluorescent proteins for use in molecular biology. Red fluorescent proteins such as TagRFP (Novagen) have been developed that have fast maturation times and produce bright fluorescence.

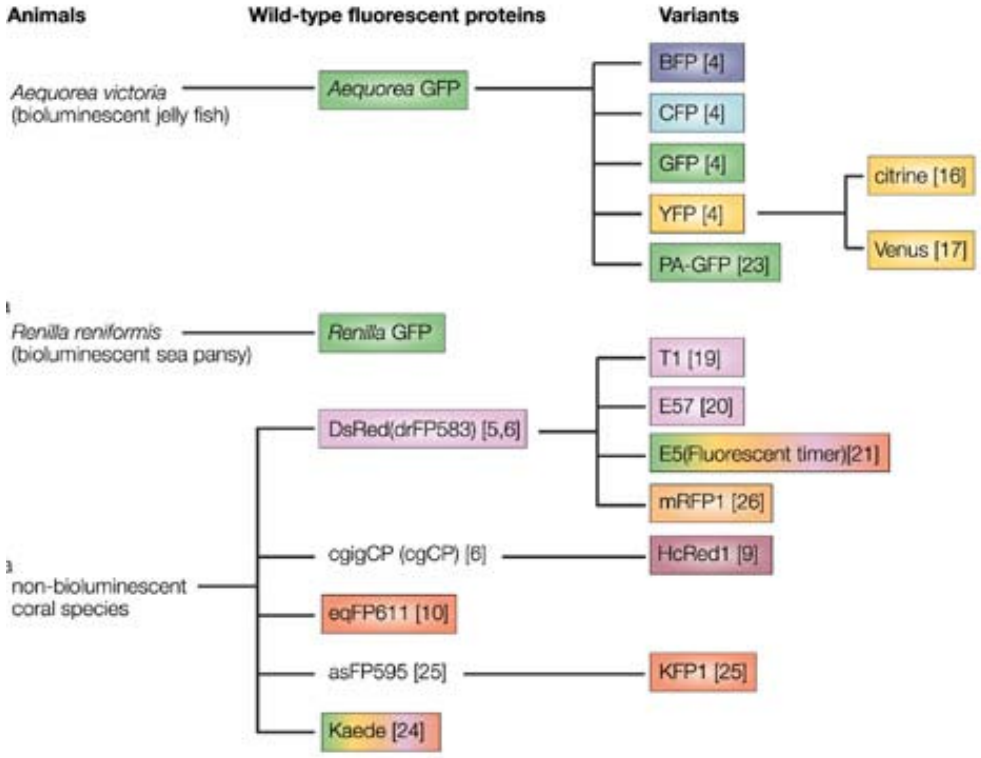

Figure 19: The origins of different fluorescent proteins that are now available for use in molecular biology. The colours represent the emission wavelength of the fluorescent proteins available from each group. (Adapted from (Miyawaki *et al.*, 2003)).

The combination of GFP and GFP-like (mRFP-1 derived) proteins and their many mutant forms have given rise to a whole range of different coloured fluorescent proteins with excitation and emission spectra discrete enough and far enough apart to allow expression and visualisation of multiple different fluorescent proteins in the same cell (Figure 20).

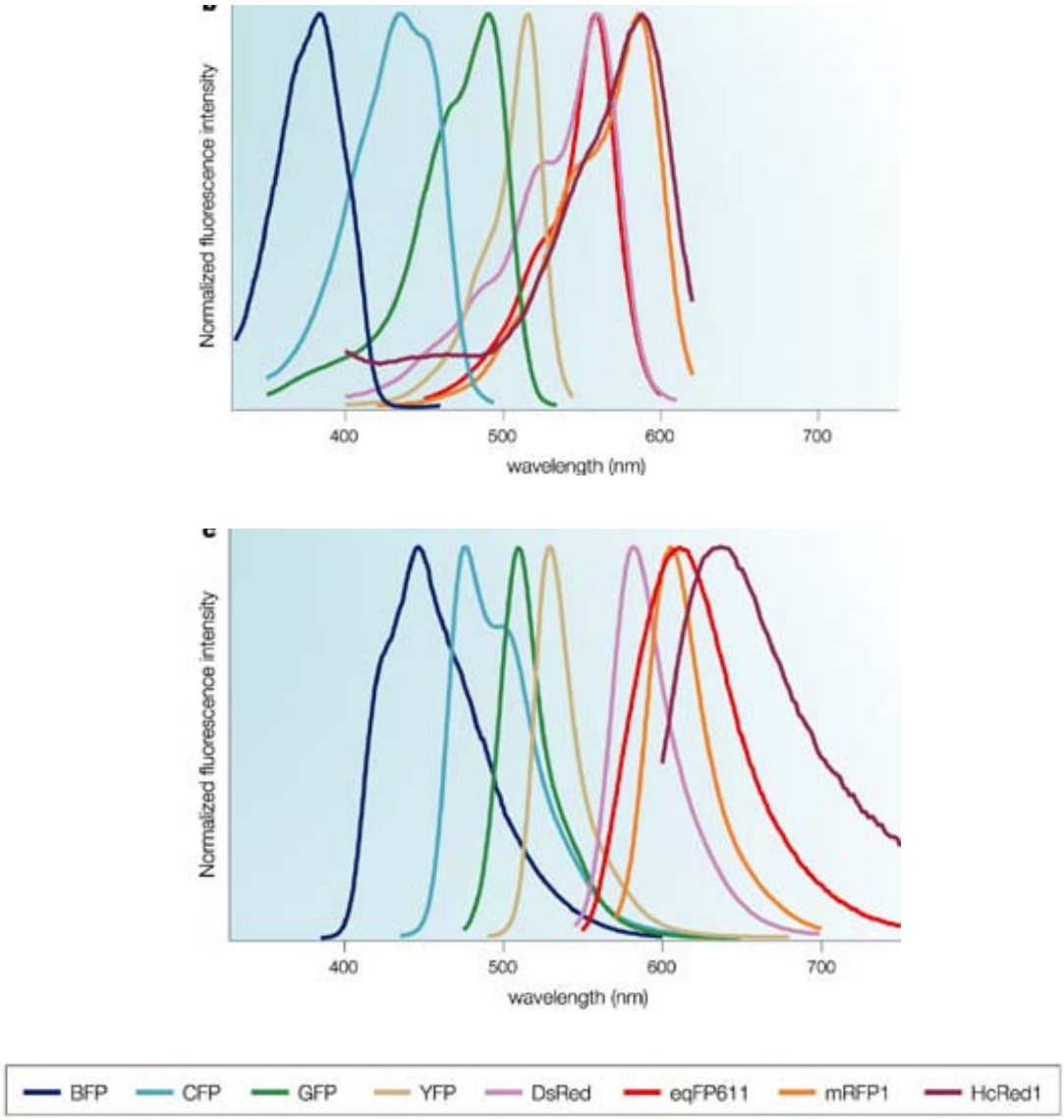

Figure 20: The excitation (top) and emission (bottom) spectra of a range of fluorescent proteins currently available. (Adapted from (Miyawaki *et al.*, 2003).

1.10 Our Biosensor

As we were aiming to create a biosensor with multiple different outputs to the same analyte, an inducible system was chosen for the reporter plasmid. Therefore, we required a promoter that would activate the expression of our

reporter in the presence of the analyte and preferably come from a system where different strength promoters for the same inducer exist in nature.

As our biosensor will produce a signal by transcriptional activation of a reporter gene, we focussed on analytes that are able to cross the membrane, initially focussing on the *E. coli* Ntr system (see section 1.7.3) as it was well characterised and met the requirement of having naturally occurring promoters of different strengths. Later in the project we explored alternative options for control of the constitutively active NtrC* transcriptional activator that enabled the output of the reporter plasmid to be linked to other analytes that can be sensed by other one component and two component systems from bacteria.

Fluorescent proteins were selected for the multi-fluorescent reporter as these provide a more stable output over time than an enzymatic reaction and would allow potential applications such as localisation of chemicals being sensed. This would not be possible with bioluminescence, colormetric or electrical biosensors as the reaction is often short lived or the genes required are simply too large to combine multiple reporter systems in the same plasmid. The use of fluorescent proteins will allow a single reporter plasmid to contain multiple output genes without becoming too large to be inserted into the host bacterium. This represents the best way to obtain a ratiometric output from the biosensor.

The reporter was put on a plasmid as we required a high signal to noise ratio to allow simple measurement of the output and any differences in copy number and

number of regulator proteins in each cell was accounted for by taking ratios of the different output proteins, effectively normalising for these issues as well as removing the need for measuring cell number or the number of live cells present in the measurement well. The expression of the constitutively active transcriptional activator (NtrC*) from a separate activator plasmid removed any issues of titrating out the activator with too many binding sites in the biosensor cell.

1.11 Aims

To recap, the aims of this project are as follows. More detail can be found in section 1.3.

1. Construct multi-fluorescent output (MFO) plasmid
2. Test MFO responses to nitrogen limitation in *E. coli*
3. Test MFO responses to nitrogen limitation in other species
4. Decouple MFO response from nitrogen limitation by creation of constitutively active transcriptional activator (NtrC*)
5. Determine if ratiometric output from MFO provides enhanced detection of analyte output for a biosensor

2. Materials and Methods

The strains (Table 5) and plasmids (Table 6) used in this study are listed below.

Strain	Species	Description	Source
XL-1 Blue	*E. coli*	General purpose cloning strain. recA1, endA1, gyrA96, thi-1, hsdR17, supE44, relA1 lac, F´ *pro*AB l*ac*IqZΔM15 Tn10 Tet^r	Stratagene
C43	*E. coli*	Expression strain. F^- ompT gal dcm $hsdS_B(r_B^- m_B^-)$(DE3)	Lucigen
RP437	*E. coli*	Wild-type K12 derivative, F-, thr-1, araC14, leuB6(Am), fhuA31, lacY1, tsx-78, λ-, eda-50, hisG4(Oc), rfbC1, rpsL136(strR), xylA5, mtl-1, metF159(Am), thiE1	(Parkinson and Houts, 1982)
S17-1λpir	*E. coli*	pInd4 mobilising strain used for conjugation. TpR SmR recA, thi, pro, hsdR-M+RP4: 2-Tc:Mu: Km Tn7 λpir	(Penfold and Pemberton, 1992)
WS8N	*R. sphaeroides*	Spontaneous naladixic acid resistant strain of the wild-type WS8	(Sockett and Armitage, 1991)
KT2440	*P. putida*	Wild-type laboratory strain	(Bagdasarian *et al.*, 1981)

Table 5: Strains used in this study

Plasmid	Description	Source
pUC19	General plasmid for cloning. Ampicillin resistance, pBM1 origin.	Pharmicia
pACYCDuet-1	Dual expression plasmid. Chloramphenicol resistance, p15A origin.	Novagen
pInd4	*R. sphaeroides* IPTG inducible expression plasmid with MCS to allow the creation of C-terminally 6 x his-tagged proteins. Kanamycin resistance	(Ind *et al.*, 2009)
pBMTBX-4	Broad host-range expression plasmid for gram negative hosts. Tetracycline resistance, bhr origin.	(Prior *et al.*, 2010)
pME6031	Shuttle vector for *Pseudomonas* strains. Tetracycline resistance. p15A and pSV1 origin.	(Heeb *et al.*, 2000)
pQE60	Expression plasmid with MCS to allow the expression of C-terminally 6 x his-tagged proteins. Ampicillin resistance.	QIAGEN
pQE60:*yfp*	A pQE60 plasmid containing the *yfp* gene.	Gift, G. Wadhams
pMFO-1	A pUC19 plasmid containing the MFO	This Study

	reporter.	
pMFO-2	A pInd4 plasmid containing the MFO reporter.	This Study
pMFO-3	A pME6031 plasmid containing the MFO reporter.	This Study
pAraNtrC*	A pBMTBX-4 plasmid containing the *NtrC** gene.	This Study
pLacNtrC*	A pACYCDuet-1 plasmid containing the *NtrC** gene.	This Study
pEYFP-N1	An ampicillin resistance plasmid that contains the *eyfp* gene for N-terminal tagging.	ClonTech
pECFP-N1	An ampicillin resistance plasmid that contains the *ecfp* gene for N-terminal tagging.	ClonTech
pTagRFP	A kanamycin resistance plasmid that contains the *tagrfp* gene for N-terminal tagging.	Evrogen

Table 6: Plasmids used in this study

2.1 Growth conditions

The antibiotic concentrations used for selective growth in *E. coli* (Table 7), *R. sphaeroides* (Table 8) and *P. putida* (Table 9) are shown below.

Antibiotics	Stock concentration (mg/ml)	Working concentration (µg/ml)
Ampicillin	100	100
Kanamycin	25	25
Chloramphenicol	30	30
Tetracycline	5	20
Streptomycin	25	25

Table 7: The antibiotic concentrations used for selective growth in *E. coli.*

Antibiotics	Stock concentration (mg/ml)	Working concentration (µg/ml)
Kanamycin	25	25
Naladixic acid	50	25

Table 8: The antibiotic concentrations used for selective growth in *R. sphaeroides.*

Antibiotics	Stock concentration (mg/ml)	Working concentration (µg/ml)
Tetracycline	5	25

Table 9: The antibiotic concentrations used for selective growth in *P. putida.*

2.1.1 Liquid cultures of *E. coli*

Liquid cultures of *E. coli* were grown in LB (Appendix A2.1), containing the appropriate antibiotics at 37°C with orbital shaking at 225 rpm.

2.1.2 Agar plates for *E. coli* growth

Agar plates for *E. coli* growth were made from LB (Appendix A2.1), solidified with 2% agar containing the appropriate antibiotics. The plates were incubated overnight at 37°C.

2.1.3 96 well plate growth of *E. coli*

Liquid cultures of *E. coli* were grown in LB (Appendix A2.1), containing the appropriate antibiotics at 37°C with orbital shaking at 225 rpm overnight. 1.5 µl of the overnight culture was used to inoculate 148.5 µl of fresh growth media in a black, clear bottom, 96-well plate with lid (Corning), to give a total volume in each well of 150 µl. The plates were then transferred to a fluorescence plate reader and incubated at 37°C. Measurements of the YFP, CFP and RFP fluorescence, along

with OD_{600}, were taken every 20 mins for 24 hrs with orbital shaking at 50 rpm in between the measurements.

2.1.4 Aerobically grown *R. sphaeroides*

R. sphaeroides were grown under aerobic conditions in succinate medium (Appendix A2.2) containing naladixic acid, and incubated at 30°C with orbital shaking at 225 rpm.

2.1.5 Photoheterotrophically grown *R. sphaeroides*

Photoheterotrophically grown *R. sphaeroides* were grown in succinate medium (Appendix A2.2) containing naladixic acid in full, sealed universals and incubated at 30 °C under light of intensity 50 µM m^{-2} s^{-1}.

2.1.6 Agar plates for *R. sphaeroides*

Agar plates for *R. sphaeroides* were made of LB (Appendix A2.1), solidified with 2% agar, containing nalidixic acid and other antibiotics as appropriate. The plates were incubated at 30°C.

2.1.7 96 well plate growth of *R. sphaeroides*

A culture of *R. sphaeroides* was grown photoheterotrophically (Section 2.1.5) for 48 hrs. 1.5 µl of this culture was used to inoculate 148.5 µl of fresh growth media in a black, clear bottom, 96-well plate with lid (Corning, to give a total volume in

each well of 150 µl. The plates were then transferred to a fluorescence plate reader and incubated at 30°C. Measurements of the YFP, CFP and RFP fluorescence as well as OD_{700} were taken every 20 mins for 24 hrs with orbital shaking at 50 rpm in between the measurements.

2.1.8 Liquid cultures of *P. putida*

Liquid cultures of *P. putida* were grown in LB (Appendix A2.1) containing the appropriate antibiotics at 28°C with orbital shaking at 225 rpm.

2.1.9 Agar plates for *P. putida*

Agar plates for *P. putida* growth were made from LB (Appendix A2.1) solidified with 2% agar, containing the appropriate antibiotics. The plates were incubated at 28°C.

2.1.10 96 well plate growth of *P. putida*

Liquid cultures of *P. putida* (Section 2.1.8) were grown overnight. 1.5 µl of the overnight culture was used to inoculate 148.5 µl of fresh growth media in a black, clear bottom, 96-well plate with lid (Corning), to give a total volume in each well of 150 µl. The plates were then transferred to a fluorescence plate reader and incubated at 28°C. Measurements of the YFP, CFP and RFP fluorescence as well as OD_{600} were taken every 20 mins for 24 hrs with orbital shaking at 50 rpm in between the measurements.

2.1.11 Storage of bacterial strains

Strains were grown to stationary phase in appropriate media under aerobic conditions, with appropriate antibiotics. These cultures were then mixed in a ratio of 3:2 with sterile glycerol (50% v/v) in a cryotube (VWR). Tubes containing culture were flash frozen in liquid nitrogen and stored immediately at – 80°C.

2.2 Genetic techniques

2.2.1 Preparation of *E. coli* genomic DNA

E. coli genomic DNA was extracted using a genomic DNA extraction kit (Sigma) following the manufacturer's protocol.

2.2.2 DNA gel electrophoresis on agarose gels

DNA fragments were separated by size by gel electrophoresis in a gel, prepared by dissolving 0.8% to 2% (w/v) agarose (Roche) in ½ x TBE (Appendix A2.15). 5 x DNA loading dye (Appendix A2.12) was added to each sample prior to loading on the gel. The gels were run at 100 – 150 V and then stained in ethidium bromide solution (1 ng/ml) for 10 minutes. The gel image was obtained using the Gel-Doc system (Bio-Rad) with UV light illumination. Gel blocks containing single bands of separated DNA were cut from the gels for use in further experiments

2.2.3 Extraction of DNA from TBE agarose gels

The Qiaquick Gel Extraction Kit (Qiagen) was used to extract DNA from the bands cut from the gels following the manufacturer's protocol.

2.2.4 Standard PCR for cloning

PCR reactions to obtain DNA for cloning purposes were carried out using *pfu* DNA polymerase (Promega) and specifically designed primers (Sigma), with the following reaction mixture:

1 µl of template DNA

1µl of each of two appropriate primers at 100 µM

5 µl of 2.5 mM dNTP mix (Invitrogen)

5 µl of 10 x *pfu* polymerase buffer (Promega)

1 µl of *pfu* DNA polymerase (Promega)

In some cases DMSO was added at up to 2% (v/v). The reaction mixture was made up to 50 µl with MilliQ. The tubes were then placed in a PCR machine (Techne TC-3000) with the following program:

10 mins at 98°C	
2 mins at 98°C	)
1.5 mins at appropriate annealing temperature	} Repeated 30 times
2 mins (per kb of DNA) at 72°C	)
5 mins at 72°C	
Hold at 4°C	

2.2.5 Splicing Overlap Extension PCR

Splicing overlap extension PCR was used to insert the mutations D54E and S160F into the *ntrC* gene of *E. coli,* in order to create the constitutively active form of the protein, NtrC* (Section 5.3). In this particular case, internal primers B and C contain a mismatch in addition to the complementary regions in order to generate the amino acid change in the final product. A summary of the basic principle is shown below (Figure 21). Where this method was used to create mutations, the mutation is represented by *.

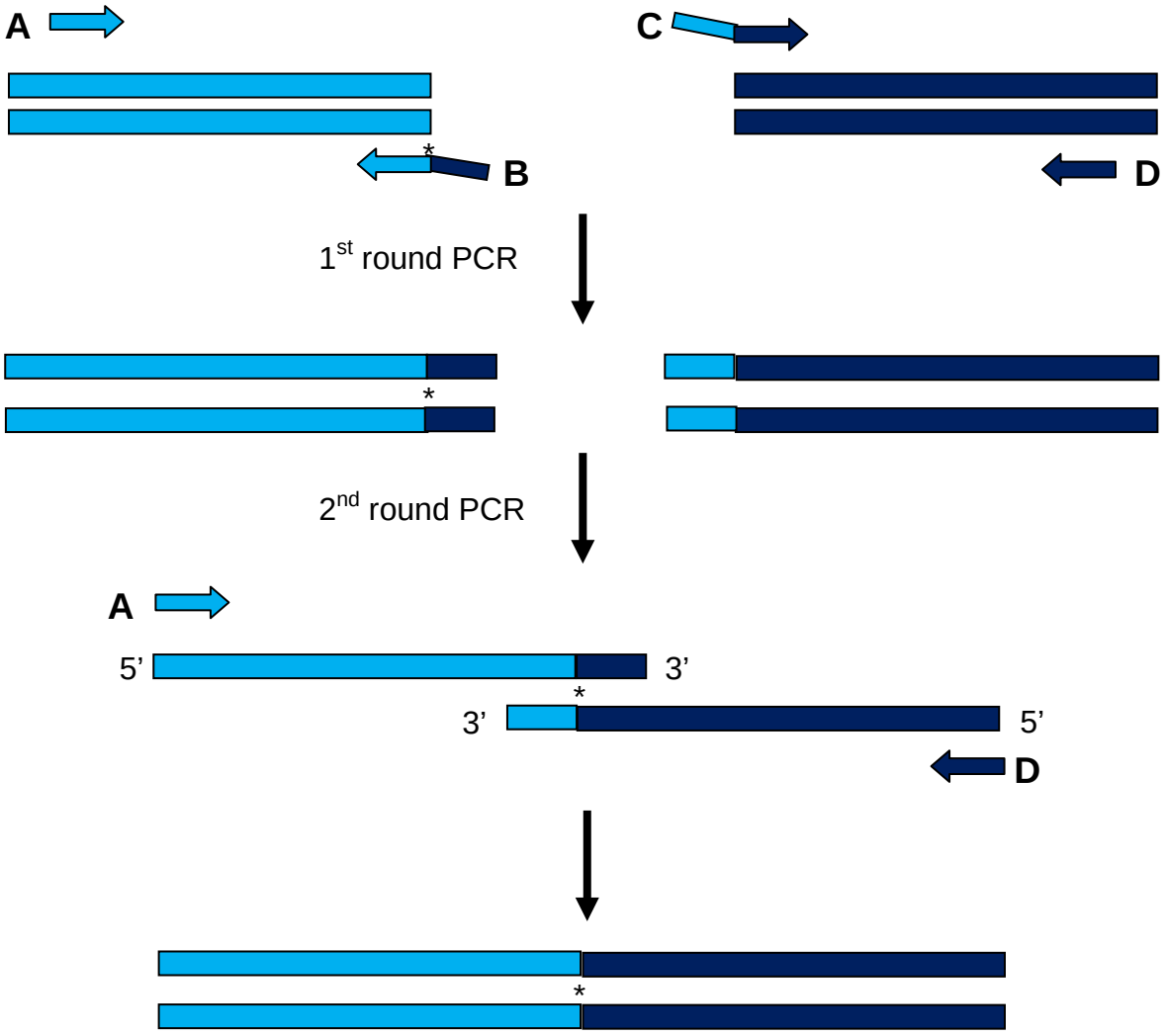

Figure 21: The principle of the splicing overlap-extension PCR technique. The two reactions in the first round of PCR use the standard PCR protocol (Section 2.2.4). In the second round of PCR 1 µl of each of the first round products was used as the template DNA for the reaction. The mutation is represented by * for the creation of NtrC*.

2.2.6 Three fragment splicing overlap-extension PCR

A variation of splicing overlap-extension PCR (Section 2.2.5) was used to fuse the promoter, fluorescent protein gene and the terminator together for each of the individual reporters in the MFO reporter fragment.

2.2.7 Restriction enzyme digests

For plasmid digests the following protocol was used:

4 µl of plasmid DNA

2 µl of appropriate 10X enzyme buffer (NEB)

1 µl of restriction enzyme 1 (NEB)

1 µl of restriction enzyme 2 (NEB)

The reaction mixture was made up to 20 µl with MilliQ and the tubes were incubated for 2 hrs at 37°C.

For PCR product digests the following protocol was used:

40 µl of PCR product

5 µl of appropriate 10X enzyme buffer (NEB)

2 µl of restriction enzyme 1 (NEB)

2 µl of restriction enzyme 2 (NEB)

The reaction mixture was made up to 50 µl with MilliQ and the tubes were incubated for 2 hrs at 37°C.

2.2.8 Dephosphorylation of plasmid DNA

Restriction enzyme digests of the plasmid were heated to 85°C for 20 mins then cooled to 4°C and then 1 µl (10 units) of calf intestinal alkaline phosphatase (NEB) was added. The mixture was incubated for 1 hr at 37°C.

2.2.9 DNA ligation mix

For ligations, the following protocol was used:

8 µl of purified and digested plasmid DNA

24 µl of purified and digested insert DNA

5 µl of 10X T4 DNA ligase buffer (NEB)

2 µl of T4 DNA ligase (NEB)

The reaction mixture was made up to 50 µl with MilliQ and the tubes were incubated overnight at 16°C.

2.2.10 Quick ligation mix

For quick ligations the following protocol was used:

1 µl of purified and digested plasmid DNA

3 µl of purified and digested insert DNA

5 µl of 2X Quick Ligase buffer (NEB)

1 µl of Quick Ligase (NEB)

The reaction mixture was incubated at 25°C for 10 mins.

2.2.11 Multi-fragment DNA ligation

The standard ligation procedure was adapted for this project to achieve a four-fragment ligation.

8 µl of digest fragment 1

8 µl of digest fragment 2

3 µl of 10X T4 DNA ligase buffer (NEB)

1 µl of T4 DNA ligase (NEB)

10 µl of MilliQ

Incubate for 30 mins at room temperature; then add:

8 µl of digest fragment 3

2 µl of 10X T4 DNA ligase buffer (NEB)

1 µl of T4 DNA ligase (NEB)

9 µl of MilliQ

Incubate for 30 mins at room temperature; then add:

2 µl of digested vector

2 µl of 10X T4 DNA ligase buffer (NEB)

1 µl of T4 DNA ligase (NEB)

15 µl of MilliQ

Incubate overnight at room temperature.

2.2.12 Chemically competent *E. coli* cells

Chemically competent *E. coli* cells were prepared (Sambrook and Russell, 2001). *E. coli* cells were grown to an OD_{600} of 0.4 – 0.5, and harvested by centrifugation at 1000 g for 10 min, at 4°C. The cell pellet was re-suspended in 2 ml of ice cold TFBI (Appendix A2.10), a further 14 ml of TFBI was then added before incubating on ice for 1 hr. The cells were then centrifuged at 2000 g, for 10 min, at 4°C. The cell pellet was re-suspended in 2 ml of ice cold TFBII (Appendix A2.11) and

separated into 200 µl aliquots in pre-chilled cryogenic tubes (VWR). Tubes were flash frozen in liquid nitrogen and stored immediately at – 80°C.

2.2.13 Heat-shock transformations

For transformations, competent cells were defrosted on ice for 20 mins. DNA was added and the cells incubated on ice for a further 1 hr. Cells were subjected to heat shock at 42°C for 2 mins, followed by incubation on ice for 2 min. 800 µl of LB was added and the mix was incubated at 37°C for 1 – 2 hrs. Transformed *E. coli* were selected for by plating onto LB agar plates containing the appropriate antibiotics.

2.2.14 Electro-competent *Pseudomonas* cells

Electro-competent *Pseudomonas putida* were made by harvesting cells by centrifugation of 1.5 ml of an overnight culture in a refrigerated bench top centrifuge at 6900 g for 4 min at 4°C and re-suspending cells in ice cold 10% (v/v) glycerol in 1 mM HEPES by the following method:

Centrifuge for 4 min at 6900 g

Pour off supernatant and re-suspend in 1 ml glycerol/HEPES

Repeat previous two steps

Centrifuge for 4 min at 6900 g

Pour off supernatant and re-suspend in 100 µl glycerol/HEPES

Store on ice until use

2.2.15 Plasmid preparation

Plasmids were extracted from cells using either mini-prep or midi-prep kits (Qiagen) depending on the final quantities required, following the manufacturer's protocol.

2.2.16 DNA sequencing

Plasmid DNA was sequenced at the in-house GeneService DNA sequenceing facility on an AB1377 Sequencer (Applied Biosystems) with the use of BigDye^{TM} dye terminators (PE Biosystems). DNA sequences were aligned using the Staden PreGap Linux plug-in (Staden *et al.*, 2000) and inspected in the Clone Manager 9 (Operations, 2004) software package.

2.2.17 Conjugation

Plasmid DNA cannot be inserted into *R. sphaeroides* cells by transformation, as they cannot be made competent. Introduction of plasmids is achieved by conjugation, which involves direct transfer of plasmid DNA from one bacterium to another via pili (Penfold and Pemberton, 1992). The pInd4 plasmid has been designed to allow transfer by bacterial conjugation. *E. coli* S17-λpir cells that contained the plasmid to be conjugated were grown to early exponential growth phase and mixed gently in a ratio of 1:10 with stationary phase *R. sphaeroides* cells. Cell mixtures were pipetted onto a 0.2 µM nitrocellulose filter that had been

placed on a 2% LB agar plate. Cells were incubated overnight at 30°C and re-suspended in LB media (Appendix A2.1) and spread plated onto 2% LB agar containing appropriate antibiotics.

2.2.18 Electroporation

To transform *P. putida* cells, 3 µl of DNA was added to 100 µl of electro-competent *P. putida* cells (Section 2.2.14). The cell/DNA mix was transferred to an ice cold 1 mm electroporation cuvette (Cell Projects). Electroporation was carried out using a Bio-Rad electroporator set to 1.75 mV and 200 Ohm. The cells were immediately mixed with 1 ml SOC media (Appendix A2.8) and incubated for 2 hrs at 28 °C with orbital shaking at 225 rpm. Cells were then spread plated onto selective 2% LB agar containing appropriate antibiotics.

2.3 Phenotypic techniques

2.3.1 Epifluorescence microscopy

The system used to acquire epifluorescence images of reporter cells was a Nikon Eclipse TE200 microscope with Differential Interference Contrast (DIC) enhancement, and a mercury lamp with a CFP/GFP/RFP filter set (Chroma, Rockingham, VT). The images were acquired using a Hamamatsu ORCA-ER CCD camera and the Simple PCI 6 software package (Nikon).

Before imaging, cell samples were immobilised on a thin layer of 1.2% agarose in water.

2.3.2 Image analysis

The epifluorescence microscopy images were analysed using the built-in analysis tool in the Simple PCI 6 software package. Regions of interest were defined by setting the lower threshold of the YFP channel of the RGB image to 300 and taking the mean fluorescence within these defined areas for the YFP, CFP and RFP channels.

2.3.3 Plate reader measurements

Growth curve and fluorescence intensity measurements were taken simultaneously using a Tecan M200 plate reader. Excitation and emission wavelengths are shown in Table 10 and OD wavelengths for growth curves are shown in Table 11. The excitation slit width was 9 nm and the emission slit width was 20 nm.

Measurements were taken in a Corning 3603 black, clear bottom, 96-well microplate with the cover on. Plates were incubated at an appropriate temperature for host cell growth with orbital shaking at 50 rpm. Each well contained 150 µl of culture. Gain values were set between 100 and 220 for analysis of host strains under nitrogen limiting conditions, depending on the host strain used. The gain values were set to 120 for all three fluorescence channels for the measurements of fluorescence output from the NtrC* induction experiments.

Biological repeats refer to experiments on different days where cells were grown from a frozen stock each time. Each biological repeat contains 6 technical well repeats for the plate reader measurement.

Fluorescent protein	Excitation ± 9 (nm)	Emission ± 20 (nm)
YFP	508	540
CFP	442	485
RFP	555	584

Table 10: Excitation and emission wavelengths used to measure fluorescence intensities.

Bacterial species	OD wavelength (nm)
E. coli	600
P. putida	600
R. sphaeroides	700

Table 11: OD wavelengths for growth curves

2.3.4 Plate reader data analysis

The data obtained from these experiments was corrected for cell number by dividing each of the fluorescence intensities by the OD_{600} at the same time point. The total fluorescence levels were then calculated by subtracting the corrected fluorescence readings of control cells containing empty plasmids from the corrected fluorescence readings from the reporter strains.

In the case of the ratio of CFP to RFP (Section 5.6) the fluorescent intensities for each of the reporter channels was corrected for cell number and background fluorescence from control cells was subtracted in the same way as described above. The maximum fluorescent output for each concentration of IPTG added was calculated by averaging the last 20 time points where the response curves had reached a plateau and normalising these as a percentage of maximum by dividing each output by the maximum level of fluorescent output seen from each reporter. The ratio was then taken by dividing the normalised value of CFP by the normalised value of RFP for each concentration of IPTG.

3. Reporter Plasmid

3.1 Introduction

The aim of this section was to increase the sensitivity and detection range for a particular input that can generate a response from a bacterial biosensor. To achieve this aim, we constructed a multi-fluorescent output (MFO) plasmid. Promoters were chosen that are activated by the same transcriptional regulator, but at different levels relative to each other. The promoters of genes involved in the Nitrogen-regulated (Ntr) response (Merrick and Edwards, 1995;Reitzer, 2003) were chosen as they naturally exhibit varying strength depending on the number and quality of response regulator (NtrC-P) binding sites that they have (Section 1.7.3).

The Ntr system is responsible for regulating gene expression in response to nitrogen availability in the environment; operons under its control are activated when nitrogen is limiting in the environment. For this experiment the promoters of *glnALG* (Magasanik, 1989;Reitzer *et al.*, 1989), *glnHPQ* (Claverie-Martin and Magasanik, 1991) and *nac* (Atkinson *et al.*, 2002) operons were chosen; these are high, medium and low affinity respectively and are all bound by NtrC-P with varying affinities (Figure 22).

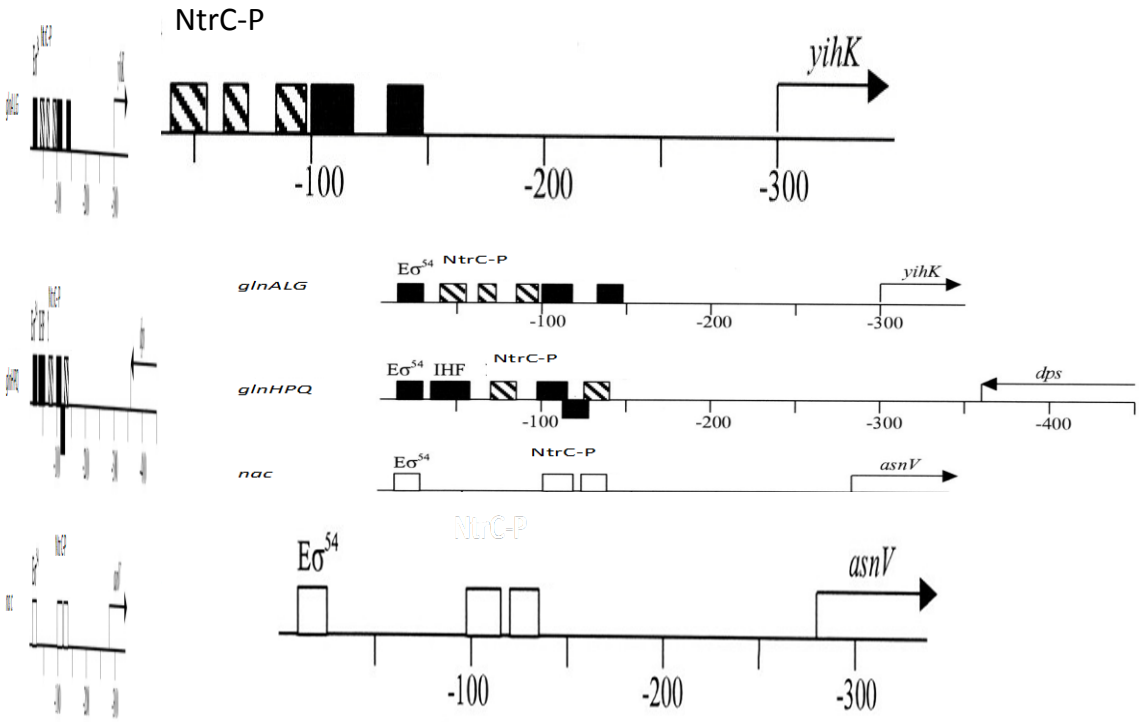

Figure 22: The NtrC-P binding sites in the promoter regions of the *glnALG*, *glnHPQ* and *nac* operons of *E. coli*. High affinity NtrC-P binding sites are shown as filled boxes, medium affinity as striped boxes and low affinity as clear boxes. (Reitzer and Schneider, 2001).

The promoters of the *glnALG*, *glnHPQ* and *nac* operons were chosen as they were the best characterised of the Ntr promoters in the literature (Atkinson *et al.*, 2002;Leigh and Dodsworth, 2007;Reitzer and Schneider, 2001) and the most likely to give the improved range of fluorescence output by allowing activation of the high affinity promoter at low concentrations of NtrC-P and when the concentration of NtrC-P increases and becomes saturating for this promoter the medium and low affinity promoters will become activated.

The fluorescent proteins EYFP, ECFP and TagRFP were selected for the multi-fluorescent reporter as these minimise any overlap in the excitation and emission spectra (Figure 23) allowing detection using fluorescence microscopy or a fluorescence plate reader.

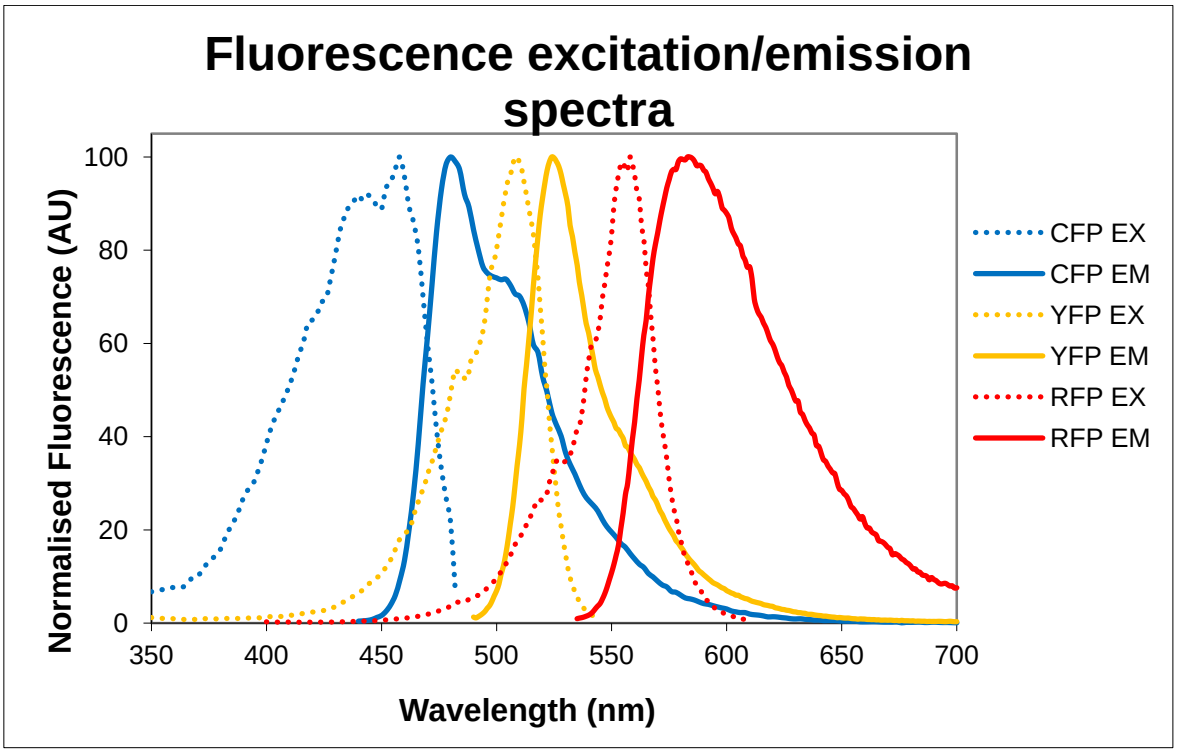

Figure 22: The normalised excitation (EX) and emission (EM) spectra for YFP, CFP and RFP. (Data obtained from Evrogen).

The high, medium and low affinity promoters were coupled to three different fluorescent protein genes; *yfp, cfp and rfp,* respectively and the *E. coli rrnB* terminator (Orosz *et al.*, 1991) was added to the end of each construct to prevent read through in transcription. RFP was selected for the low affinity promoter as this reporter is likely to produce the least fluorescence signal and will therefore

require a longer exposure time to observe the signal. The longer wavelength light used to excite RFP will be the least damaging to the cell (Frigault *et al.*, 2009). YFP was selected for the high affinity promoter as this then provides the biggest spectral difference between adjacent reporters on the plasmid.

3.2 Construction of a multi-fluorescent reporter plasmid, pMFO-1

To create a genetic fusion between the three promoters and the different fluorescent protein encoding genes it was important to design a cloning strategy to ensure that the promoters were lined up with the fluorescent protein genes. The natural ATG start codon was mimicked so that the ATG start codon of the corresponding fluorescent protein gene was in the same position relative to the promoter. To prevent read-through from one reporter to the next, the *E. coli rrnB* transcriptional terminator (Orosz *et al.*, 1991) (Section 1.11) was inserted after each of the fluorescent protein genes. In addition to this, the three reporters were inserted in the order, low, medium and then high affinity so that any read-through would not affect the output of the reporter as the subsequent reporter gene on the plasmid would already be activated.

Three fragment overlap-extension PCR (Section 2.2.6) was used to create each section of the multi-fluorescent reporter plasmid. All primer sequences are listed in Appendix A1.1. In the first round of PCR primers were designed to amplify the individual parts of the reporter fragment. For the high affinity reporter, P*glnALG* was amplified from *E. coli* genomic DNA using primers fmdA and fmdB. In a separate reaction, *yfp* was amplified from the plasmid pEYFP-N1 using primers

fmdC and fmdD and in a third reaction the *rrnB* terminator sequence was amplified from *E. coli* genomic DNA using primers fmdE and fmdF. In the second round of PCR the products from the first round, the *glnALG* promoter, *yfp* gene and *rrnB* terminator, were used as the template and annealed, extended and amplified using the external primers fmdA and fmdF. Fusion of the three fragments was made possible as the internal primers, fmdB/fmdC and fmdD/fmdE, were designed to have complementary regions. The product of this reaction was the high affinity reporter, P*glnALG-yfp-rrnB.*

The medium affinity reporter was made in a similar way. In this case P*glnHPQ* was amplified from *E. coli* genomic DNA using primers fmdG and fmdH. In a separate reaction, *cfp* was amplified from the plasmid pECFP-N1 using primers fmdI and fmdJ and in a third reaction the *rrnB* terminator sequence was amplified from *E. coli* genomic DNA, using primers fmdK and fmdL. In the second round of PCR the products from the first round, the *glnHPQ* promoter, *cfp* gene and *rrnB* terminator, were used as the template and annealed, extended and amplified using the external primers fmdG and fmdL. Fusion of the three fragments was made possible as the internal primers, fmdH/fmdI and fmdJ/fmdK, were designed to have complementary regions. The product of this reaction was the medium affinity reporter, P*glnHPQ-cfp-rrnB*.

The low affinity reporter was made in a similar way. In this case P*nac* was amplified from *E. coli* genomic DNA using primers fmdM and fmdN. In a separate reaction, *rfp* was amplified from the plasmid ptagRFP using primers fmdO and

fmdP and in a third reaction, the *rrnB* terminator sequence was amplified from *E. coli* genomic DNA, using primers fmdQ and fmdR. In the second round of PCR the products from the first round, the *nac* promoter, *rfp* gene and *rrnB* terminator, were used as the template and annealed, extended and amplified using the external primers fmdM and fmdR. Fusion of the three fragments was made possible as the internal primers, fmdN/fmdO and fmdP/fmdQ, were designed to have complementary regions. The product of this reaction was the low affinity reporter, P*nac-rfp-rrnB*.

A four-fragment ligation (Section 2.2.11) was used to generate the construct of the multi-fluorescent reporter plasmid (Figure 24). The three products from the overlap-extension PCR reactions were cloned into a pUC19 vector. The P*glnALG-yfp-rrnB* overlap-extension PCR product was digested with *Xba*I and *Hin*dIII (primer fmdA was designed so that it was flanked with an *Xba*I site and primer fmdF was designed so that it was flanked by a *Hin*dIII site). The P*glnHPQ-cfp-rrnB* overlap extension PCR product was digested with *Kpn*I and *Xba*I (primer fmdG was designed so that it was flanked with a *Kpn*I site and primer fmdL was designed so that it was flanked with an *Xba*I site). The P*nac-rfp-rrnB* overlap extension PCR product was digested with *Eco*RI and *Kpn*I (primer fmdM was designed so that it was flanked with an *Eco*RI site and primer fmdR was designed so that it was flanked with a *Kpn*I site). The pUC19 vector was digested with *Eco*RI and *Hin*dIII and then de-phosphorylated (Section 2.2.8). The digested P*nac-rfp-rrnB* fragment was mixed with the digested P*glnHPQ-cfp-rrnB* fragment and left to ligate for 30 mins, then the digested P*glnALG-yfp-rrnB* fragment was added and left to ligate for 30 mins, finally the digested pUC19 vector was added

and left to ligate overnight. The resulting product was the 6226 bp pMFO-1 multi-fluorescent reporter plasmid (Figure 24).

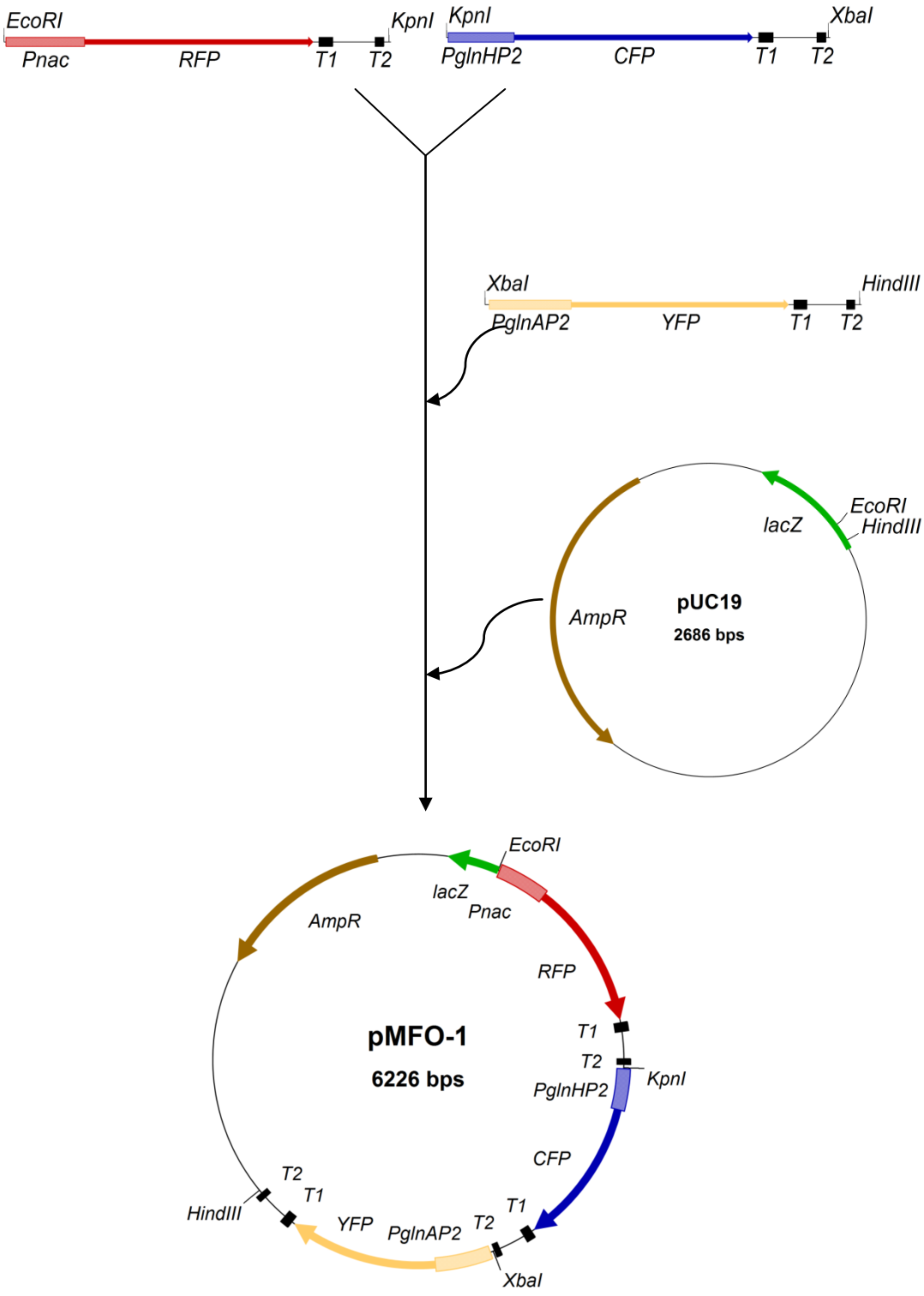

Figure 23: Four fragment ligation strategy for construction of the reporter plasmid, pMFO-1. The RFP fragment was digested with *Eco*RI and *Kpn*I, the CFP fragment was digested with *Kpn*I and *Xba*I, the YFP fragment was digested with *Xba*I and *Hin*dIII, and the pUC19 plasmid was digested with *Eco*RI and *Hin*dIII. The digested RFP and CFP fragments were allowed to ligate before the addition of the digested YFP fragment and finally the digested pUC19 plasmid (Section 2.2.11). This forms the pMFO-1 construct to report nitrogen limitation in the environment.

3.3 Testing of the pMFO-1 reporter plasmid

To test the output of the different strength reporters the pMFO-1 plasmid was transferred into *E. coli* XL-1 blue cells and grown to stationary phase in LB. This is predicted to deplete the nitrogen from the media and hence the activation of transcription of the fluorescent protein genes on the reporter plasmid. When the nitrogen levels in the growth media become limiting the nitrogen sensor, NtrB/C, indirectly detects the low level of nitrogen and this results in an increase in the amount of activated NtrC-P in the cell. The increase in the level of phosphorylated NtrC in the cell should activate transcription from the three reporter genes in a stepwise manner, with the YFP being expressed first, followed by the CFP, and finally the RFP.

An overnight culture of the reporter strain was diluted 1 in 100 into 150 µl of fresh LB (Appendix A2.1) containing appropriate antibiotics. The fluorescent output of the reporter was measured in a fluorescence plate reader in a 96 well plate. Measurements were taken of the three fluorescent channels (YFP, CFP and RFP) as well as the OD_{600} every 20 mins with shaking in between each set of measurements (For a detailed protocol see Methods section 2.3.3). *E. coli* XL-1 Blue cells containing the empty pUC19 plasmid were used as a control for background fluorescence of the growth medium and the cells. The results of these experiments are shown for the YFP channel (Figure 25), the CFP channel (Figure 26), and the RFP channel (Figure 27) after normalisation for cell number and subtraction of fluorescence from control cells.

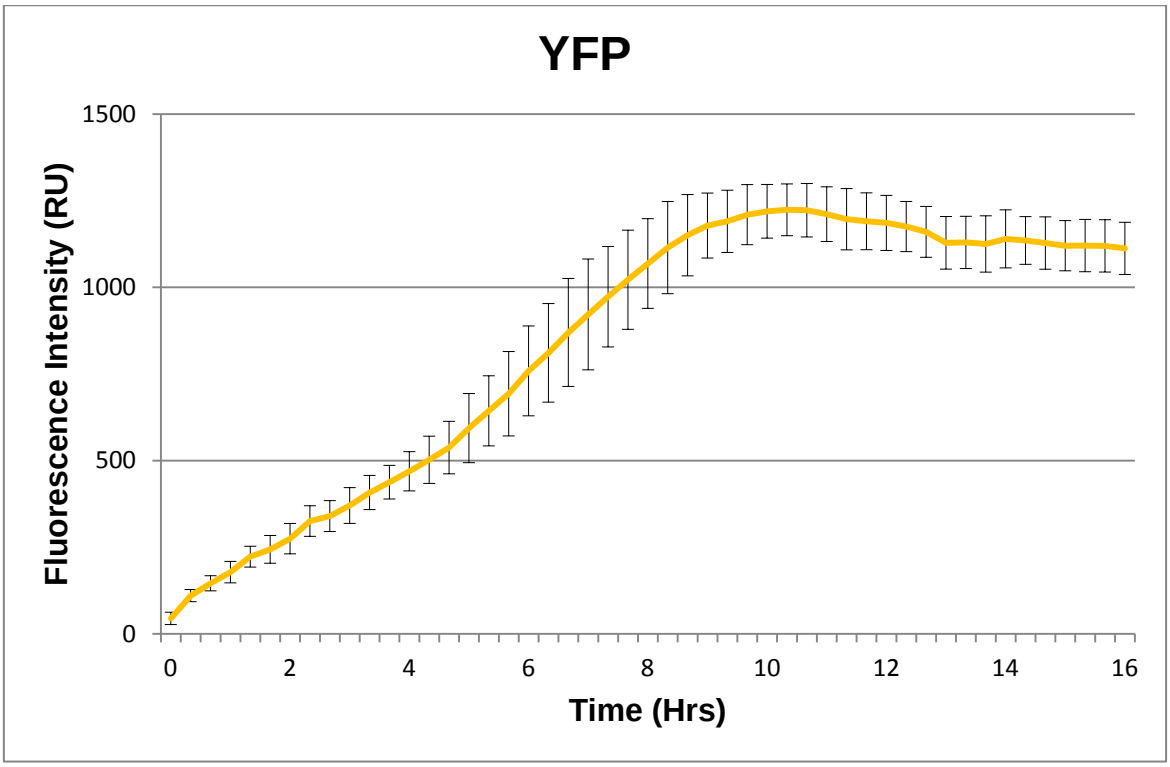

Figure 24: The level of YFP expression in the reporter strain, XL-1 pMFO-1, in response to nitrogen depletion. The results have been corrected for cell number by dividing the raw fluorescence data by the OD_{600} from the same time point, followed by the subtraction of values obtained for non-fluorescent control cells, containing an empty pUC19 plasmid. Error bars represent the standard error of the mean obtained from three biological repeats.

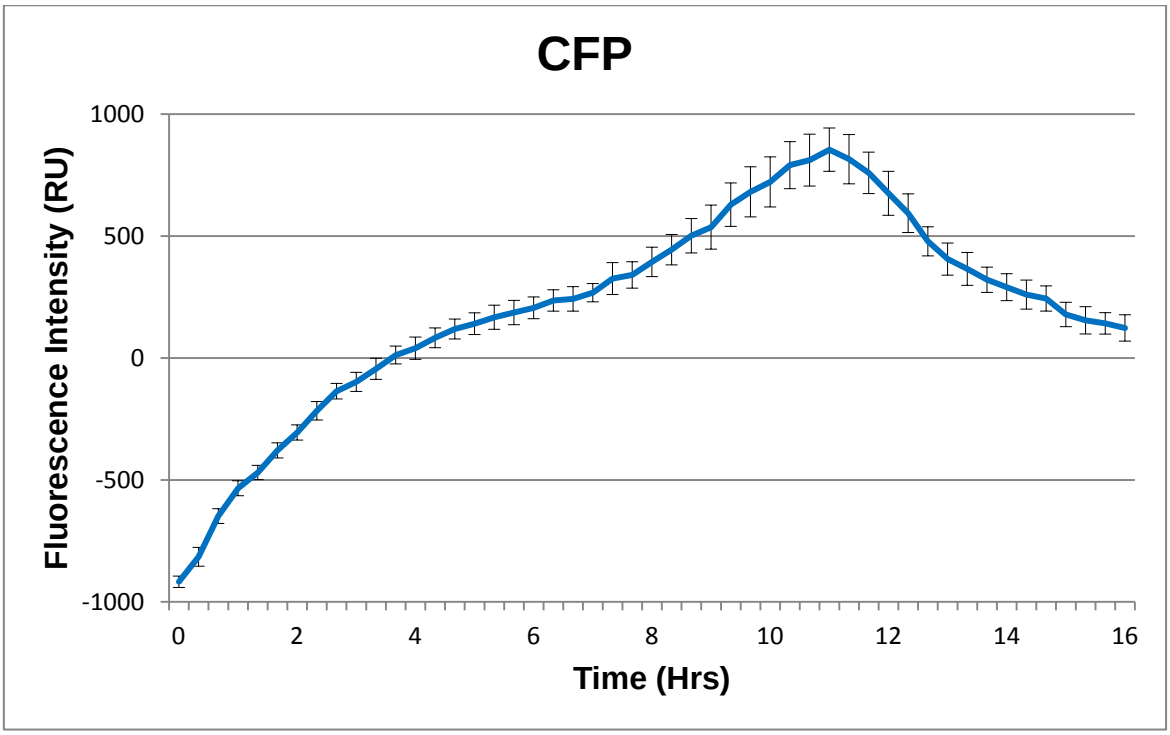

Figure 25: The level of CFP expression in the reporter strain, XL-1 pMFO-1, in response to nitrogen depletion. The results have been corrected for cell number by dividing the raw fluorescence data by the OD_{600} from the same time point, followed by the subtraction of values obtained for non-fluorescent control cells, containing an empty pUC19 plasmid. Error bars represent the standard error of the mean obtained from three biological repeats.

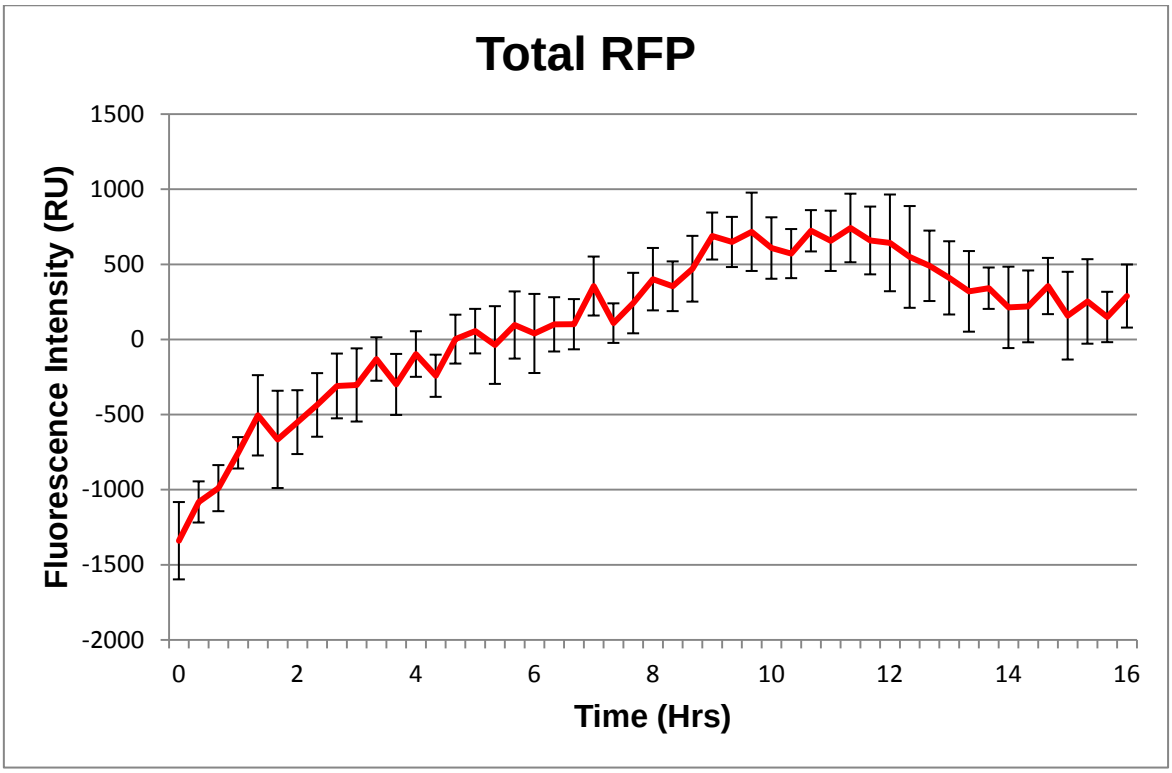

Figure 26: The total level of RFP expression in the reporter strain, XL-1 pMFO-1, in response to nitrogen depletion. The results have been corrected for cell number by dividing the raw fluorescence data by the OD_{600} from the same time point, followed by the subtraction of values obtained for non-fluorescent control cells, containing an empty pUC19 plasmid. Error bars represent the standard error of the mean obtained from three biological repeats.

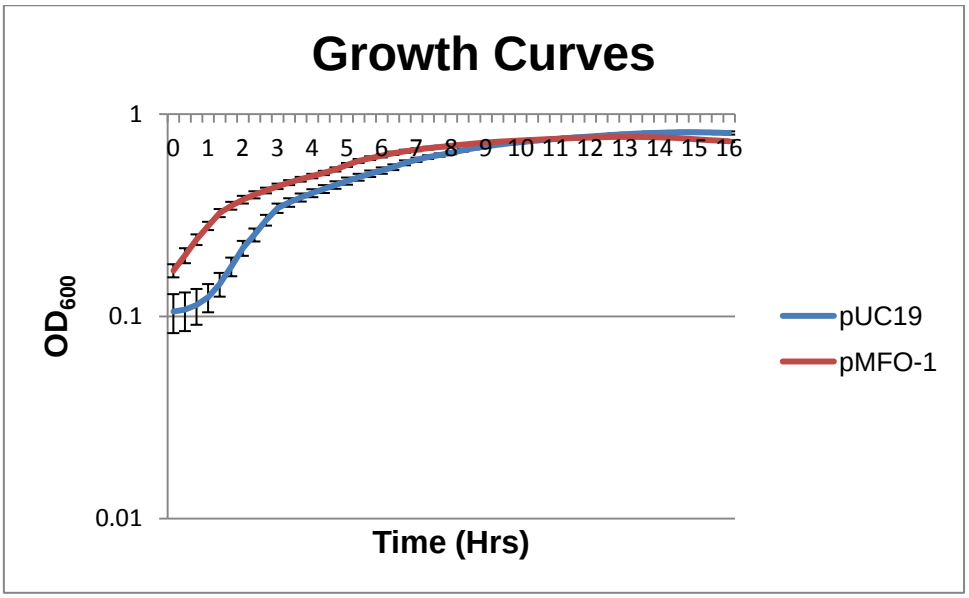

Figure 27: Growth curves of cells containing the pMFO-1 reporter plasmid and wild type control containing only the pUC19 backbone. Error bars represent standard deviation of the mean obtained from three biological repeats.

The XL-1 blue cells show a measurable response to the drop in nitrogen availability in the environment as the cells deplete the nitrogen in the LB media. A full response curve is seen from the YFP reporter, which is under the control of the high affinity promoter, however, the response appears to be constitutive expression from the promoter rather than an induction in response to nitrogen depletion. The CFP reporter shows negative values at the start, but increases steadily up to a maximum and then drops off. The RFP reporter is very noisy, due to the low level of signal from the low affinity promoter being hard to detect above the background auto fluorescence of the growth medium, but appears to follow a similar pattern to that seen for the CFP promoter. Growth curves are shown in Figure 28, however, the cells are clearly suffering from the high levels of protein expression under nitrogen limiting conditions as microscopy images show that the

cells are not dividing but forming long, filamentous cells (Figure 29), possibly due to the lack of ATP inhibiting cell division (Higashitani *et al.*, 1997). If the host cells are growing as filamentous cells then the OD_{600} measurements may not be an accurate reflection of cell number. Hence the normalised values for fluorescence may not be correct and the subtraction of control cell fluorescence may result in negative values. This may also explain the negative values seen after the background subtraction in the CFP and RFP channels. The difference in cell number between the control cells and the reporter cells combined with the low levels of signal obtained from the CFP and RFP channels may result in negative values after correction for cell number and subtraction of background fluorescence due to the higher error in plate reader measurements when fluorescence levels are low. In order to address these issues, a variety of different *E. coli* strains were tested to find a host that was robust enough to cope with the high demands of protein expression that the reporter plasmid puts on the cell. It is also possible that the large numbers of high affinity promoters on pMFO-1 are quenching all of the available NtrC-P in the cell before activation can take place at the medium and low promoters, accounting for the low signal to noise values obtained in these affinity channels. It is also important to maintain similar inoculum densities for the reporter cells and the control cells in future experiments to address the issue of negative values after subtraction of control cell auto fluorescence

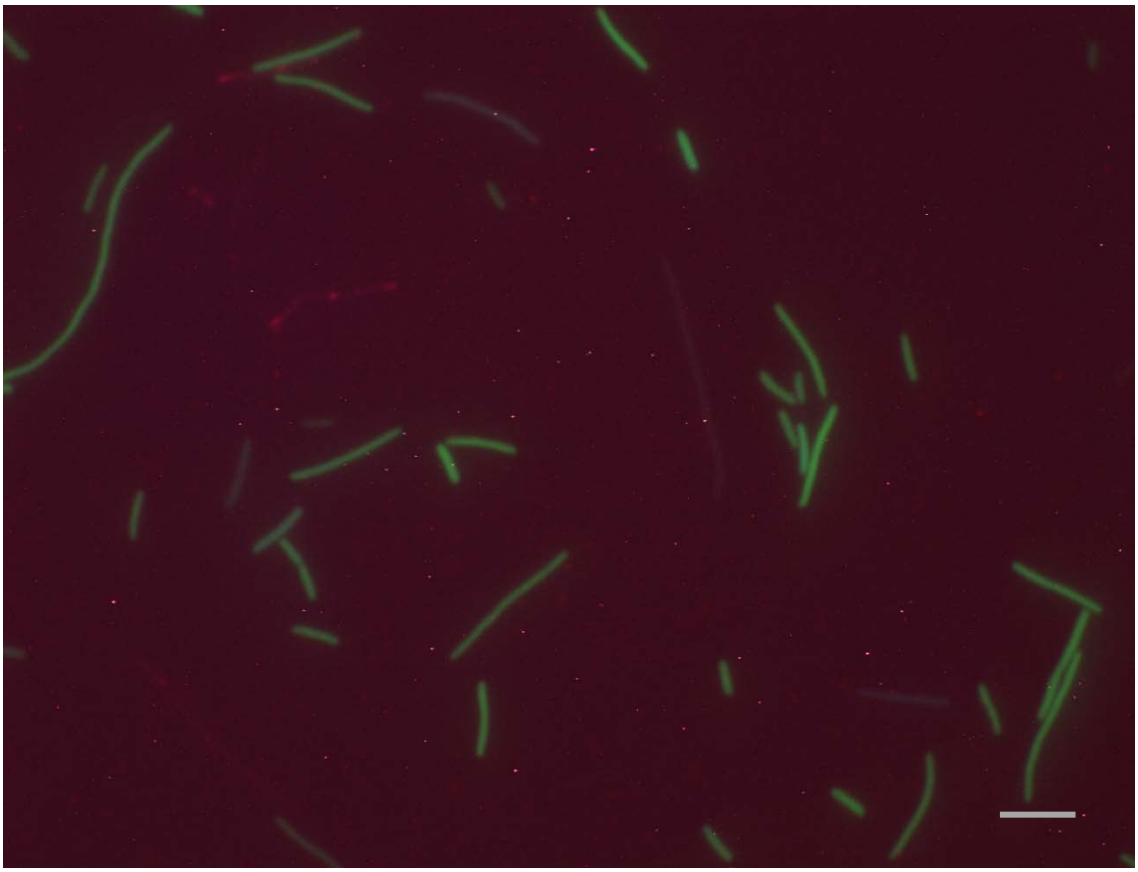

Figure 28: Epifluorescence image of XL-1 Blue cells containing the pMFO-1 plasmid after 24 hr growth in LB. This shows that the cells are struggling to divide and are growing as long, filamentous cells. Scale bar = 10 µM. See section 2.3.1 for microscope details.

3.4 Strain test

To try and reduce the potential adverse effect of high levels of protein production on the viability of the host cells, different strains of *E. coli* were tested for their ability to grow well and produce a good signal when transformed with a YFP expression vector (pQE60-*yfp*). This plasmid has the *yfp* gene under the control of the *lac* promoter so that high levels of expression can be achieved by the addition of IPTG. The plasmid was selected as it could be more easily transferred into the different strains than the pMFO-1 and would allow a high level of fluorescent

protein expression to be achieved to stress the cells. This would allow us to test if the high levels of protein expression were negatively affecting the cells or if it was another issue like titrating out the transcriptional activation proteins that reduced expression from the medium and low affinity promoters. The strains selected were a wild-type K-12 strain RP437, and a high protein expression strain, C43; these were compared to the XL-1 Blue strain currently used as the host strain. The cells were grown in overnight in LB, and diluted 1 in 100 into fresh LB containing either 0 µM or 200 µM IPTG. The growth curves (Figure 30) and YFP expression levels (Figure 31) were measured using a fluorescence plate reader. Fluorescence intensity and OD_{600} readings were taken every 20 mins for 24 hrs.

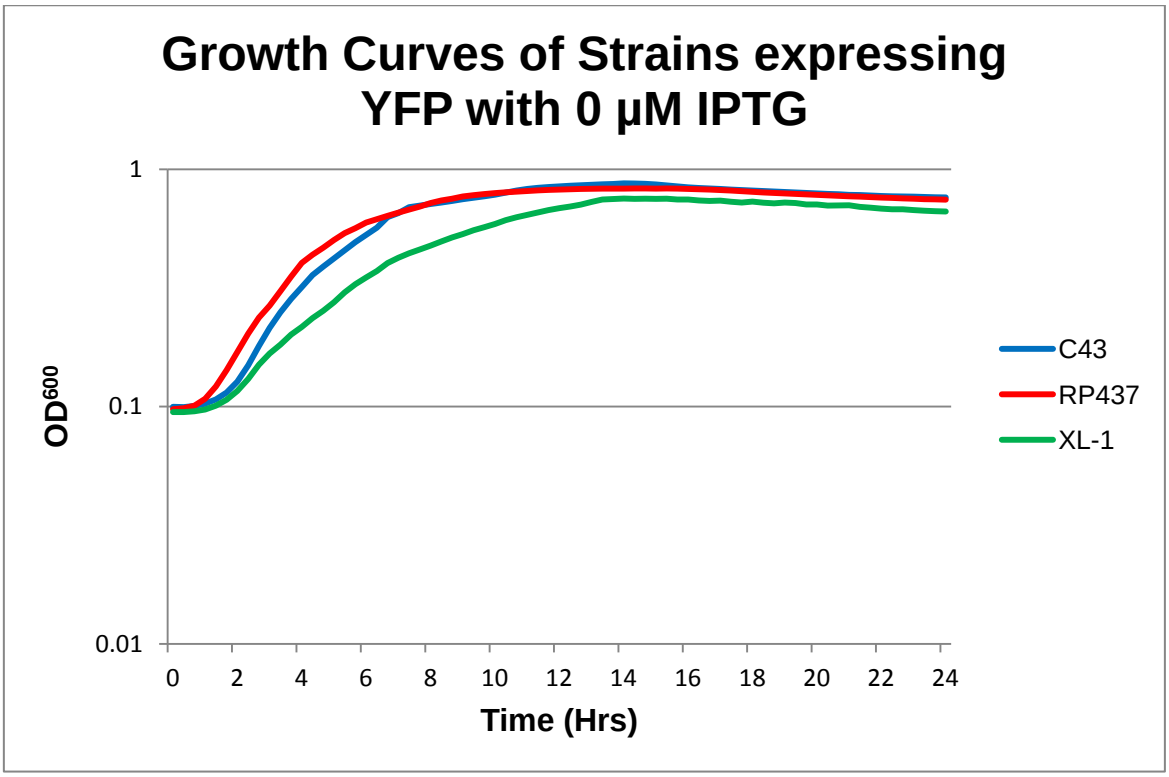

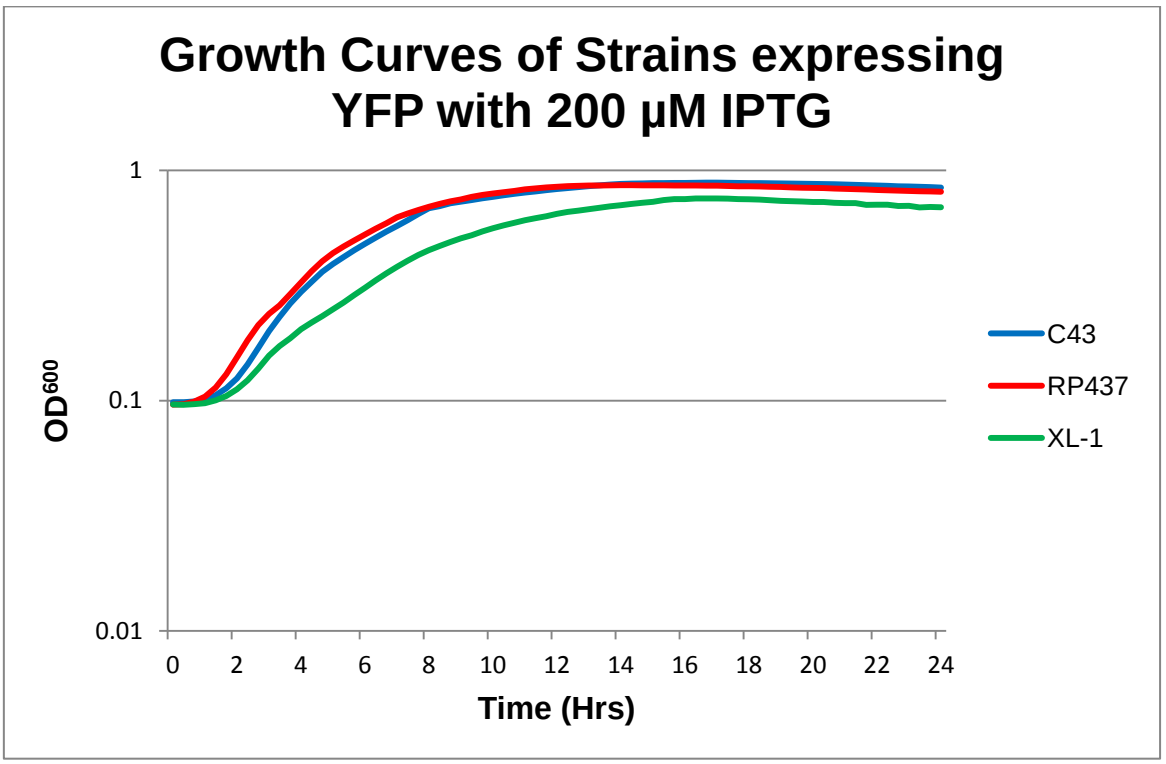

Figure 29: Growth curves of *E. coli* strains XL-1 blue, RP437, and C43 expressing YFP from an IPTG inducible plasmid (pQE60-*yfp*) in the presence and absence of the inducer IPTG.

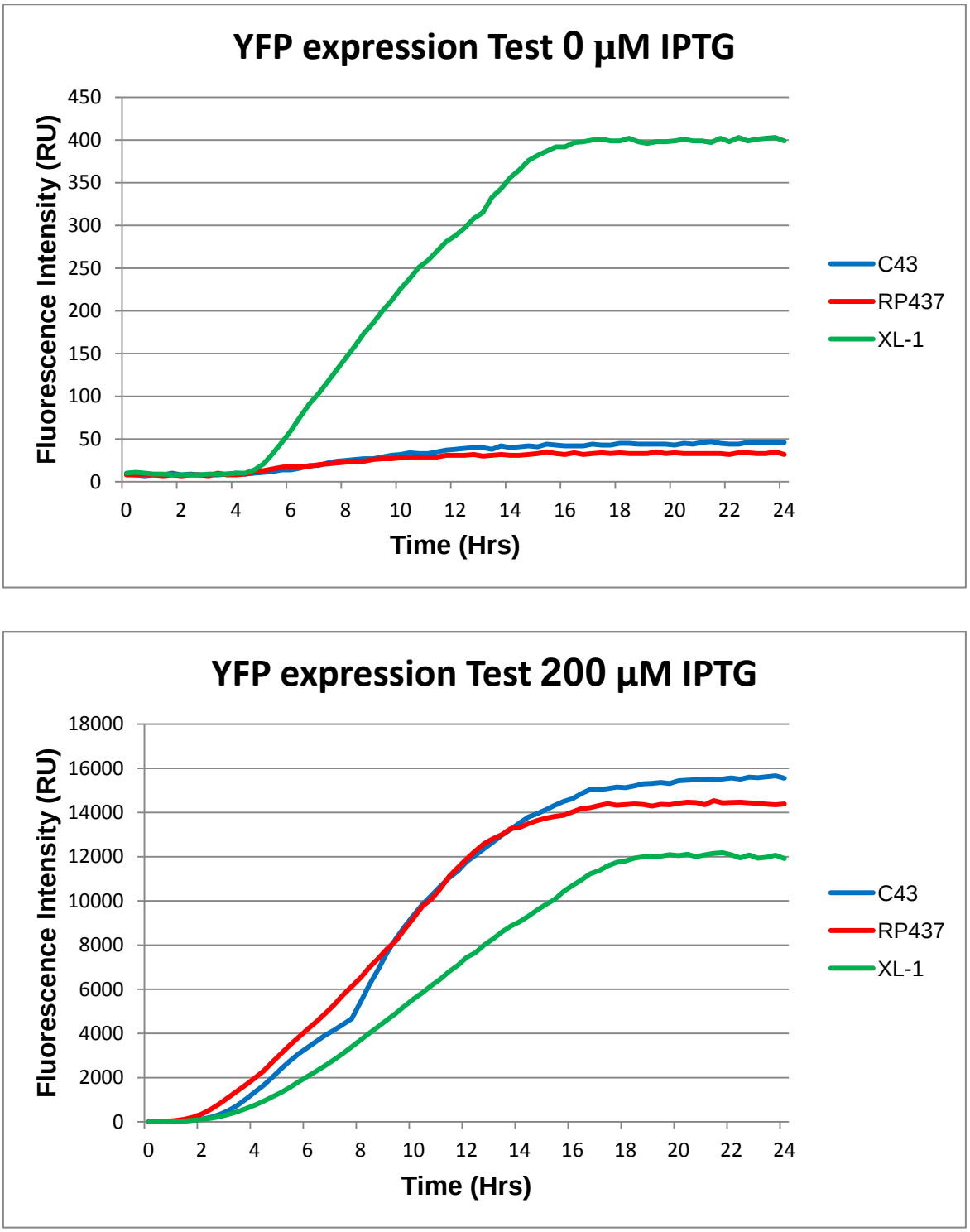

Figure 30: Fluorescence intensity of YFP produced by *E. coli* strains XL-1 blue RP437 and C43 containing an IPTG inducible plasmid (pQE60-*yfp)* in the presence and absence of IPTG. The results have been corrected for cell number by dividing the raw fluorescence data by the OD_{600} from the same time point, followed by the subtraction of fluorescence produced by non-fluorescent control cells containing an empty pQE60 plasmid that have been corrected in the same way as the YFP expression cells. Note the change in Y-axis scale between the two graphs.

The results show that even with very high levels of induction of YFP, the growth curves of all three *E. coli* strains are not adversely affected. This suggests that in the reporter strain XL-1 pMFO-1 there is either a higher demand on the protein expression of the cell or that the additional NtrC-P binding sites on the reporter plasmid are sequestering the cellular NtrC-P and as a result the cells are not able to properly regulate their nitrogen metabolism during nitrogen limitation.

The high protein expression strain, C43, was selected to use as the host for the MFO reporter plasmid as this showed the highest level of fluorescent output of YFP from the IPTG inducible expression plasmid at 22 hrs. This strain has been optimised to be more tolerant than the wild-type *E. coli* strain when expressing high levels of toxic proteins such as subunits of the F-ATPase (Miroux and Walker, 1996). These characteristics may be beneficial when producing large amounts of fluorescent protein as a biosensor host and we need the host cell to be as robust as possible to the demands put on it as a biosensor.

3.5 MFO in a lower copy plasmid, pMFO-2

In order to address the potential problem of the large number of high affinity promoters on the reporter plasmids sequestering all of the active NtrC-P in the cells, the reporter fragment was transferred from pMFO-1 into the lower copy number plasmid pInd4 (Ind *et al.*, 2009). The pMFO-1 reporter plasmid has a copy number of ~400 per cell and each of the YFP reporter fragments contains 2 high affinity binding sites, so there could potentially be ~800 high affinity binding sites per cell. The pInd4 plasmid has a copy number of ~100 per cell, thus reducing the

number of high affinity binding sites 4 fold. This will reduce the number of high affinity NtrC-P binding sites to ~200 in each cell and should allow the weaker promoters to become activated by NtrC-P before the cells run out of nitrogen in the growth medium and are unable to produce any more fluorescent proteins.

In any biosensor there is a trade off to be made between the higher copy number of a reporter giving greater signal strength but potentially titrating out the regulator and having physiological consequences for the host organism. In this case the final biosensor will not rely on host produced NtrC-P response to nitrogen limitation (See chapter 5) and therefore a 100 copy number plasmid was judged to be an acceptable compromise.

The MFO reporter fragment from pMFO-1 was transferred into the lower copy number plasmid pInd4 (8367 bp) (Ind *et al.*, 2009). The pMFO-1 plasmid was digested with *Eco*RI and *Hin*dIII to give a 3591 bp reporter fragment. pInd4 was also digested with *Eco*RI and *Hin*dIII, to give a linearised 6748 bp plasmid, and de-phosphorylated (Section 2.2.8). The reporter fragment was then ligated into pInd4 to produce the 10339 bp product, pMFO-2. The ligation mix was used to transform XL-1 Blue competent cells and successful colonies were picked and grown up for plasmid extraction.

The purified pMFO-2 plasmid was transferred into *E. coli* C43 competent cells and the resulting strain was grown in an overnight culture and diluted 1 in 100 into fresh LB containing appropriate antibiotics in a total volume of 150 µl. The culture

was transferred to a 96-well plate and the fluorescence output of the reporter plasmid measured every 10 minutes for 21 hours in a plate reader. The results were compared to C43 cells containing the pMFO-1 plasmid grown under the same conditions. The normalised and background corrected results for the YFP channel (Figure 32), CFP channel (Figure 33) and RFP channel (Figure 34) are shown below.

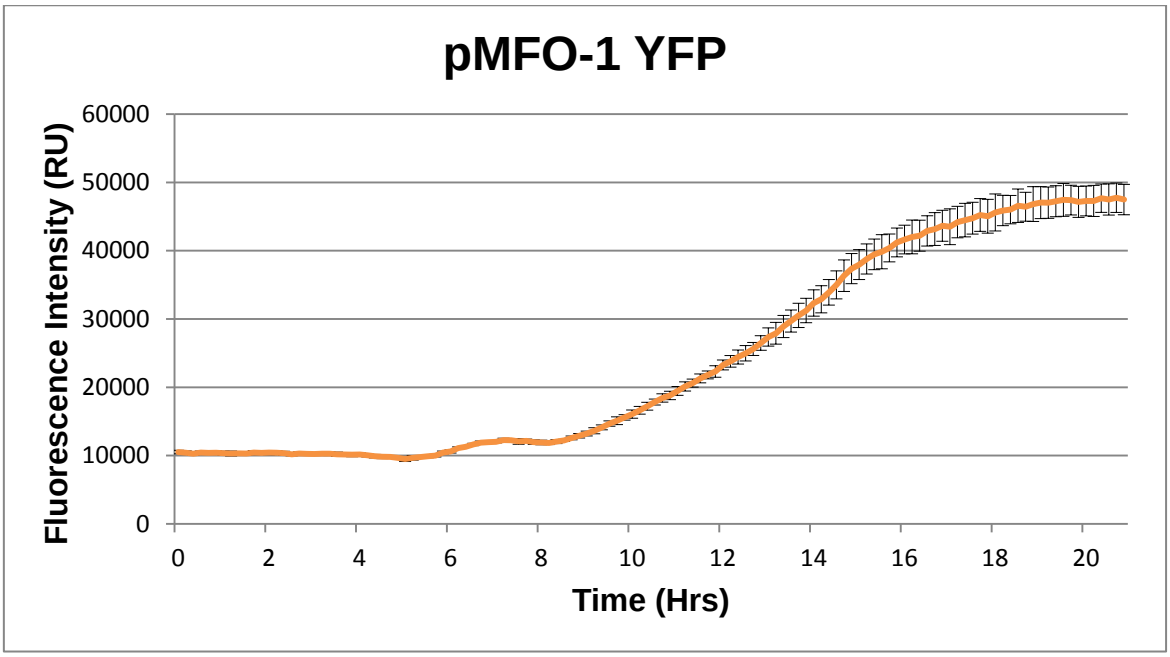

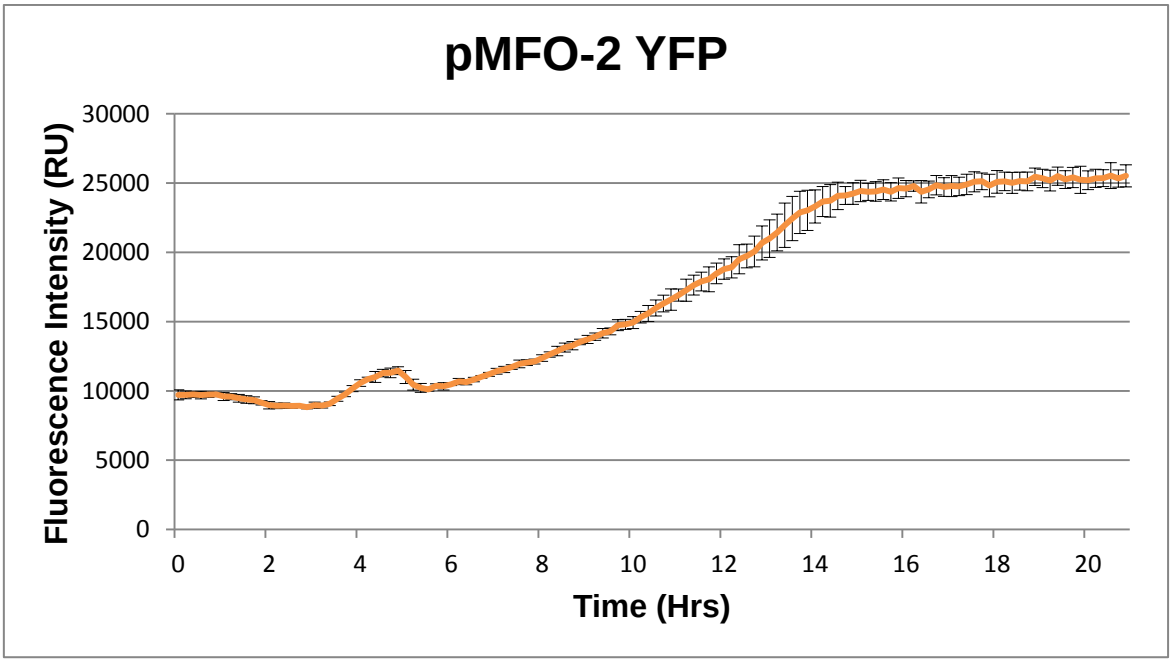

Figure 31: Total YFP fluorescence produced by *E. coli* C43 cells containing either pMFO-1 or pMFO-2. The results have been corrected for cell number by dividing the raw fluorescence data by the OD_{600} from the same time point, followed by the subtraction of fluorescence produced by non-fluorescent control cells containing either an empty pUC19 or pInd4 plasmid. The error bars represent the standard error of the mean for three biological repeats.

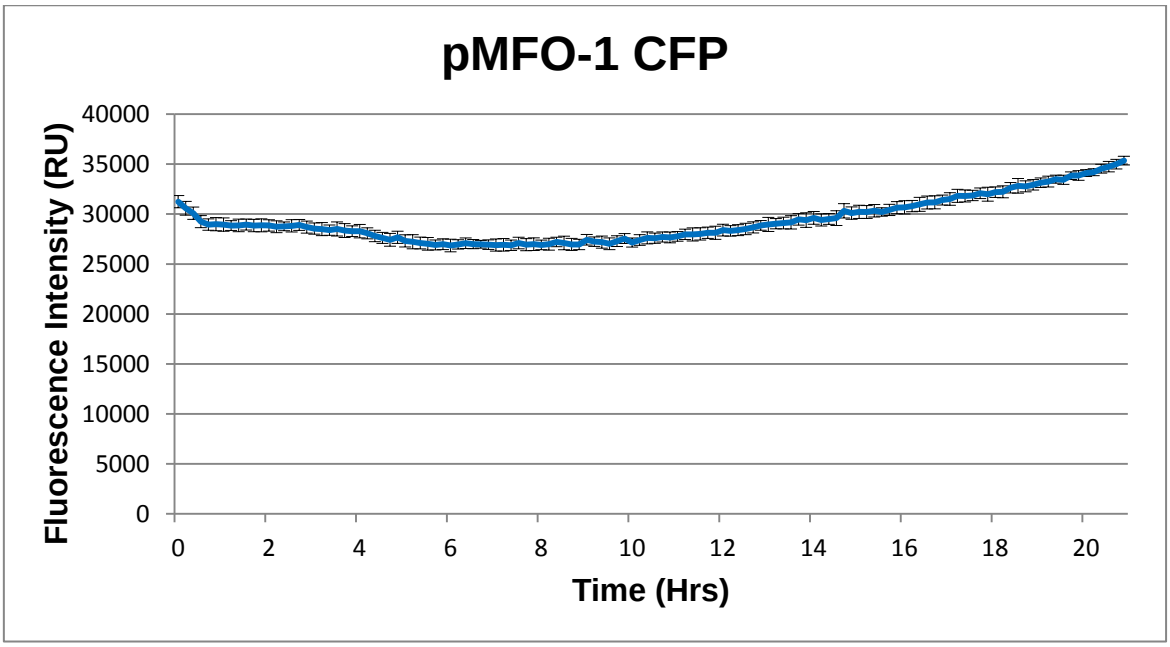

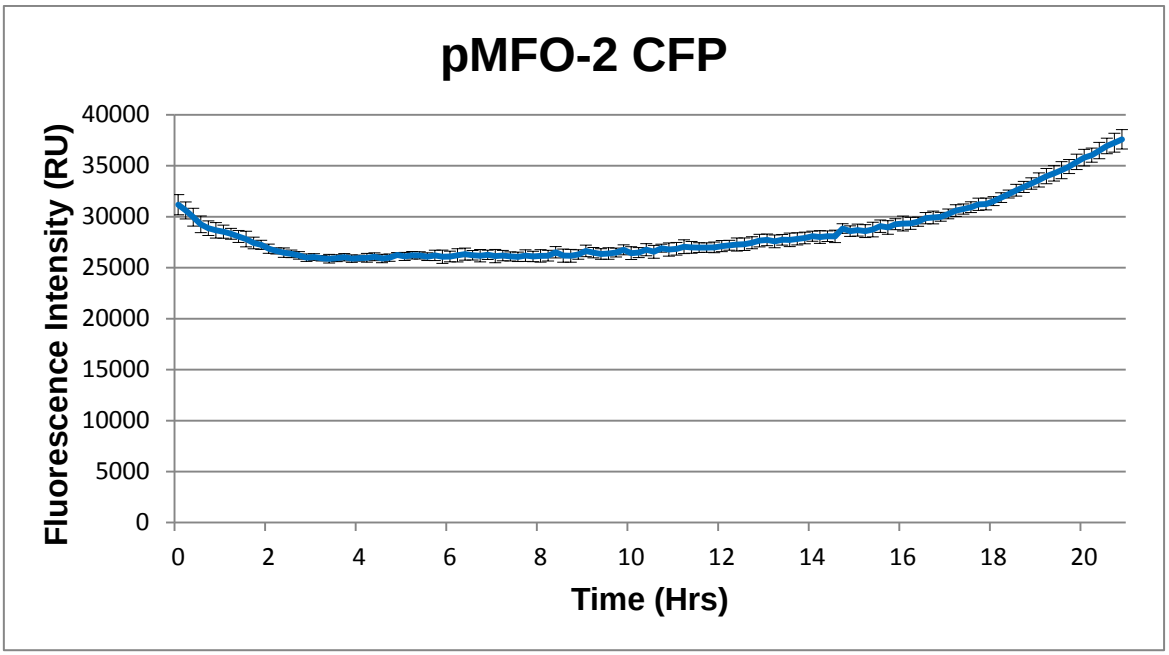

Figure 32: Total CFP fluorescence produced by *E. coli* C43 cells containing either pMFO-1 or pMFO-2. The results have been corrected for cell number by dividing the raw fluorescence data by the OD_{600} from the same time point, followed by the subtraction of fluorescence produced by non-fluorescent control cells containing either an empty pUC19 or pInd4 plasmid. The error bars represent the standard error of the mean for three biological repeats.

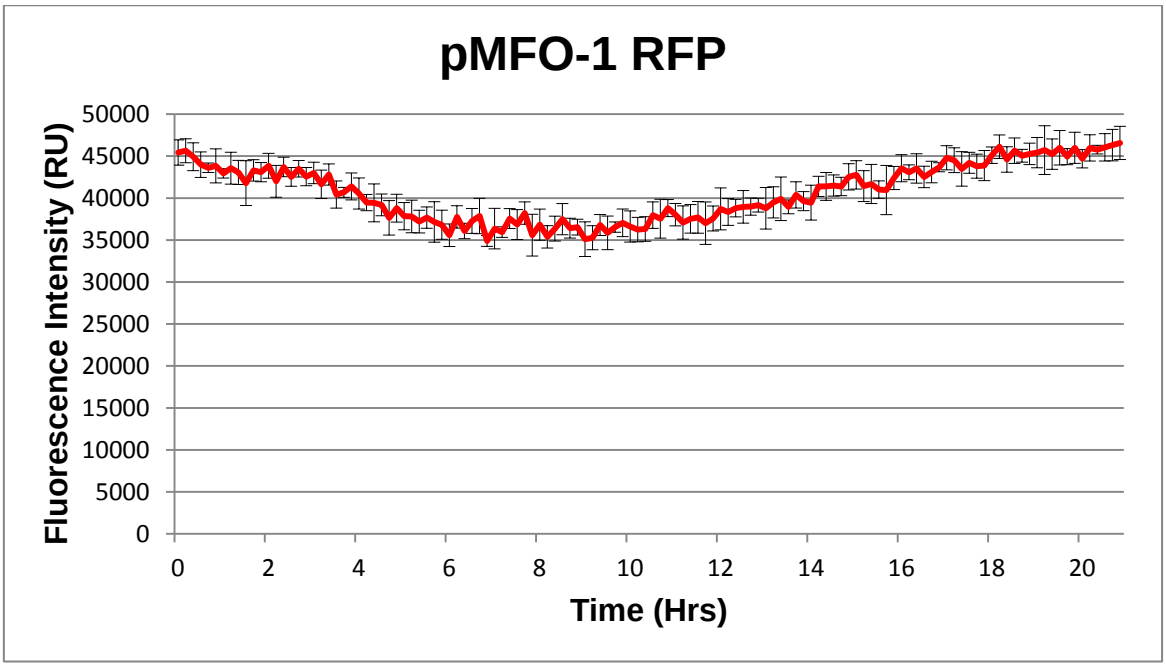

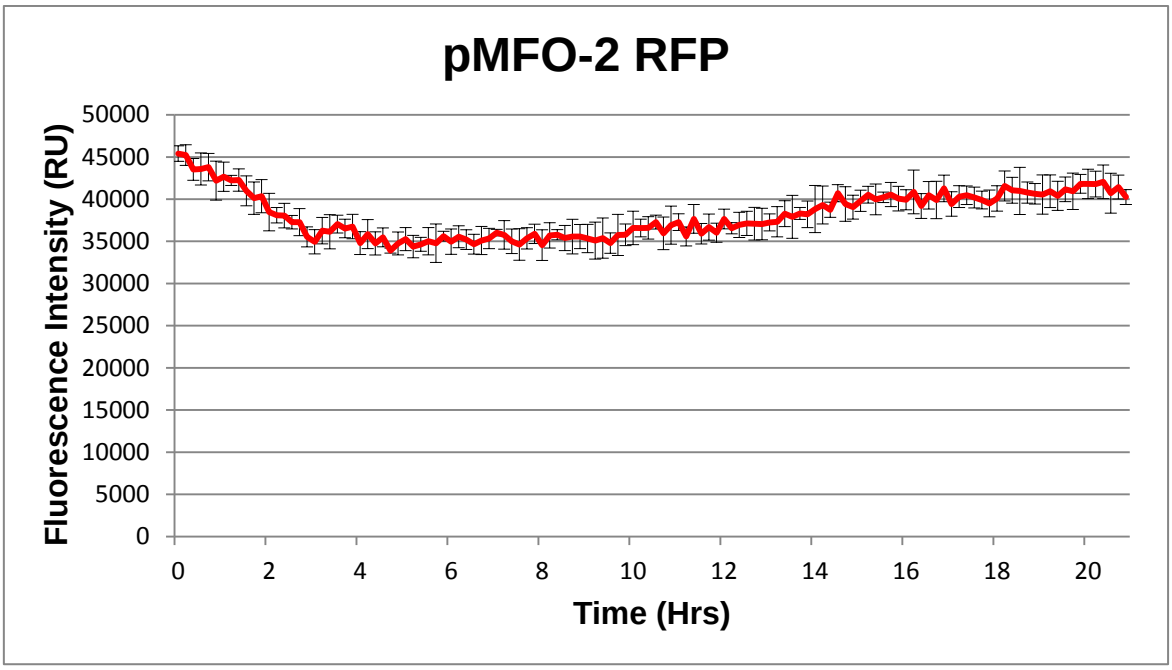

Figure 33: Total RFP fluorescence produced by *E. coli* C43 cells containing either pMFO-1 or pMFO-2. The results have been corrected for cell number by dividing the raw fluorescence data by the OD_{600} from the same time point, followed by the subtraction of fluorescence produced by non-fluorescent control cells containing either an empty pUC19 or pInd4 plasmid. The error bars represent the standard error of the mean for three biological repeats.

The results show that when the MFO reporter fragment is transferred to a lower copy number plasmid, pMFO-2, the maximum level of fluorescence in the YFP channel is reduced to approximately half of the level seen in the high copy number plasmid, pMFO-1, ~25,000 RU compared to ~50,000 RU at 18 hrs. However, the levels of fluorescent output from the CFP and RFP channels does not change in the lower copy pMFO-2 compared to the original higher copy pMFO-1. It appears that even with the lower number of *ntr* promoters located on pMFO-2 (~200), this may still be high enough to sequester much of the activated NtrC-P in the host cells before a high level of activation is seen in the CFP and RFP reporters. The number of NtrC-P dimers in a fully activated cell are thought to be ~70 under complete nitrogen limiting conditions (Section 1.7.3) (Reitzer and Magasanik, 1983). It is also possible that, under these growth conditions, the cells use up all of the resources in the media whilst growing and producing YFP and run out of nutrients before the medium and low affinity promoters are fully activated by NtrC-P. The negative values seen in the CFP and RFP channels when pMFO-1 was tested in XL-1 Blue cells are not seen in the results from the C43 cells (Figure 35). This suggests that the cells are coping better with the high levels of protein expression and are managing to divide, rather than producing long filamentous cells, therefore the cell number correction and subtraction of control cell fluorescence is working as expected, this was confirmed by microscopy (Figure 35).

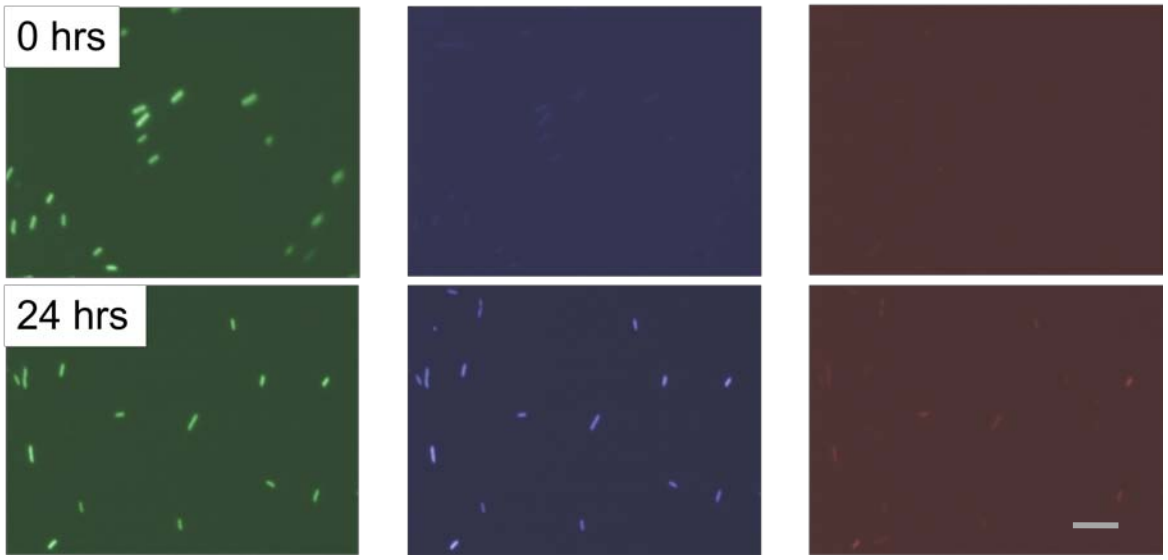

Figure 34: Epifluorescence image of C43 cells containing the pMFO-1 plasmid. This shows that the cells are now able to divide and are not growing as long, filamentous cells. Images were taken at 0 hr and 24 hr after transfer from 50 mM NH_4^+ to 0 mM NH_4^+ growth media. YFP (expressed from the high affinity promoter) is seen in the green channel, CFP (medium affinity) in the blue channel and RFP (low affinity) in the red channel. Scale bar = 10 µM. See section 2.3.1 for microscope details.

3.6 Varying ammonium concentrations

To test the response to different amounts of ammonium in the growth media, *E. coli* C43 strains containing the pMFO-1 and pMFO-2 reporter plasmids were grown up in an overnight culture of LB. The overnight LB culture was then diluted 1 in 100 into a final volume of 150 µl of fresh LB containing appropriate antibiotics and supplemented with either 0 mM, 20 mM, 50 mM, or 100 mM additional ammonium. The addition of extra ammonium should result in carbon being limiting rather than nitrogen at higher concentrations of added ammonium. The cells were then transferred to a 96-well plate and grown to stationary phase in a plate reader. The fluorescence output of the reporter plasmids and the OD_{600} was measured,

and the maximum level of fluorescence output in each of the three channels is shown below (Figure 36).

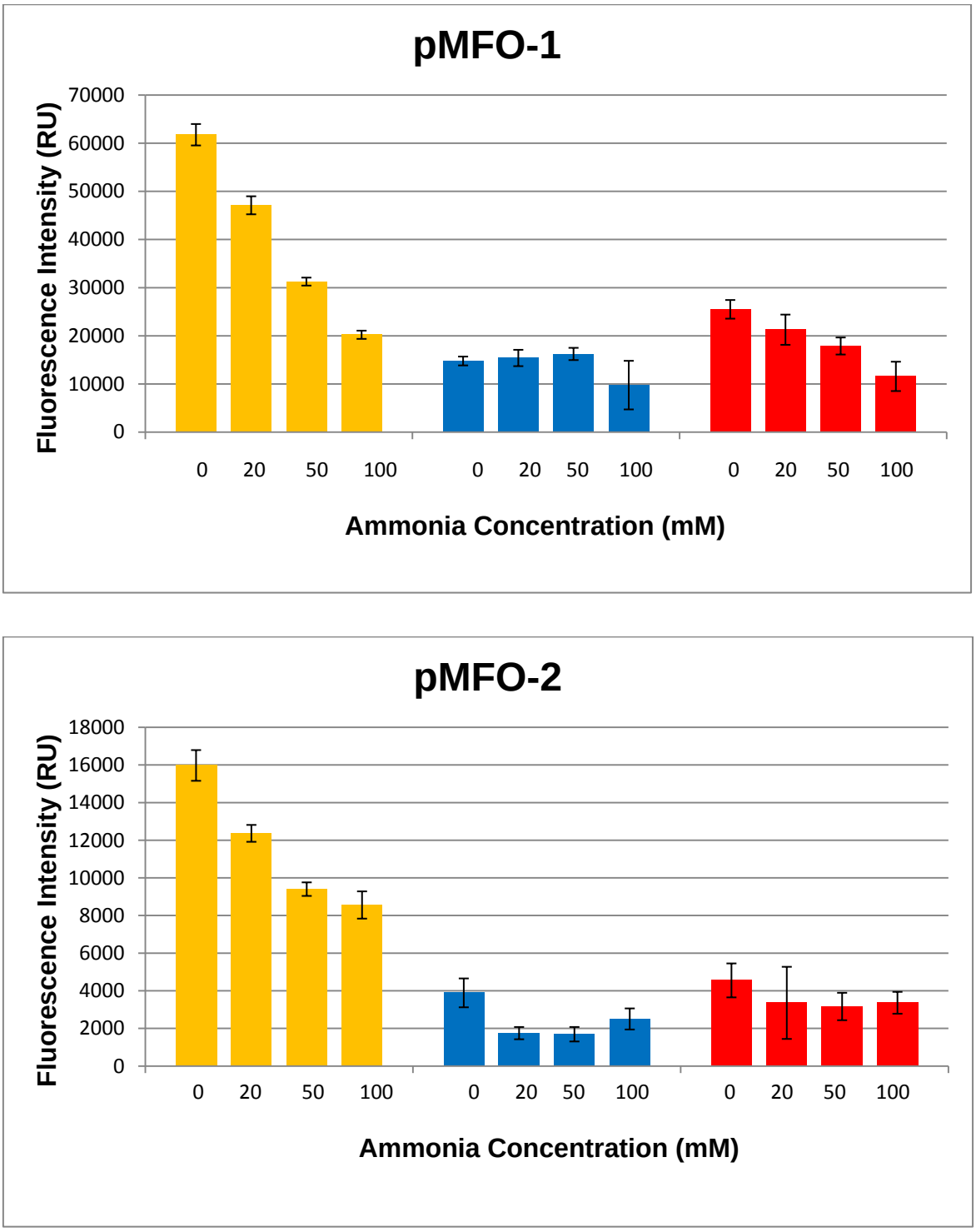

Figure 35: The maximum output of YFP, CFP, and RFP fluorescence from pMFO-1 and pMFO-2 in *E. coli* C43 when grown to stationary phase in LB supplemented with 0 mM, 20 mM, 50 mM, and 100 mM ammonium. The results have been corrected for cell number by dividing the raw fluorescence data by the OD_{600} from the same time point, followed by the subtraction of values obtained for non-fluorescent control cells, containing an empty pUC19 plasmid for pMFO-1 and an empty pInd4 plasmid for pMFO-2. Error bars represent 1 standard error of the mean for three biological repeats.

The results show that in the high copy number, pMFO-1, plasmid as the concentration of supplemented ammonium is increased, the maximum level of fluorescence output in the YFP and RFP channels decreases. This is encouraging for future applications of the MFO reporter as a biosensor as the decreasing levels of fluorescence being produced with increasing of ammonium suggest that this is due to the different concentrations of NtrC-P that are present in the cell. The fluorescence output of the CFP does not show the decrease in response to an increase in ammonium concentration that is seen from the YFP and RFP reporters This may be due to the release of amino acids and other cell contents during stationary phase due to cell lysis, resulting in a high level of background auto-fluorescence being produced in the CFP channel and masking the signal seen from the reporter plasmid.

The results of the lower copy number, pMFO-2 reporter plasmid also show a reduction in the maximum level of YFP fluorescence in response to increasing ammonium concentrations in the growth media. However, this is not seen in the CFP and RFP channels. The lower levels of signal from pMFO-2 may have resulted in it being harder to measure the signal from the reporter above the background noise from cell lysis in the CFP and RFP channels.

From these experiments it can be seen that more signal needs to be generated from the reporter plasmid in the CFP and RFP channels in order to be able to clearly detect it above the background fluorescence of the media and the cells.

3.7 Media test

In order to get the maximum signal to noise ratio from the reporter plasmid, a growth medium must be selected that gives the lowest level of auto-fluorescence possible. This will allow small changes in fluorescence output from the reporter plasmid to be measured above the background auto fluorescence of the growth media and the cell culture. To test the suitability of different growth media a series of experiments were repeated in LB and M9 minimal media (Appendix A2.3), to investigate which gave the lowest level of background auto-fluorescence when used as the growth media for cells containing the reporter plasmid pMFO-2. LB has higher levels of amino acids and peptides (Sezonov *et al.*, 2007) and is therefore expected to have higher levels of autofluorescence that M9 minimal media. These amino acids are thought to contribute greatly to background auto fluorescence, especially in the CFP channel.

An overnight culture of C43 cells containing the pMFO-2 reporter plasmid was diluted 1 in 100 in either 150 µl of LB or M9 minimal media. The fluorescence output of the reporter was measured over time in a plate reader and the results of the YFP (Figure 37), CFP (Figure 38) and RFP (Figure 39) channels after subtraction of control cells containing C43 cells containing the empty pInd4 plasmid, grown in the same conditions are shown.

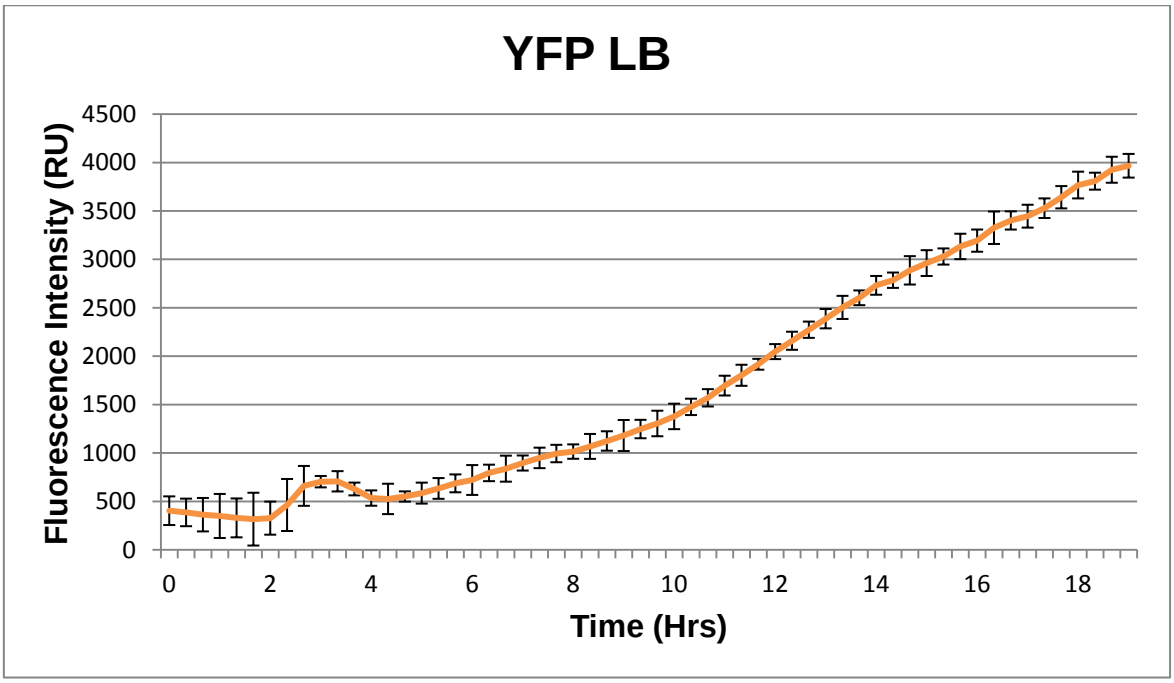

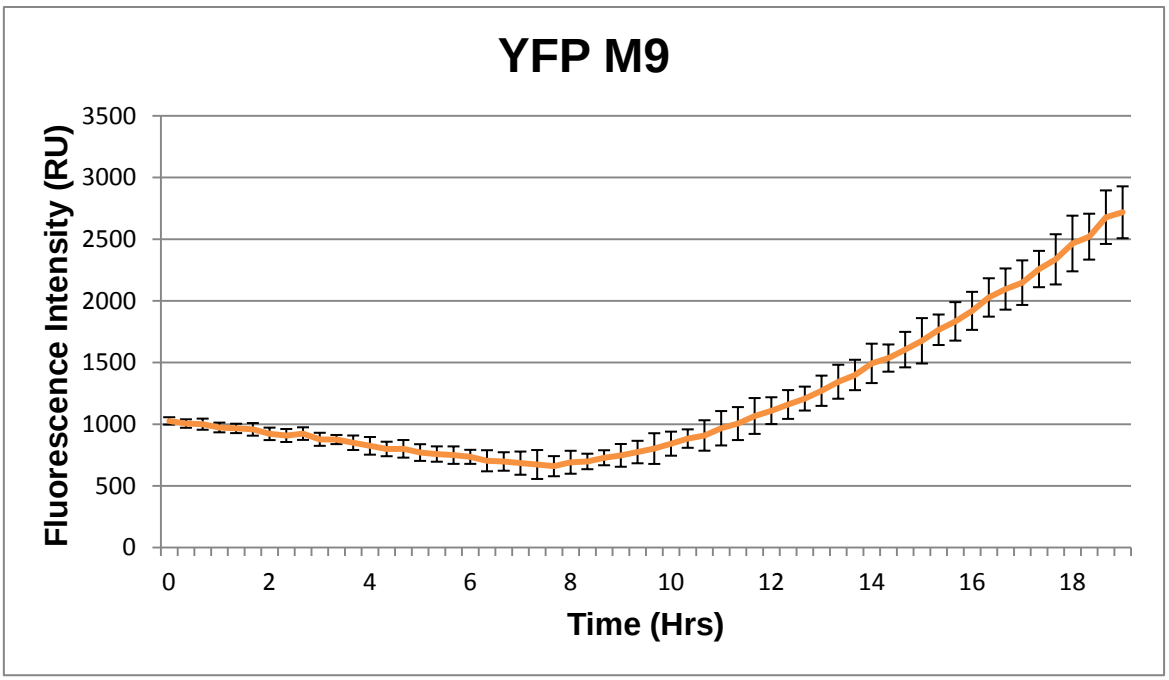

Figure 36: The YFP response to nitrogen limitation in *E. coli* C43 cells containing pMFO-2 when grown in LB and M9 growth media. The results have been corrected for cell number by dividing the raw fluorescence data by the OD_{600} from the same time point, followed by the subtraction of fluorescence produced by non-fluorescent control cells containing an empty pInd4 plasmid. The error bars represent the standard error of the mean for three biological repeats.

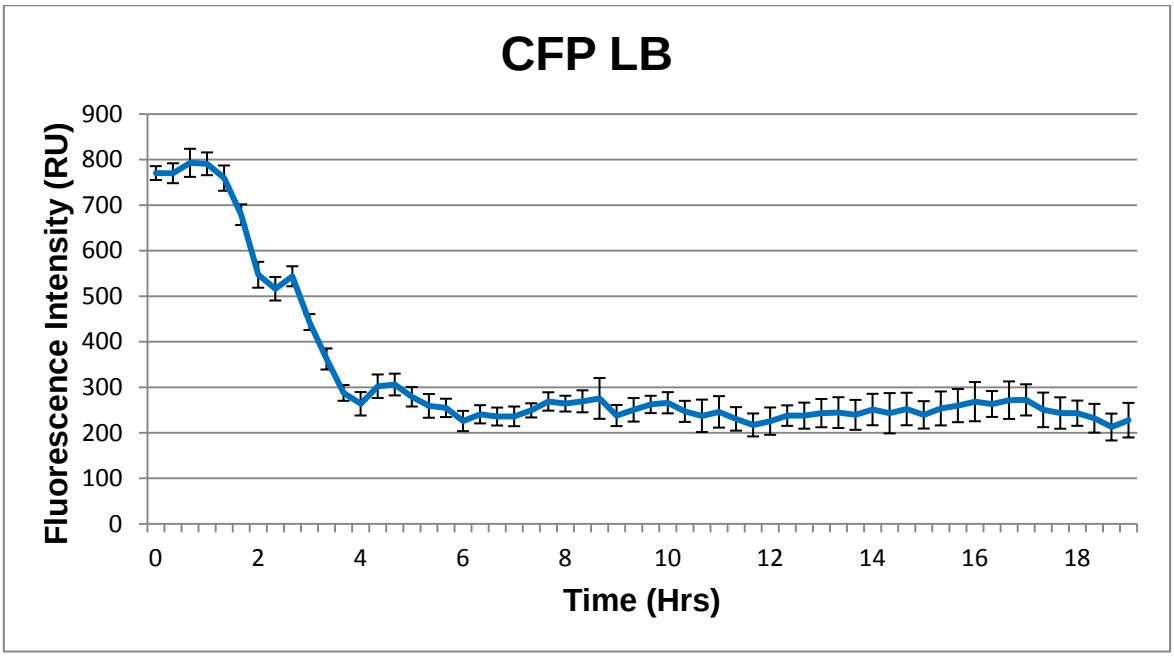

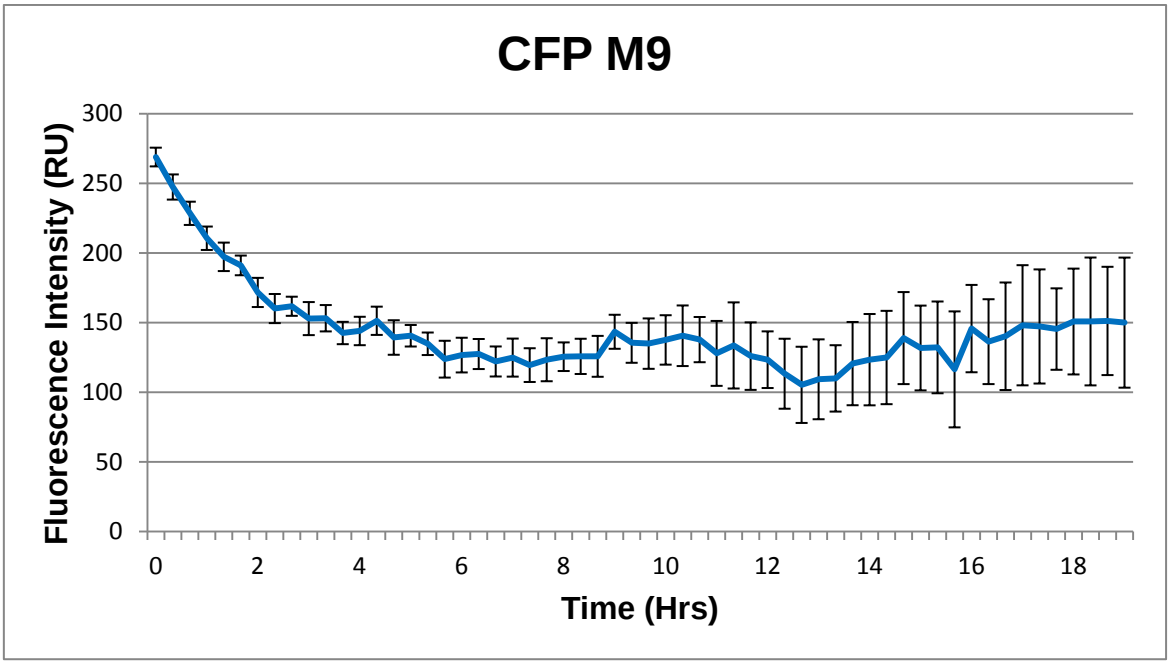

Figure 37: The CFP response to nitrogen limitation in *E. coli* C43 cells containing pMFO-2 when grown in LB and M9 growth media. The results have been corrected for cell number by dividing the raw fluorescence data by the OD_{600} from the same time point, followed by the subtraction of fluorescence produced by non-fluorescent control cells containing an empty pInd4 plasmid. The error bars represent the standard error of the mean for three biological repeats.

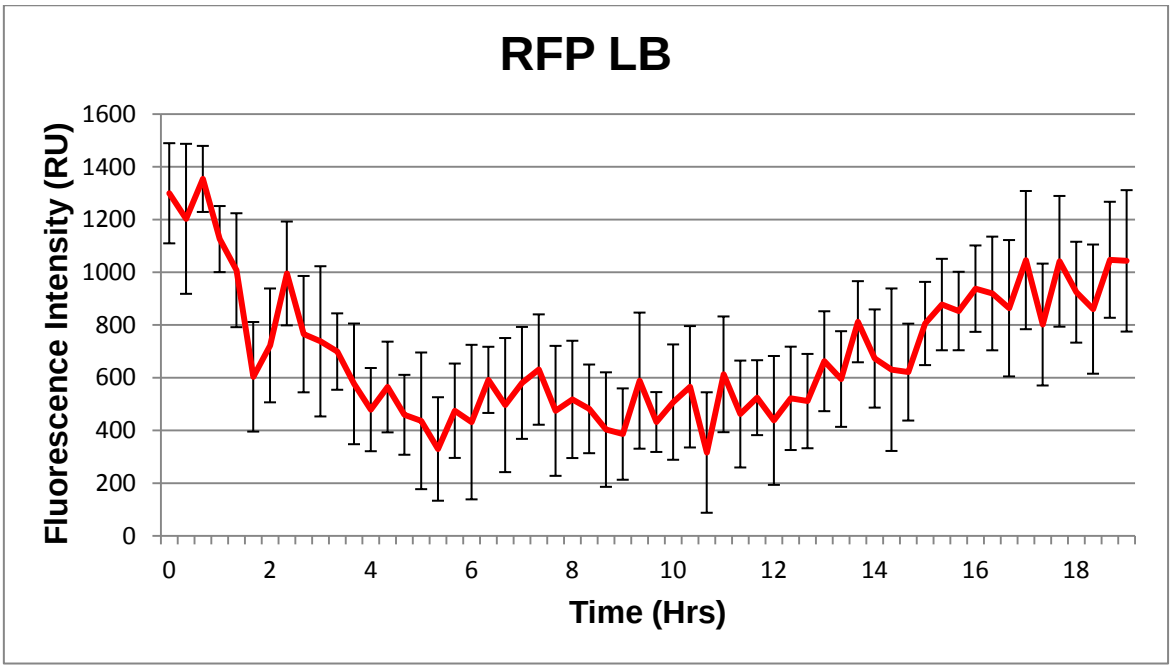

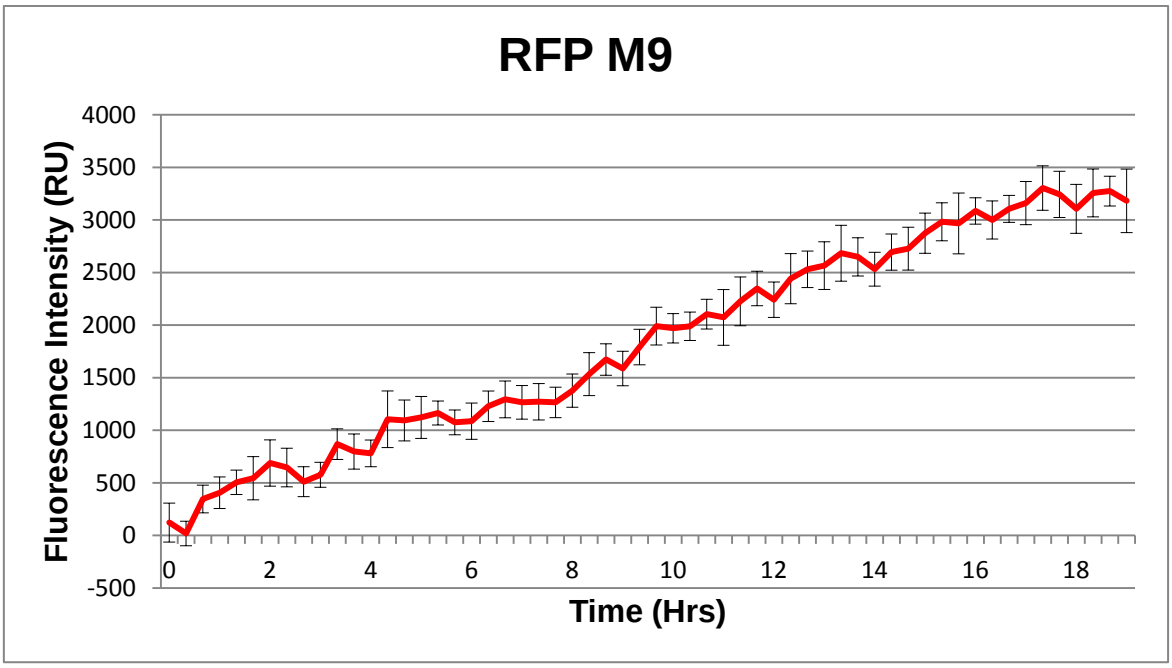

Figure 38: The RFP response to nitrogen limitation in *E. coli* C43 cells containing pMFO-2 when grown in LB and M9 growth media. The results have been corrected for cell number by dividing the raw fluorescence data by the OD_{600} from the same time point, followed by the subtraction of fluorescence produced by non-fluorescent control cells containing an empty pInd4 plasmid. The error bars represent the standard error of the mean for three biological repeats.

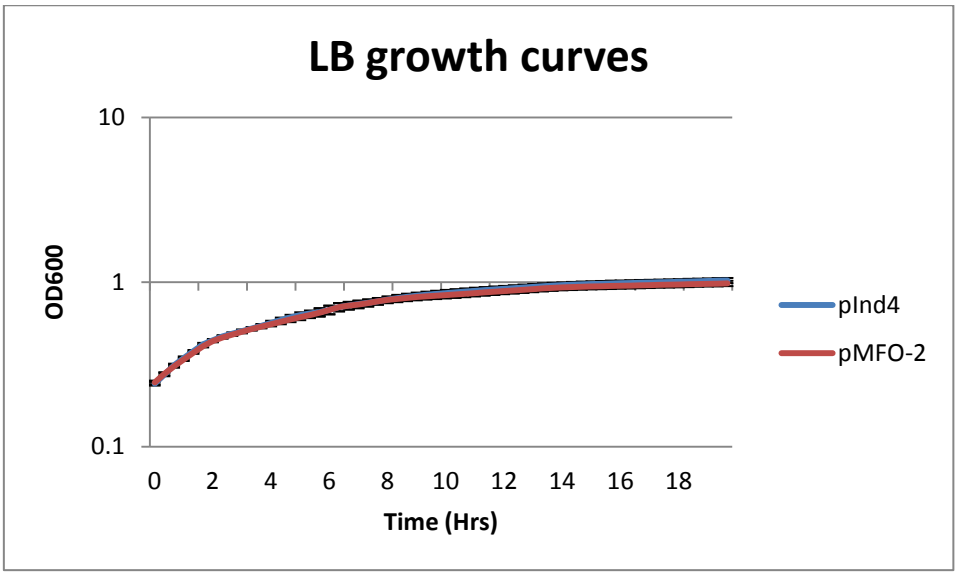

Figure 39: Growth curves of cells containing the pMFO-2 reporter plasmid and wild type control containing only the pInd4 backbone. Error bars represent standard deviation of 3 biological repeats.

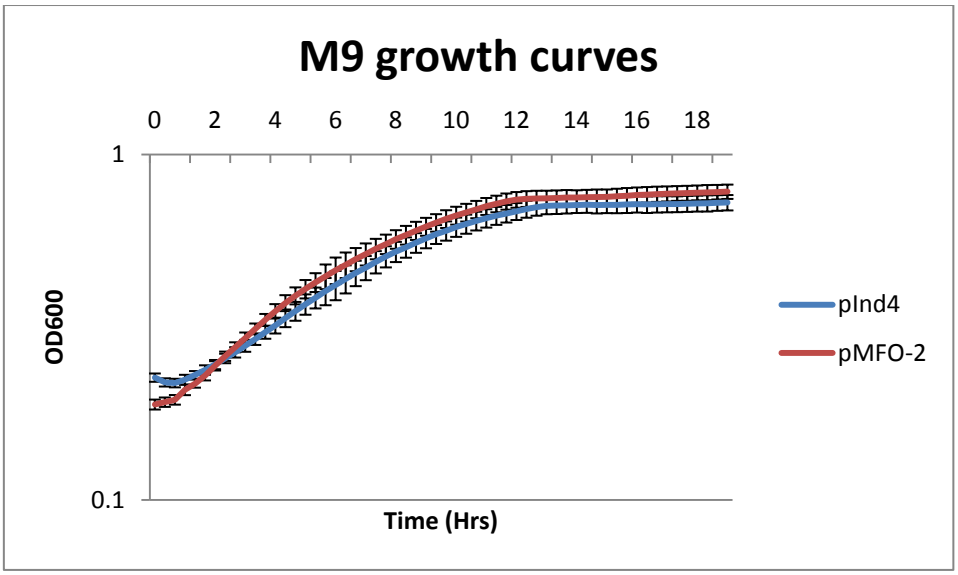

Figure 40: Growth curves of cells containing the pMFO-2 reporter plasmid and wild type control containing only the pInd4 backbone. Error bars represent standard deviation of 3 biological repeats.

The graphs show the total fluorescence produced by each of the reporters on pMFO-2 after subtraction of a control sample in which C43 cells are grown in the same conditions, but containing the empty pInd4 plasmid. It can be seen that in comparison with LB growth media the M9 growth media gives a much stronger and less noisy signal in the RFP channel from the low affinity promoter. This is possibly due to a higher level of starvation being experienced by the cells at an early stage in the M9 media resulting in a stronger activation of the low affinity promoter. The signal from the medium affinity promoter in the CFP channel is low in both LB and M9; this may be due to a high level of background auto fluorescence produced by the cells growing in the medium. There is evidence to suggest that auto fluoresce is increased during *E. coli* stress response (Renggli *et al.*, 2013). This may impact fluorescence readings in both the reporter cells and the control cells as nutrients become limiting in the growth media. In this case the control cells produce an increase in the level of signal seen from the CFP channel as the cells grow and therefore it is not possible to detect a good signal from the reporter above the background fluorescence of the control. The level of fluorescence in the YFP channel from the high affinity promoter is less in M9 than in LB, 2700 units compared to 4000 units. This may be due to there being fewer nutrients available to the cells in M9 to produce as much YFP as the cells grown in LB. However, there is still sufficient signal to have an output that is easily measurable above the background level of fluorescence in the control cells.

The cells grown in M9 minimal media give a better overall response across the three fluorescent reporters as signal responses are seen in both the YFP and RFP channels and are therefore likely to give a better output from a biosensor than

cells grown in LB. The lower level of background fluorescence in M9, due to the absence of auto fluorescent amino acids such as Tryptophan, will allow detection of lower concentrations of an analyte and we need to obtain a measurable signal across all three fluorescent channels for the multi-fluorescent output reporter to be successful. It is also possible that the higher level of the RFP response is due to the more severe nitrogen limitation experienced by the cells transferred into M9 compared to previous results in LB, this may produce a stronger response from the Ntr system resulting in increased output from the low affinity promoter.

3.8 New experimental approach

In order to minimise the amount of nutrients used by the cells for growth and to try and maximise the fluorescent protein production by the cells the experimental procedure was altered. Instead of using an overnight culture at the start of the experiments and allowing the cells to grow in the plate reader, the overnight culture was diluted 1 in 50 into fresh LB containing appropriate antibiotics and grown to an OD_{600} of 0.6. 1 ml of the mid-log phase culture was spun down in a bench-top centrifuge and re-suspended in 1 ml of M9 minimal media (Appendix A2.3) supplemented with different concentrations of ammonium. 150 µl of sample was transferred to a 96-well plate and the fluorescence output of the reporter plasmids measured in a plate reader.

This is a more realistic approach for a biosensor, with a sample added to a large number of reporter cells and the output of the reporter measured. To test the new experimental approach, *E. coli* C43 cells containing either the pMFO-1 or the

pMFO-2 reporter plasmid were analysed. The fluorescence output of the YFP channel (Figure 42), CFP channel (Figure 43) and RFP channel (Figure 44) after normalisation for cell number and subtraction of background fluorescence from control cells are shown below.

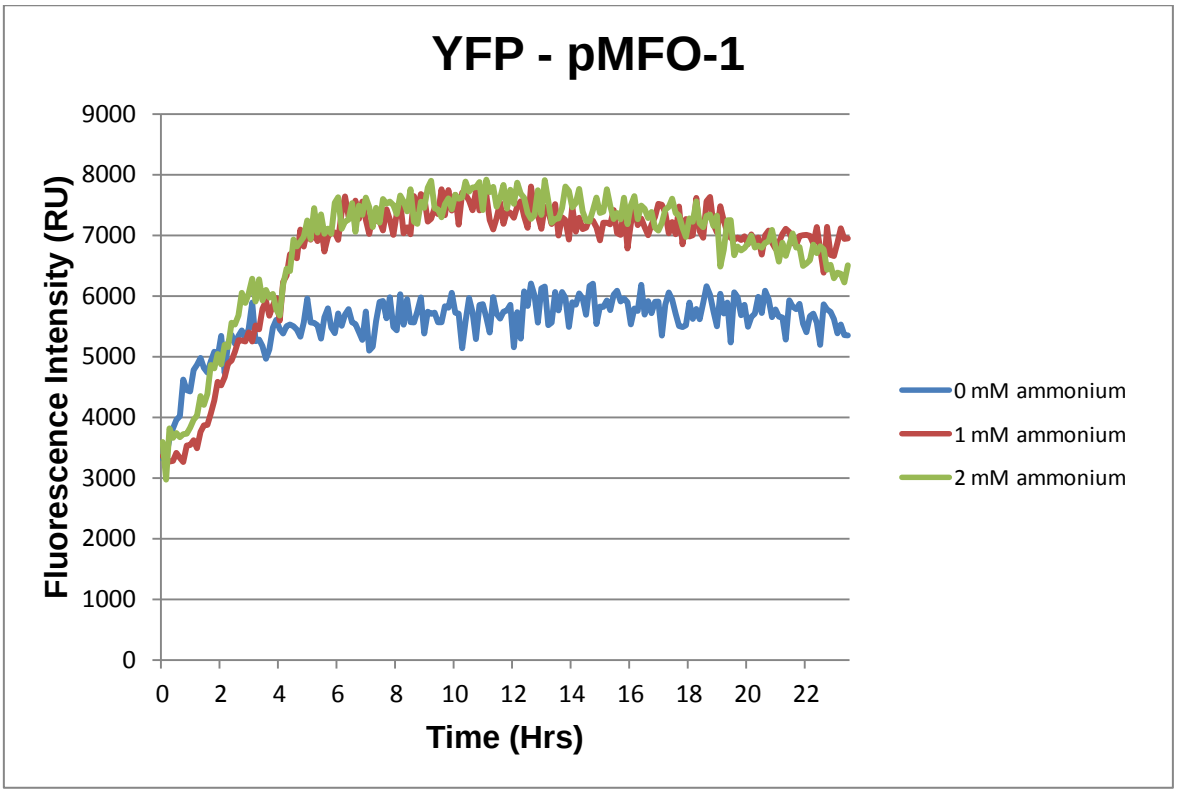

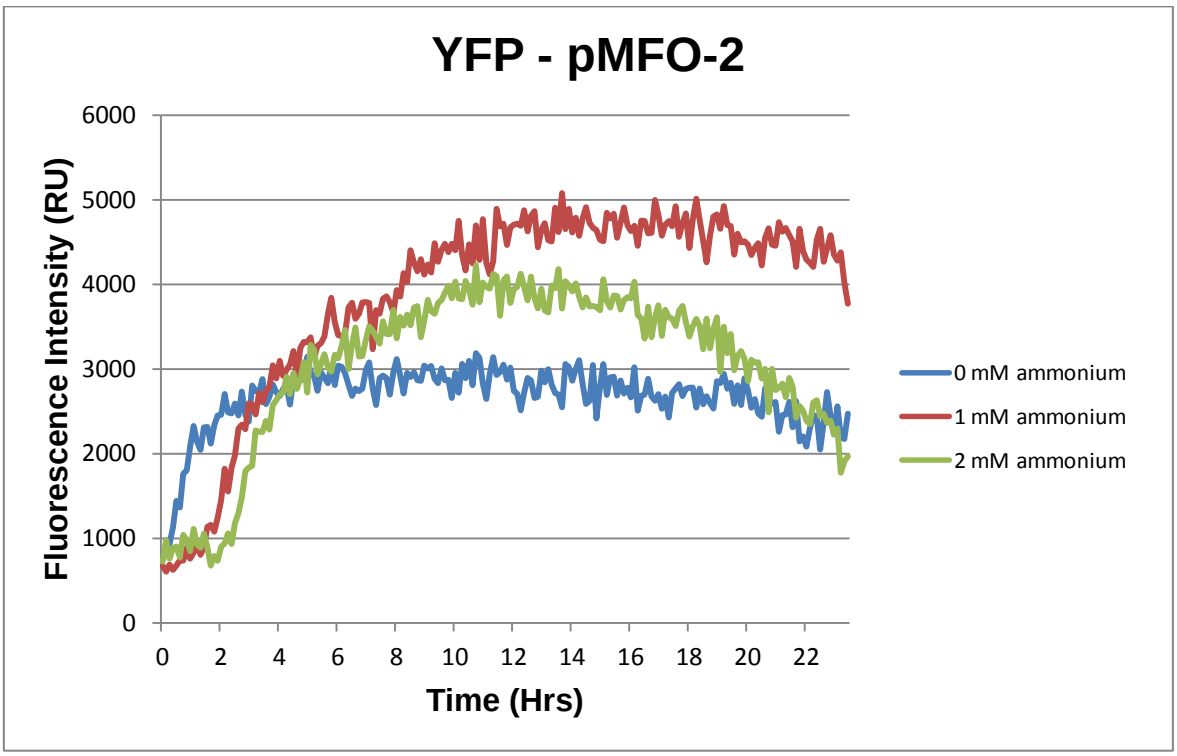

Figure 41: The total level of YFP expression in the reporter strain, C43 pMFO-1 and C43 pMFO-2, in M9 supplemented with 0 mM, 1 mM or 2 mM ammonium. The results have been corrected for cell number by dividing the raw fluorescence data by the OD_{600} from the same time point, followed by the subtraction fluorescence from normalised non-fluorescent control cells, containing an empty pUC19 or pInd4 plasmid.

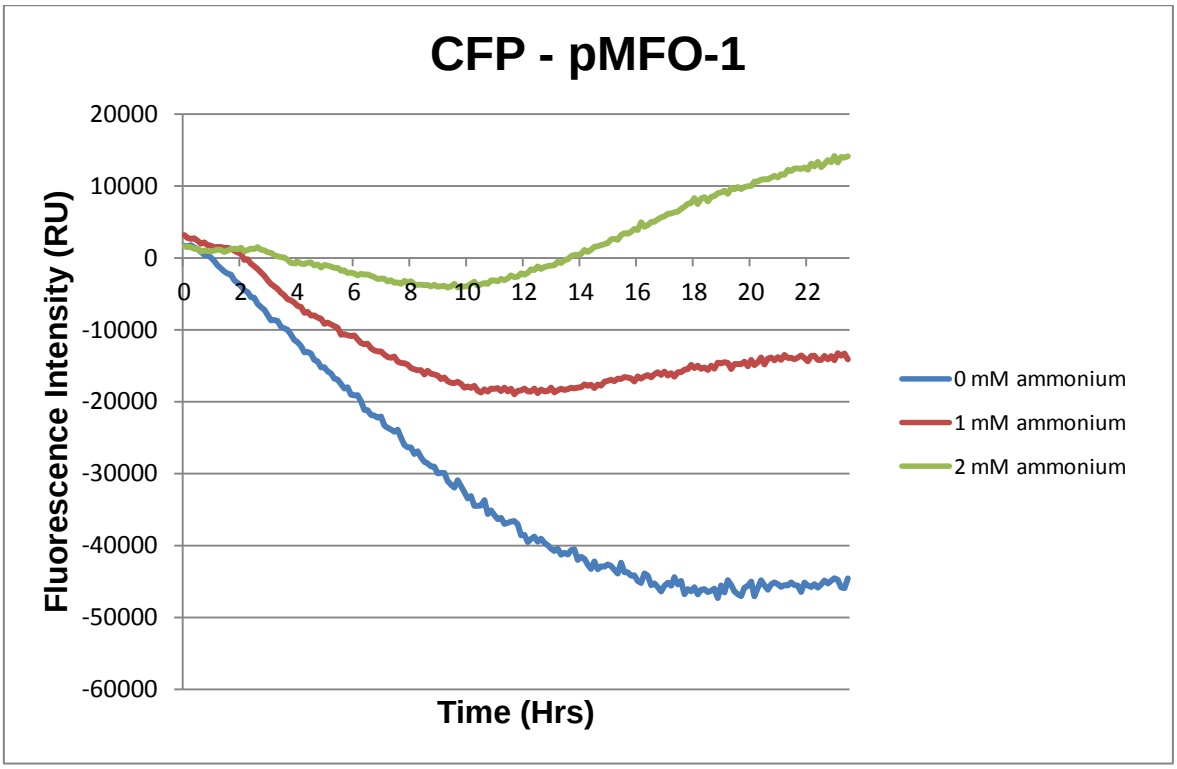

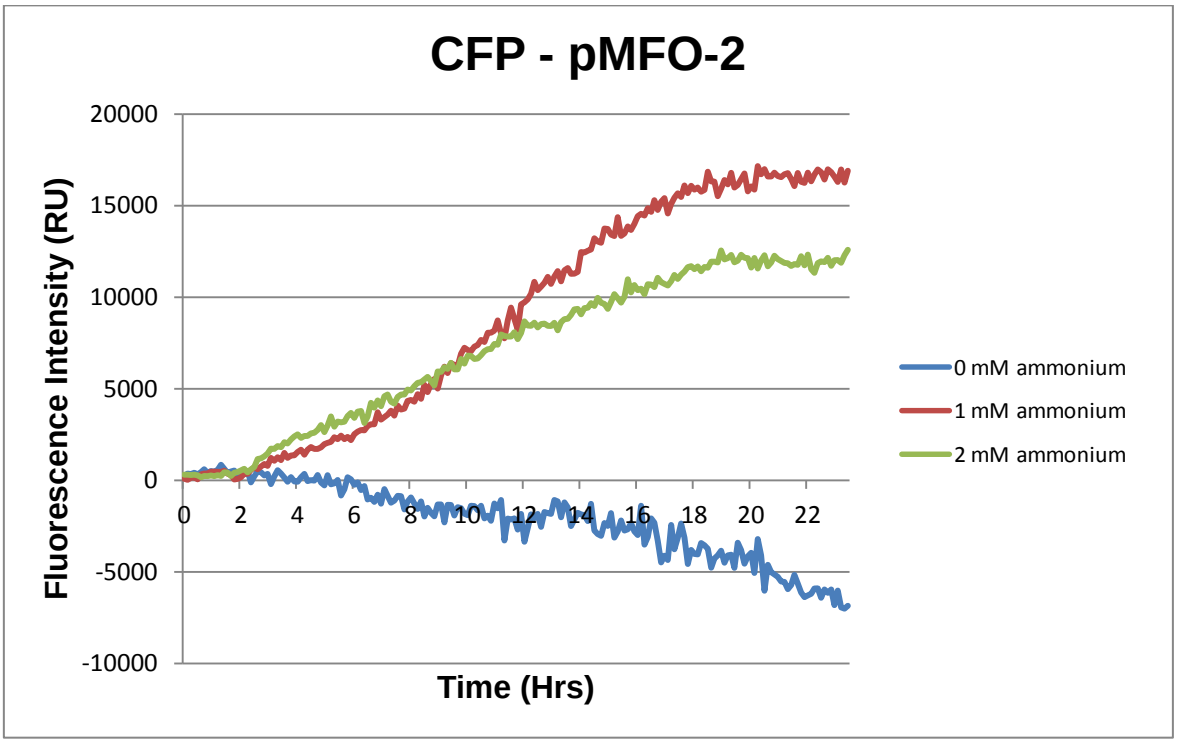

Figure 42: The total level of CFP expression in the reporter strain, C43 pMFO-1 and C43 pMFO-2, in M9 supplemented with 0 mM, 1 mM or 2 mM ammonium. The results have been corrected for cell number by dividing the raw fluorescence data by the OD_{600} from the same time point, followed by the subtraction fluorescence from normalised non-fluorescent control cells, containing an empty pUC19 or pInd4 plasmid.

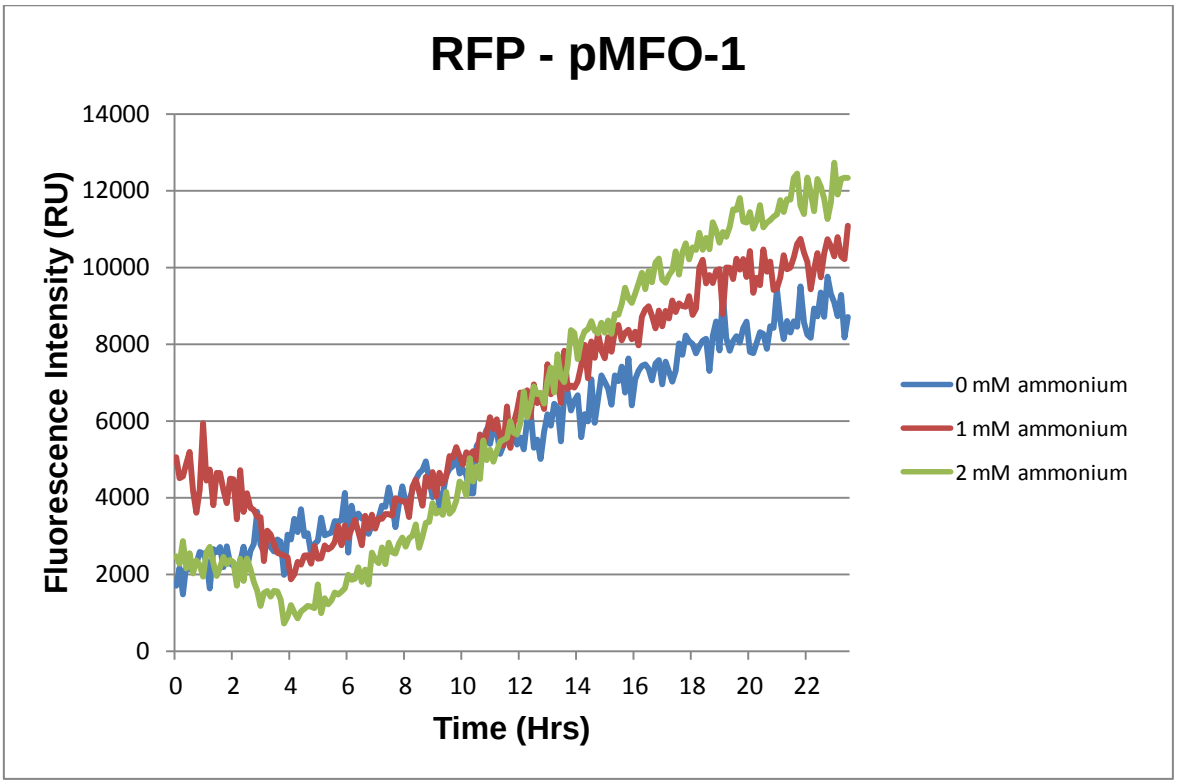

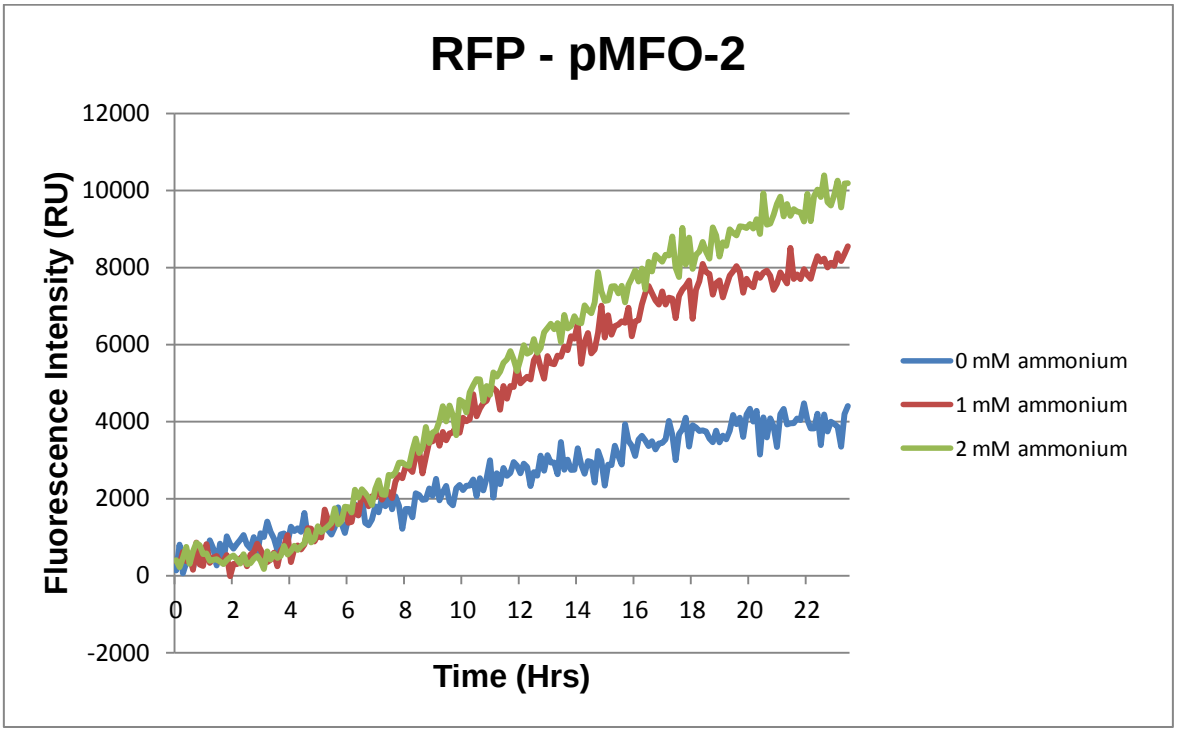

Figure 43: The total level of RFP expression in the reporter strain, C43 pMFO-1 and C43 pMFO-2, in M9 supplemented with 0 mM, 1 mM or 2 mM ammonium. The results have been corrected for cell number by dividing the raw fluorescence data by the OD_{600} from the same time point, followed by the subtraction fluorescence from normalised non-fluorescent control cells, containing an empty pUC19 or pInd4 plasmid.

The results show that with the new experimental approach a measurable signal is produced by all three of the reporter channels. In all cases both in pMFO-1 and pMFO-2, the level of fluorescence output from the cells grown with no supplemented ammonium is lower than when 1 mM or 2 mM ammonium is added to the growth media. This is contrary to the expected response where lower ammonium levels results in higher levels of NtrC-P but could be explained by the lack of nitrogen available to the cells to produce the fluorescent proteins. In fact, the absence of any nitrogen source in the 0mM ammonium conditions is probably preventing any protein synthesis and hence any reporter output and is therefore not a valid condition to use.

This is supported by comparison of the relative levels of fluorescence output from cells containing pMFO-1 grown in media supplemented with 1 mM and 2 mM ammonium. The high affinity reporters show that cells supplemented with 1 mM ammonium produce the same amount of YFP fluorescence than cells supplemented with 2 mM ammonium and in both the CFP and RFP reporters the cells supplemented with 1 mM ammonium produce less fluorescence than cells supplemented with 2 mM ammonium. This is not what is expected if ammonium is repressing activation from these promoters, supporting the idea that there are not enough nutrients available for high levels of protein synthesis.

The cells containing pMFO-2 show the expected fluorescence output in the YFP and CFP channels, the 1 mM ammonium signal is higher than the 2 mM signal, but not in the RFP channels. This suggests that the lower number of high affinity

YFP promoters and the lower demand for YFP production means that there is sufficient nitrogen left to produce a good level of CFP from the medium affinity promoter but not enough for RFP production from the low affinity promoter under these conditions.

These results suggest that the low levels of fluorescence output seen in the CFP and RFP reporter channels are probably a result of the cells not having enough nitrogen present to be able to synthesise the fluorescent proteins even if the level of NtrC-P in the cell is high enough to activate transcription from these promoters because the remaining nitrogen has already been used synthesising the YFP from the high affinity promoter.

3.9 Discussion

A three output multi-fluorescent reporter that responds to limitation of nitrogen in the environment by expression of YFP, CFP and RFP, has successfully been constructed. The fluorescence output of the reporter is easily monitored using a fluorescence plate reader; this gives information about the fluorescence intensity produced by each of the three reporters on the reporter plasmid as well as the OD_{600} of the culture at that particular time point.

The reporter plasmid, pMFO-1 has been tested by growing to stationary phase and monitoring the fluorescent output. This has shown a good response to nitrogen limitation in the YFP channel, corresponding to the high affinity promoter; however the signal from the CFP and RFP channels, corresponding to the

medium and low affinity promoters respectively, was difficult to detect above the background fluorescence of the LB growth media and the cell culture. This resulted in the apparent fluorescence in the CFP and RFP channels being higher in the control cells than in the reporter at some time points. This may be due to the cell cultures producing different levels of auto-fluorescence throughout the experiment and the signal from the reporter not being high enough to be detected above this, or could be due to the fact that the reporter plasmid sequesters the host cell's NtrC-P resulting in filamentous cells and hence the OD_{600} values not being representative of the cell number, making the determination of fluorescence per cell inaccurate. The increased error in the plate reader measurements at low signal levels may result in the negative values observed in the CFP and RFP channels. The high numbers of fluorescent proteins present in each cell may also lead to fluorescence quenching due to overlap in excitation and emission curves of the reporter proteins and the proximity of the protein to each other in the cell may lead to FRET or self-quenching (Wang *et al.*, 2005), possibly resulting in lower signal output from the reporter.

The low level of signal seen in the CFP and RFP channels could be a result of the high affinity promoters on the YFP reporter sequestering all of the NtrC-P needed to activate transcription of CFP and RFP. This is possible as the copy number of pMFO-1 is ~400 in *E. coli* and each of the YFP promoters contains 2 high affinity NtrC-P binding sites, giving in excess of ~800 high affinity binding sites in the cell. It has been shown previously that in nitrogen rich media there are ~5 NtrC dimers per cell and during nitrogen limitation this number increased to ~70 (Reitzer and Magasanik, 1983), it is therefore possible that there is not enough NtrC-P present

in the cell to activate a good level of transcription from all of the different affinity promoters.

To address this problem the MFO reporter fragment was transferred in to the lower copy number plasmid pInd4, which has a copy number of ~100 in *E. coli*. This will reduce the number of high affinity binding sites in the host cell by a factor of 4. The results showed that the level of YFP signal was reduced by half, but there was little improvement in the level of total output in the CFP and RFP channels. This is may be a result of the lower signal level produced by the low copy number plasmid being masked by background noise from the cell culture, or that the number of high affinity binding sites was still sequestering all of the host cell's NtrC-P.

In order to get a good level of detection across all three fluorescent reporters it was necessary to reduce the level of background fluorescence. It is not possible to reduce the auto-fluorescence of the cells, but it is possible to reduce the auto-fluorescence of the growth media. The cells were grown in M9 minimal media which produces less background fluorescence than LB. The results of *E. coli* C43 cells grown in M9 showed that an improved signal was seen in the RFP channel, but the CFP channel showed little increase in signal above the background control cells. Overall however, the fluorescence output from the reporter plasmid is better when grown in M9 then when host cells are grown in LB. The growth in LB appears to produce more of a constitutive level of YFP production rather than an induction of YFP production from the promoter. This suggests that the cells are not

nitrogen limited during this experiment. Previous work on *E. coli* growth in LB suggests that the cells become carbon limited, before the nitrogen source is depleted (Sezonov *et al.*, 2007).

A new experimental approach was developed to provide a more realistic assay for a biosensor. An overnight culture of the host cells was diluted 1 in 50 in LB and grown to an OD_{600} of 0.6 before measurement. This improves the assay in two ways; firstly the cells now have a high supply of nitrogen from the fresh LB media, resulting in the level of NtrC-P in the cell being at its lowest and secondly, there are now more cells in the starting sample, which gives a higher level of signal from the sample. The results of the new experiments show that when the cells are transferred into media with 0 mM ammonium the cells struggle to produce a high level of fluorescent proteins, however, if 1 mM ammonium is added to the M9 media the cells produce a measurable response in all three fluorescent reporter channels. This indicates that the reason why the CFP and RFP signals are so low in cells grown to stationary phase may be that the cells simply run out of nutrients after the production of YFP from the high affinity reporter and are unable to produce a good signal in the CFP and RFP channels. This is not surprising as the natural Ntr response is to conserve the cells energy and this has been altered to activate high levels of transcription, a highly energy consuming process. This is a highly promising result however, as if the MFO reporter was used to detect compounds other than nitrogen, then the nitrogen levels could be kept high to ensure that the cells were able to produce a strong, detectable signal from all three fluorescent reporters on the plasmid. The lower levels of fluorescence from

pMFO-2 may also be useful when fine tuning the output of a biosensor giving more flexibility in the design of the system.

There may also be problems with fluorescence scattering when collecting data from the plate reader in dense cell cultures and there could also be problems with reading multiple fluorescent signals from the same well, such as photobleaching, or FRET between different fluorescent proteins in the cell affecting the total output observed from the biosensor.

The issue of titrating out the transcriptional activator, NtrC and the limiting nitrogen levels in the growth media preventing sufficient synthesis of reporter protein in medium and low affinity reporters will be addressed in chapter 5, where constitutively active form of NtrC (NtrC*) is engineered to activate the reporter plasmid. This serves three purposes in the biosensor, firstly it ensures that there can be a sufficient level of transcriptional activation of the high, medium and low affinity reporters, even if the reporter plasmid has a high copy number ensuring a high signal to noise ratio. Secondly, the production of NtrC* can be put under the control of different promoter sequences, this enables the input of the biosensor to be easily switched to detect different compounds that effect the level of transcription of that specific promoter. Thirdly, as the activation of NtrC is no longer dependent on the nitrogen levels in the environment, then excess levels of ammonium can be added to the growth media to ensure sufficient nutrients are available to sustain the high levels of fluorescent protein synthesis required by this biosensor. The high levels of ammonium also serve to shut down any interference

from the host cells' Ntr system that might cause increased activation of the reporter plasmid.

4. Characterization in other species

4.1 Introduction

The work done in *E. coli* indicated that it may not be sufficiently robust to cope with the high levels of protein expression required by the multi-fluorescent reporter plasmid under the conditions tested. This may be a result of the nitrogen limiting conditions that the cells are being tested in, or it could be a result of the extra NtrC-P binding sites in the cell interfering with the host's normal transcriptional regulation. To create a successful biosensor a robust host is needed that can tolerate high levels of fluorescent protein production and be able to survive in the chemicals being detected.

To try to identify a more robust host than *E. coli*, the MFO reporter fragment was transferred into suitable plasmids that were capable of replicating in the new host cell. These were put into alternative host strains and the fluorescent output of the reporter was measured to discover whether the *E. coli* promoters that control the expression of each of the fluorescent protein genes on the reporter plasmid could be activated by the host cells' NtrC-P in other species, as the Ntr system is highly conserved amongst bacterial species. It is expected that the new host cell NtrC-P will interact with the *E. coli* NtrC binding sites due to sequence similarities, *E. coli* – TGCACCn5GGTGCA, *R. sphaeroides* – TGCACAn5AGGGCG, although whether the affinities will be similar is unknown. *P. putida*, however lacks a *nac* orthologue (Hervas *et al.*, 2010) so the regulatory mechanisms of NtrC genes may differ but previous work has shown that *P. putida* NtrC functions in *E. coli* (Hervas *et al.*, 2009)so it is probable that the reverse will also happen.

The hosts selected to test were *Rhodobacter sphaeroides*, an α-subgroup proteobacterium, as the pMFO-2 reporter plasmid is also able to replicate in this species, and *Pseudomonas putida*, a γ-subgroup proteobacterium, as this is a common host for biosensors because of its high tolerance for toxins such as arsenate (Chang *et al.*, 2008a).

4.2 MFO reporter in *Pseudomonas putida*

P. putida is often used as a host for biosensors due to its high level of tolerance for toxins such as arsenate (Fernandez *et al.*, 2014) and its ability to sense these as well as petrochemical pollutants (Fernandez *et al.*, 2012). It was therefore interesting to investigate how well the strain coped with production of fluorescent proteins from the MFO reporter. Another area of interest is that the level of nitrogen in the environment is an important factor that affects the virulence of *Pseudomonas* species that are plant pathogens (Snoeijers *et al.*, 2000) so a reporter of the nitrogen level in the immediate environment of these bacteria during pathogenesis would allow researchers to compare this directly with the bacterial infection on a plant specimen.

In order to transfer the MFO fragment to *P. putida,* it was necessary to transfer the reporter fragment into a plasmid capable of replicating in *Pseudomonas* strains. This was not straightforward, as the highly repetitive nature of the DNA in the reporter fragment meant that it could not be amplified by PCR in order to change the restriction sites. Thus a plasmid with a suitable multiple cloning site, containing *Eco*RI and *Hin*dIII cut sites, was required. The plasmid chosen was pME6031

(Heeb *et al.*, 2000), a shuttle vector with a pSV1 replicon, giving a low copy number (5.9 ± 1.8 per cell) for replication in *Pseudomonas* strains (Heeb *et al.*, 2000).

To create the *Pseudomonas* reporter plasmid, the MFO fragment was digested out of pMFO-1 using *Eco*RI and *Hin*dIII to give a 3591 bp reporter fragment. pME6031 was also digested with *Eco*RI and *Hin*dIII to give a 8306 bp plasmid fragment. The two digest products were ligated to give an 11897 bp *Pseudomonas* reporter plasmid, pMFO-3. The pMFO-3 plasmid was used to transform electro-competent (Section 2.2.14) wild-type *P. putida* strain KT2440 by electroporation (Section 2.2.18). Cells that successfully took up the plasmid were grown up in a 5 ml overnight culture of LB, and then diluted 1 in 100 into fresh LB in a final volume of 150 µl. The cells were transferred to a 96-well plate and grown to deplete nitrogen levels at 28°C with orbital shaking at 50 rpm. The fluorescent output of the reporter plasmid was measured along with OD_{600} and the normalised and background corrected results are shown below for the YFP channel (Figure 45), CFP channel (Figure 46) and RFP channel (Figure 47).

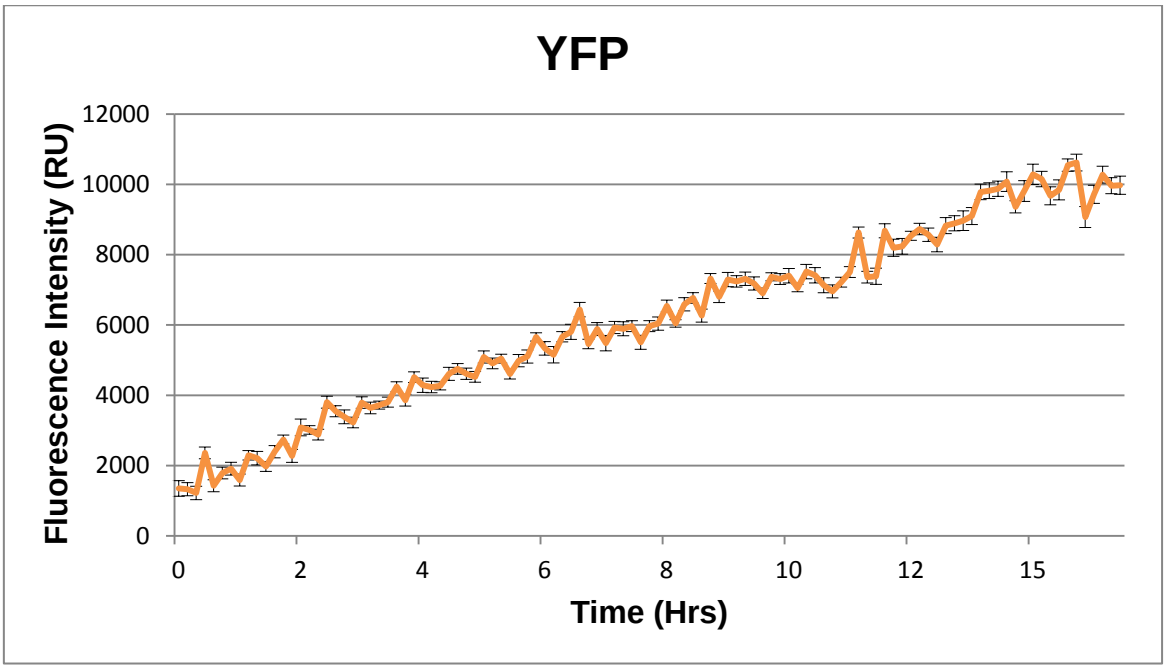

Figure 44: The total YFP output of pMFO-3 in *P. putida*. The results have been corrected for cell number by dividing the raw fluorescence data by the OD_{600} from the same time point, followed by the subtraction of fluorescence produced by non-fluorescent control cells containing an empty pME6031 plasmid. The error bars represent the standard error of the mean for three repeats.

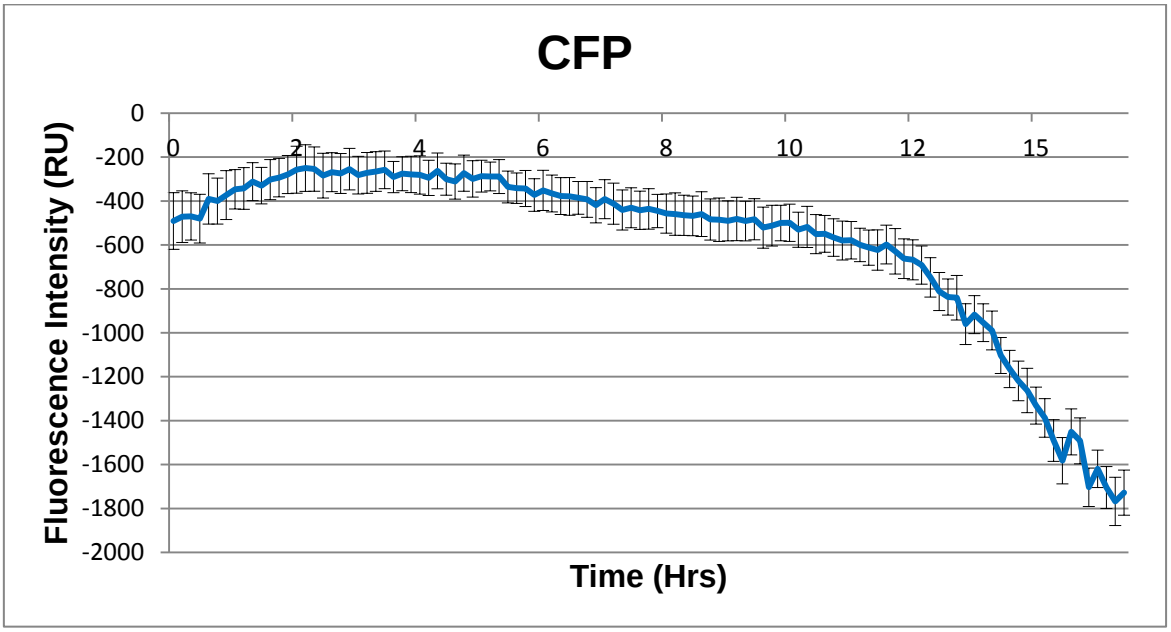

Figure 45: The total CFP output of pMFO-3 in *P. putida*. The results have been corrected for cell number by dividing the raw fluorescence data by the OD_{600} from the same time point, followed by the subtraction of fluorescence produced by non-fluorescent control cells containing an empty pME6031 plasmid. The error bars represent the standard error of the mean for three repeats.

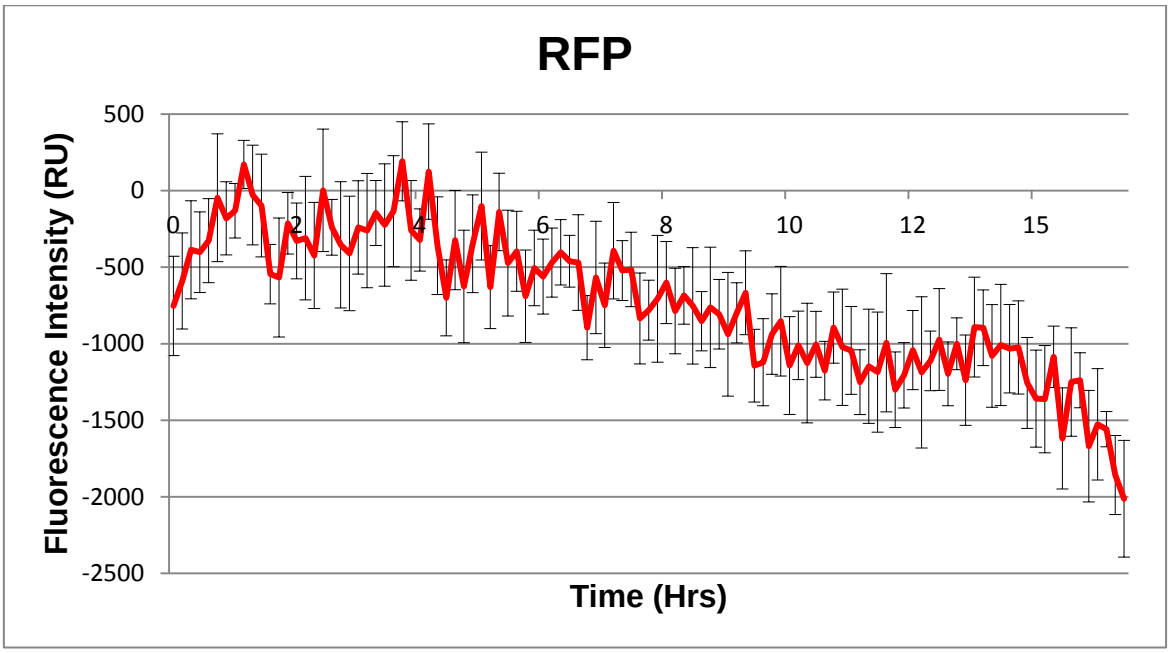

Figure 46: The total RFP output of pMFO-3 in *P. putida*. The results have been corrected for cell number by dividing the raw fluorescence data by the OD_{600} from the same time point, followed by the subtraction of fluorescence produced by non-fluorescent control cells containing an empty pME6031 plasmid. The error bars represent the standard error of the mean for three repeats.

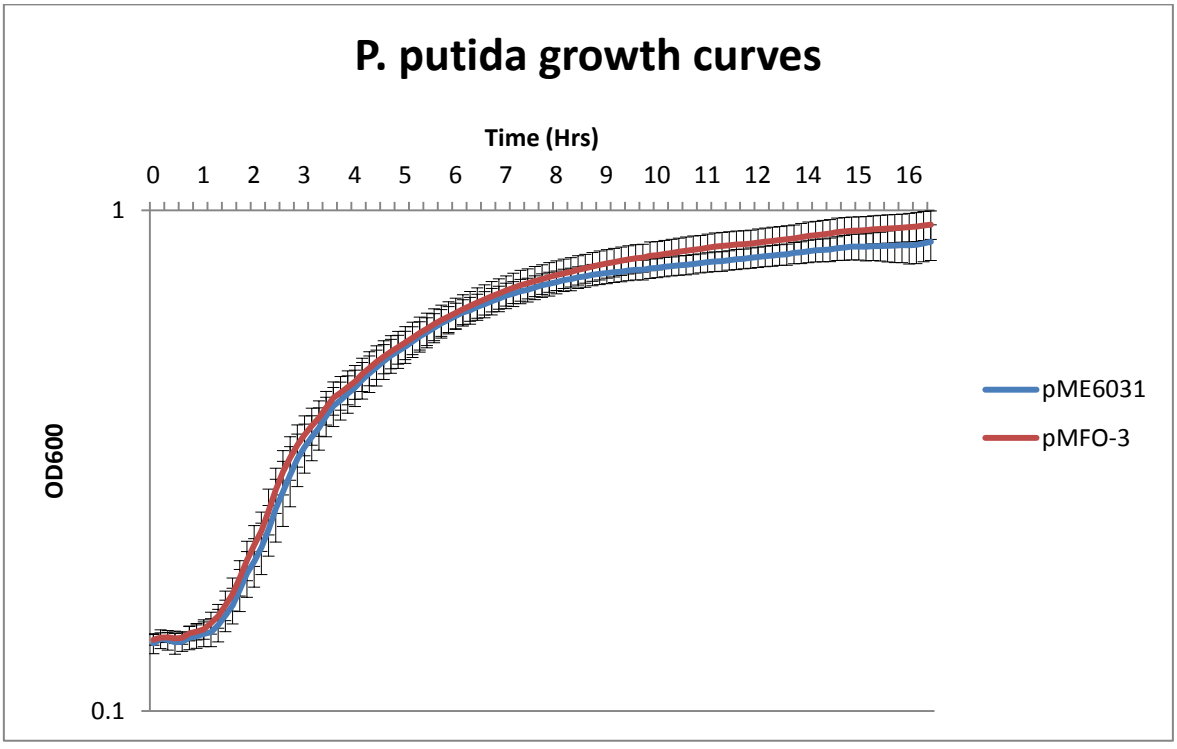

Figure 47: Growth curves of cells containing the pMFO-3 reporter plasmid and wild type control containing only the pME6031 backbone. Error bars represent standard deviation of three repeats.

The results show a response similar to that seen in *E. coli* for the YFP channel of the reporter, giving a good response curve as nitrogen levels become limiting in the growth media. It is also more of a constitutive expression, rather than aninduction. This suggests that the *P. putida* NtrC-P is capable of binding to and activating transcription from the *E. coli glnALG* promoter. However, the CFP and RFP channels of the reporter do not give a useful signal relating to the nitrogen levels in the growth media, often producing less fluorescence in these channels than seen in the wild-type control cells. This may be a result of the high levels of auto-fluorescence produced by *Pseudomonas* strains as a result of siderophore synthesis during starvation (Ponraj *et al.*, 2012) and the signal from the reporter may simply be undetectable above this background noise or due to too few NtrC present in the cells and this being titrated out by the high affinity promoter resulting in a level of output that is beyond the detection limits of the plate reader, giving higher errors in the values obtained. This could result in the negative values seen from the background subtraction after normalisation for cell number. From these results, it seems that *P. putida* performs in a similar manner to *E. coli* when grown under these conditions.

4.3 pMFO-2 in *R. sphaeroides*

The reporter plasmid, pMFO-2, was transferred into *R. sphaeroides*. *R. sphaeroides* contains two homologues of the Ntr system, an NtrB/C two component system similar to that found in *E. coli,* and an additional NtrY/X system that has a membrane bound sensory component in the two-component pathway

(Gregor *et al.*, 2007). This means that there are two potential activators of the *E. coli* promoters found on the reporter plasmid.

The reporter plasmid, pMFO-2, was used to transform *E. coli* S17-1λpir competent cells. The S17-1λpir cells were then used for conjugal transfer of the reporter plasmid into the *R. sphaeroides* cells (Section 2.2.17). The cells that took up the plasmid were grown in succinate medium (Appendix A2.4) containing appropriate antibiotics under photosynthetic conditions in a light cabinet, and then diluted 1 in 100 in a total volume of 150 µl in succinate medium and transferred to a 96 well plate. The cells were then grown in a plate reader at 30°C with orbital shaking at 50 rpm to deplete nitrogen levels in the medium. The fluorescent output of the reporter plasmid was measured as well as the OD_{700} at each time point. The cell number corrected results after subtraction of background fluorescence from control cells containing the empty pInd4 plasmid are shown for the YFP channel (Figure 49), CFP channel (Figure 50) and RFP channel (Figure 51).

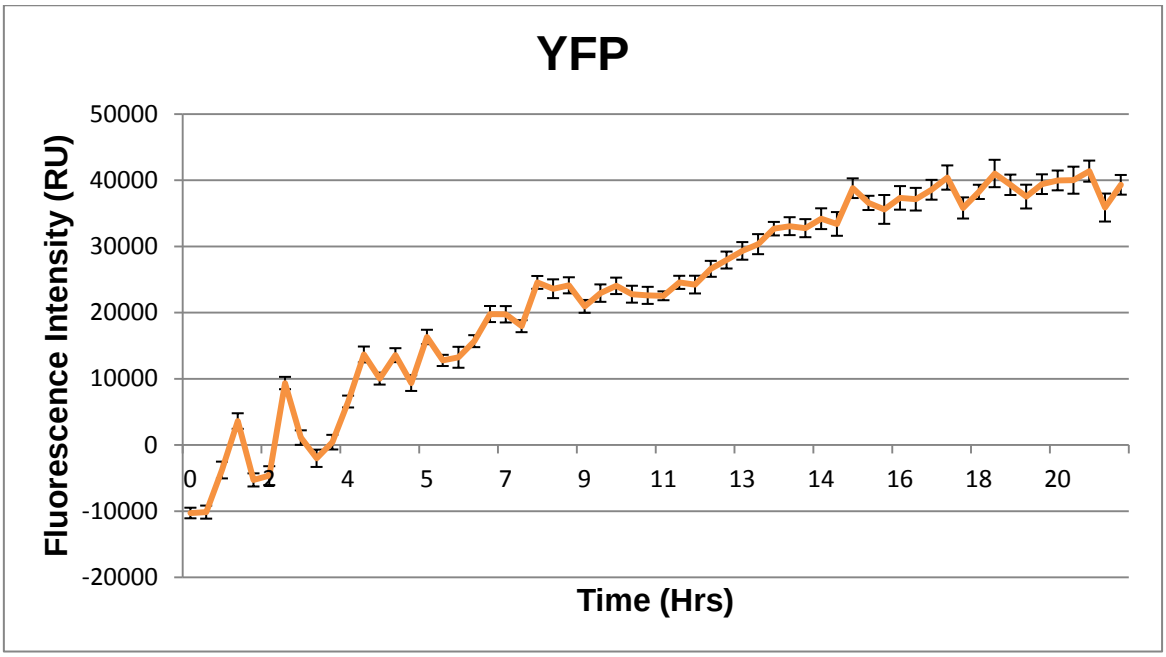

Figure 48: The total YFP output of pMFO-2 in *R. sphaeroides*. The results have been corrected for cell number by dividing the raw fluorescence data by the OD_{700} from the same time point, followed by the subtraction of fluorescence produced by non-fluorescent control cells containing an empty pInd4 plasmid. The error bars represent the standard error of the mean for three repeats.

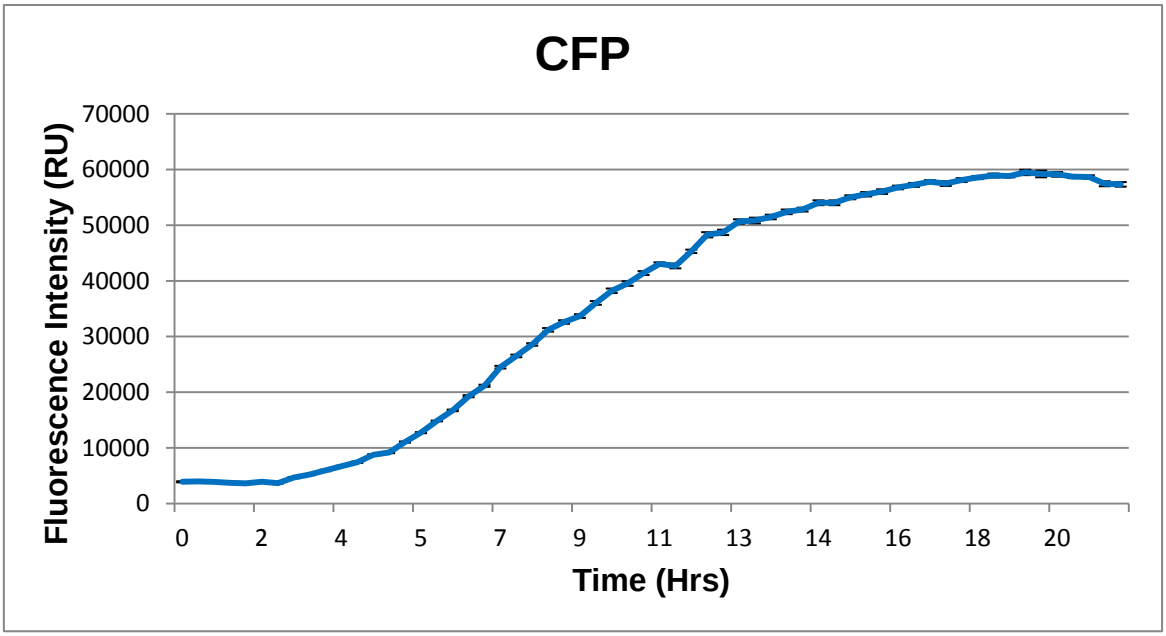

Figure 49: The total CFP output of pMFO-2 in *R. sphaeroides*. The results have been corrected for cell number by dividing the raw fluorescence data by the OD_{700} from the same time point, followed by the subtraction of fluorescence produced by non-fluorescent control cells containing an empty pInd4 plasmid. The error bars represent the standard error of the mean for three repeats.

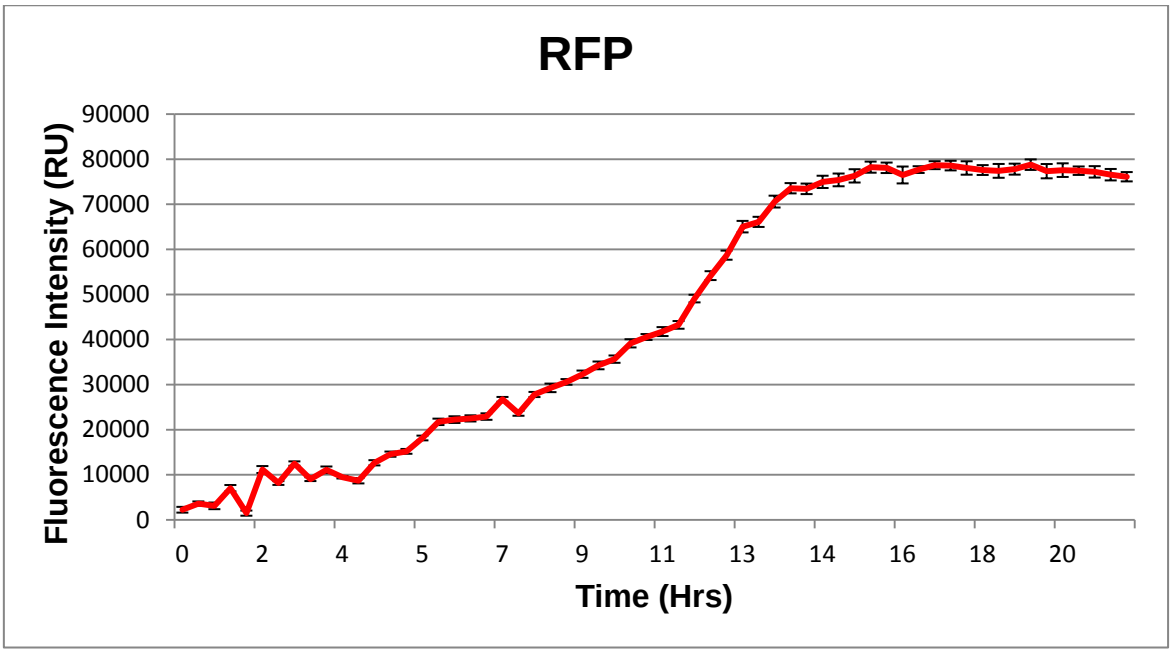

Figure 50: The total RFP output of pMFO-2 in *R. sphaeroides*. The results have been corrected for cell number by dividing the raw fluorescence data by the OD_{700} from the same time point, followed by the subtraction of fluorescence produced by non-fluorescent control cells containing an empty pInd4 plasmid. The error bars represent the standard error of the mean for three repeats.

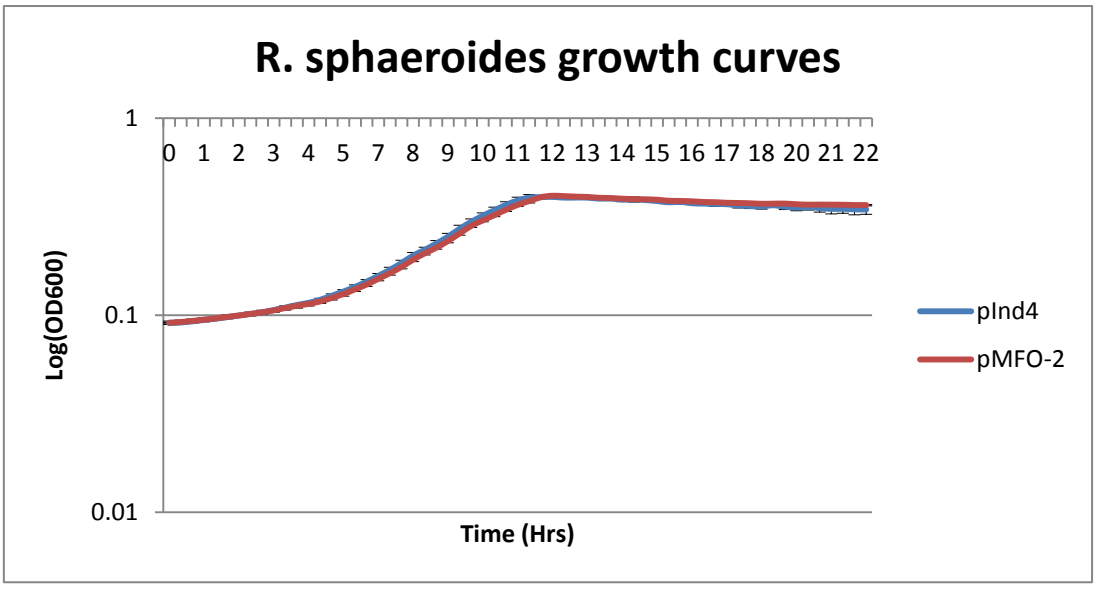

Figure 51: Growth curves of cells containing the pMFO-2 reporter plasmid and wild type control containing only the pInd4 backbone. Error bars represent standard deviation of error of the mean for 3 repeats.

The results show that either the *R. sphaeroides* NtrC-P or NtrX-P is capable of activating expression from all three of the *E. coli* promoters, as a high level of fluorescence output is observed in the YFP, CFP and RFP channels. It is possible that as the copy number of the reporter plasmid in *R. sphaeroides* is only ~20, all of the reporters are fully activated as there is sufficient NtrC-P or NtrX-P to activate them all. Although the YFP expression still appears to be constitutive, the CFP and RFP reporters respond in an induced manner.

4.4 Varying ammonium concentrations in *R. sphaeroides* growth media

To investigate whether the maximum level of fluorescent protein produced in *R. sphaeroides* is affected by the level of nitrogen in the growth media, the cells were grown up under photosynthetic conditions and then transferred into succinate media supplemented with 0 mM, 10 mM, 20 mM, or 50 mM ammonium (Figure 53).

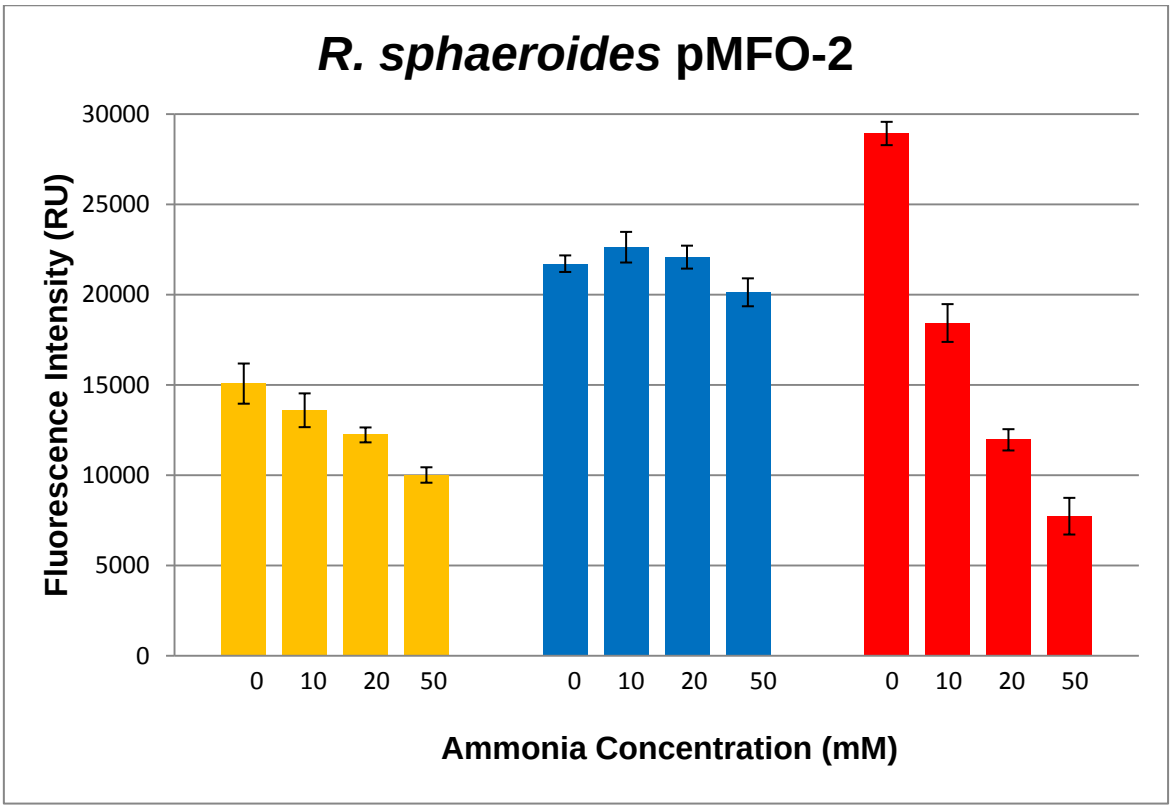

Figure 52: The maximum output of YFP, CFP, and RFP fluorescence from pMFO-2 in *R. sphaeroides* when grown to stationary phase in succinate media; supplemented with 0 mM, 10 mM, 20 mM, and 50mM ammonium. The results have been corrected for cell number by dividing the raw fluorescence data by the OD_{700} from the same time point, followed by the subtraction of fluorescence produced by non-fluorescent control cells containing an empty pInd plasmid. The error bars represent the standard error of the mean for three biological repeats.

The results show that when the level of supplemented ammonium is increased in the succinate growth media, the level of maximum florescence output in the RFP and YFP channels of the reporter plasmid steadily decreases. There is also a decrease in the CFP channel between 10 mM and 50 mM ammonium concentrations, although the output level at 0 mM is lower than that at 10 mM.

4.5 Discussion

The MFO reporter fragment was transferred into plasmids capable of replication in *P. putida* (pMFO-3) and *R. sphaeroides* (pMFO-2). The production of fluorescent proteins from the MFO reporter was observed in both *P. putida* and *R. sphaeroides,* showing that the *E. coli* promoters used in the reporter fragment could be bound by the NtrC-P of the new host species (or potentially NtrX-P in *R. sphaeroides*) and that these response regulators could successfully activate transcription from the promoters.

The expression of fluorescence from pMFO-3 in *P. putida* is similar to that of wild-type *E. coli.* A good response is seen in the YFP channel from the high affinity promoter, but the CFP and RFP channels show very little fluorescence above the background auto-fluorescence measured in the control cells. This is likely to be a result of the release of compounds from cell lysis during starvation and possibly due to auto-fluorescence associated with *Pseudomonas* strains. It is also possible that filamentous cells are forming, resulting in inaccurate background subtraction after cell number correction due to OD values no longer corresponding to cell number or the copy number of the plasmid is still too high and titrating out all of the NtrC-P.

The expression of fluorescence from the pMFO-2 reporter plasmid in *R. sphaeroides* shows a strong level of fluorescence output in all three channels. This could be a result of the additional response regulator NtrX that is found in *R. sphaeroides.* Alternatively, the low copy number of pMFO-2 in *R. sphaeroides*

(~20 copies per cell) may result in the high affinity promoters not sequestering all of the available NtrC-P, therefore allowing induction from the medium and low affinity promoters.

The reporter plasmid pMFO-2 in *R. sphaeroides* also shows a good response to the supplementation of ammonium in the growth media, showing a decrease in fluorescence as the level of supplemented ammonium is increased in all reporter channels with the exception of the CFP channel when 0 mM ammonium was added.

The results here demonstrate the potential for the use of the MFO reporter in other species in order to expand the repertoire of potential analytes to apply the MFO reporter for a biosensor or to have a more robust host to detect environmental pollutants.

The results so far from *E. coli* and from other species show that the MFO plasmid can respond in the required manner to report the level of ammonium in the environment. However, the fact that this system is tightly bound to the host cell's mechanism for conservation of nitrogen (and hence ability to synthesise proteins, including the fluorescent proteins used as the output) complicates its analysis. There is also the problem of a limited amount of NtrC-P in the cell when expressed from its native gene on the genome. This could be addressed by using a very low copy number reporter plasmid, but would result in a low signal output from the reporter, which may not be detectable above background noise. The over

expression of any protein in the cell has the potential to limit amino acid availability for synthesis of other essential proteins that the cell needs, putting additional stress on the host cell.

To address this issue the production of the output from the MFO reporter could also be decoupled from nitrogen limitation to get a cleaner response from the system by using a constitutively active form of NtrC, NtrC* produced from a second plasmid in the host cell. This would allow a high copy number reporter to be used for a high signal to noise ratio and a higher amount of the transcriptional activator (NtrC*) to be made so that the high affinity promoters do not sequester all of it. This would also enable the use of nutrient rich medium to sustain the levels of protein expression needed for the biosensor to function.

5. Constitutively active NtrC

5.1 Introduction

It has been shown that the MFO reporter plasmid can give a fluorescent output in response to different concentrations of nitrogen in the growth media. However our aim is to use the MFO reporter to respond to other chemicals in a sample. Therefore, we need to link the production of NtrC-P to something other than nitrogen availability. Previously, it has been shown that a number of different point mutations can convert NtrC into a constitutively active form (NtrC*) which will activate transcription even when not phosphorylated by NtrB (Flashner *et al.*, 1995). We therefore decided to see whether the induction of NtrC* would generate an output from the MFO reporter plasmid (Figure 54).

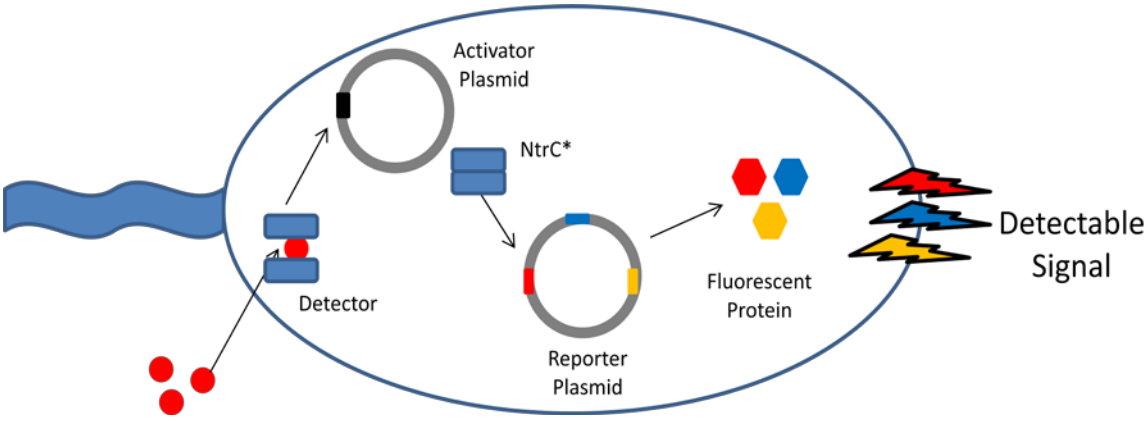

Figure 53: The MFO reporter plasmid under the control of NtrC*. The production of NtrC* is under the control of an activator plasmid containing the *NtrC** gene under the control of an inducible promoter.

The activator plasmid would allow large amounts of NtrC* to be produced in excess of the ~70 dimers from the genomic *ntrC* gene. This would also remove the requirement for the activation of the host NtrC regulon for the system to work. The plasmids pACYCDuet-1 and pBMTBX-4 were chosen as they were compatible with the pMFO-1 reporter plasmid and had IPTG and arabinose inducible promoters respectively upstream of a multiple cloning site. This would allow the induction of NtrC* production from an activator plasmid to test the reporter system without the need for nitrogen depletion.

5.2 Alignment of *ntrC* genes

Constitutively active forms of NtrC have been engineered and studied in *S. typhimurium* (Flashner *et al.*, 1995). This showed that a number of mutations in NtrC of *S. typhimurium* resulted in activation of transcription from NtrC-P regulated promoters without the need for its phosphorylation by NtrB. The highest level of transcriptional activation was seen from the double mutation D54E, a mutation in the phosphorylation site, and S160F, a mutation in the central domain of NtrC. This produces transcriptional activation close to that of wild-type NtrC-P, even in the absence of the kinase NtrB (Klose *et al.*, 1993). The NtrC proteins of *S. typhimurium* and *E. coli* were aligned using Clone Manager (Figure 55), which showed that the two proteins had 96 % identity in their amino acid sequence and therefore it is probable that the mutations which produced constitutively active forms of NtrC in *S. typhimurium* would also make *E. coli* NtrC constitutively active. Primers were designed to create the equivalent D54E and S160F mutations in the *E. coli ntrC* gene.

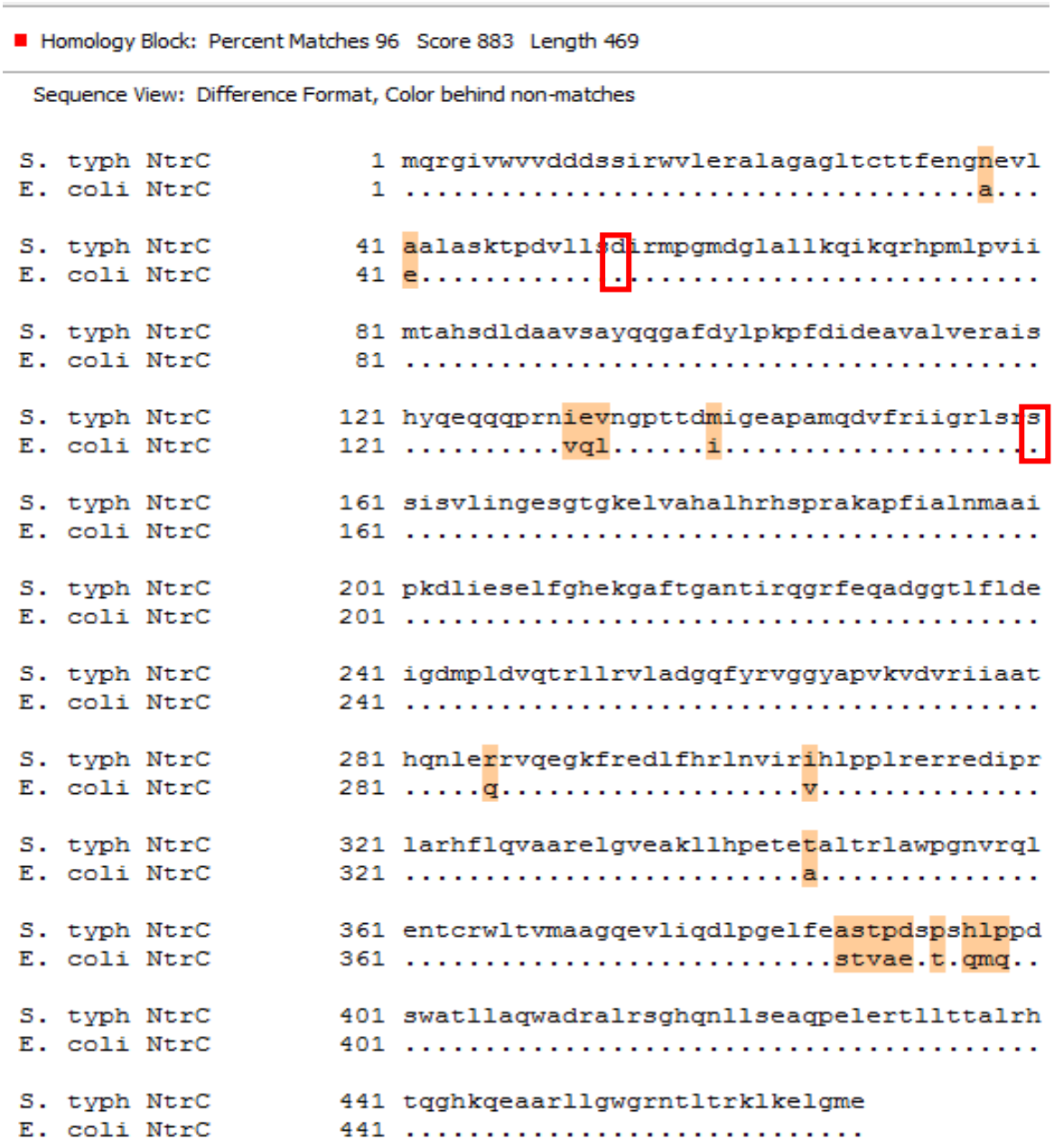

Figure 54: Alignment of the *S. typhimurium* and *E. coli* NtrC protein sequences showing 96% identity between the two proteins. The highlighted residues are where the *E. coli* sequence differs from that of *S. typhimurium* NtrC. The conserved residues D54 and S160 which make *S. typhimurium* NtrC constitutively active are highlighted in red.

5.3 Construction of *ntrC**

The alignment of the *S. typhimurium* and *E. coli* NtrC proteins was used to create the equivalent mutations in *E. coli* to those that successfully activated transcription in *S. typhimurium* (Figure 55). The highest level of transcriptional activation in the *S. typhimurium* mutants was seen in a double mutant NtrC containing the amino acid changes D54E and S160F.

Site-directed mutagenesis of the *ntrC* gene was carried out using overlap-extension PCR (Section 2.2.5). Primers (Appendix A1.2) were designed to introduce a mismatch mutation into the *ntrC* gene, the mismatch mutation C479T results in the amino acid change S160F.

In the first round of PCR, the first 479 bps of the *E. coli ntrC* gene were amplified from *E. coli* genomic DNA using primers S160FA and S160FB and in a separate reaction the last 928 bps were amplified from *E. coli* genomic DNA using primers S160FC and S160FD. In the second overlap-extension PCR, the products from the first round were annealed and extended using the external primers S160FA and S160FD. Fusion of the two fragments of the *E. coli ntrC* gene was made possible as the internal primers, S160FB and S160FC, were designed to contain complementary regions as well as the point mutation required to mutate the amino acid from serine to phenylalanine. This process is summarised in Figure 21 and resulted in the formation of *ntrC*.*

The *ntrC** overlap-extension PCR product was digested with *Nco*I and *Hin*dIII (primer S160FA was designed so that it was flanked with *Nco*I and primer S160FD was designed so that it was flanked with *Hin*dIII), and ligated into similarly digested pBMTBX-4 (Prior *et al.*, 2010) resulting in a 6.8 kb pAraNtrC* activator plasmid.

Primers (Appendix A1.2) were also designed to introduce the second mismatch mutation into the *ntrC** gene, the mismatch mutation C162A results in the amino acid change D54E.

In the first round of PCR the first 162 bps of the *E. coli ntrC** gene were amplified from pAraNtrC* using primers D54EA and D54EB and in a separate reaction the last 1245 bps were amplified from pAraNtrC* using primers D54EC and D54ED. In the second overlap-extension PCR, the products from the first round were annealed and extended using the external primers D54EA and D54ED. Fusion of the two fragments of the *E. coli ntrC* gene was made possible as the internal primers, D54EB and D54EC, were designed to contain complementary regions as well as the point mutation required to mutate the amino acid from aspartate to glutamate. This process resulted in the formation of *ntrC***.*

The *ntrC*** overlap-extension PCR product was digested with *Nco*I and *Hin*dIII (primer D54EA was designed so that it was flanked with *Nco*I and primer D54ED was designed so that it was flanked with *Hin*dIII), and ligated into similarly

digested pBMTBX-4 (Prior *et al.*, 2010) resulting in a 6.8 kb pAraNtrC** activator plasmid.

Cells transformed with pAraNtrC** containing both point mutations did not grow. However, as the pAraNtrC* plasmid with the single S160F point mutation had already been grown successfully in XL-1 blue cells, this was used to test the constitutively active *E. coli* NtrC* as this mutation alone produced a good level of transcriptional activation in the absence of NtrB in the equivalent *S. typhimurium* experiments (Flashner *et al.*, 1995).

pAraNtrC* was transformed into competent C43 *E. coli* that already contained the pMFO-1 reporter plasmid. It was possible to use both plasmids in the same cell as the pMFO-1 plasmid contains the ColE1 origin of replication and confers resistance to ampicillin, whereas the pBMTBM-4 plasmid contains the BHR origin of replication and confers resistance to tetracycline. This allows both plasmids to replicate and to be selected for using the two different antibiotics. Activation of transcription by NtrC* was tested by incubating the cells with different concentrations of L-arabinose and measuring the fluorescence output from the pMFO-1 reporter plasmid.

5.4 Arabinose induction of *ntrC**

The *E. coli* strain C43 containing both pMFO-1 and pAraNtrC* plasmids, and as a control for background fluorescence the *E. coli* strain C43 containing only the pAraNtrC* plasmid, were grown overnight in LB containing appropriate antibiotics.

The overnight cultures were then sub-cultured 1 in 50 into fresh LB containing appropriate antibiotics and grown to an OD_{600} of 0.6. 1 ml of the culture was centrifuged in a bench top centrifuge at 4000 g and re-suspended in M9 minimal media (Appendix A2.3) containing appropriate antibiotics, 128 mM NH_4Cl to suppress phosphorylation of the natural NtrC, and either 0% or 0.05% L-arabinose to induce expression of NtrC*. 0% L-arabinose acts as the control as it should not induce any expression of NtrC*. 150 µl of the cell culture was transferred to a 96-well plate and incubated at 30°C to allow induction of NtrC*. The fluorescence output of the reporter plasmid was measured for each different concentration of L-arabinose in a plate reader. The total YFP (Figure 56), CFP (Figure 57) and RFP (Figure 58) after normalisation for cell number and subtraction of C43 control cells containing only the pAraNtrC* were calculated.

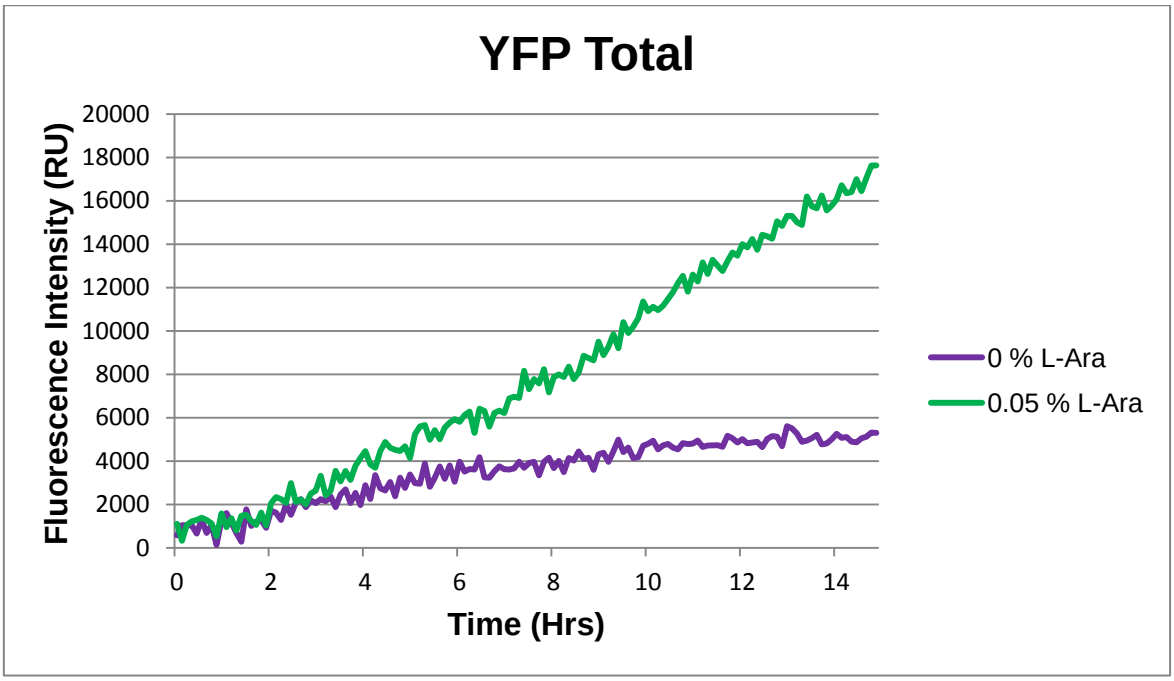

Figure 55: The total fluorescence response in the YFP channel in response to the presence and absence of the inducer L-arabinose. The results have been corrected for cell number by dividing the raw fluorescence data by the OD_{600} from the same time point, followed by the subtraction of fluorescence produced by non-fluorescent control cells containing the pAraNtrC* plasmid.

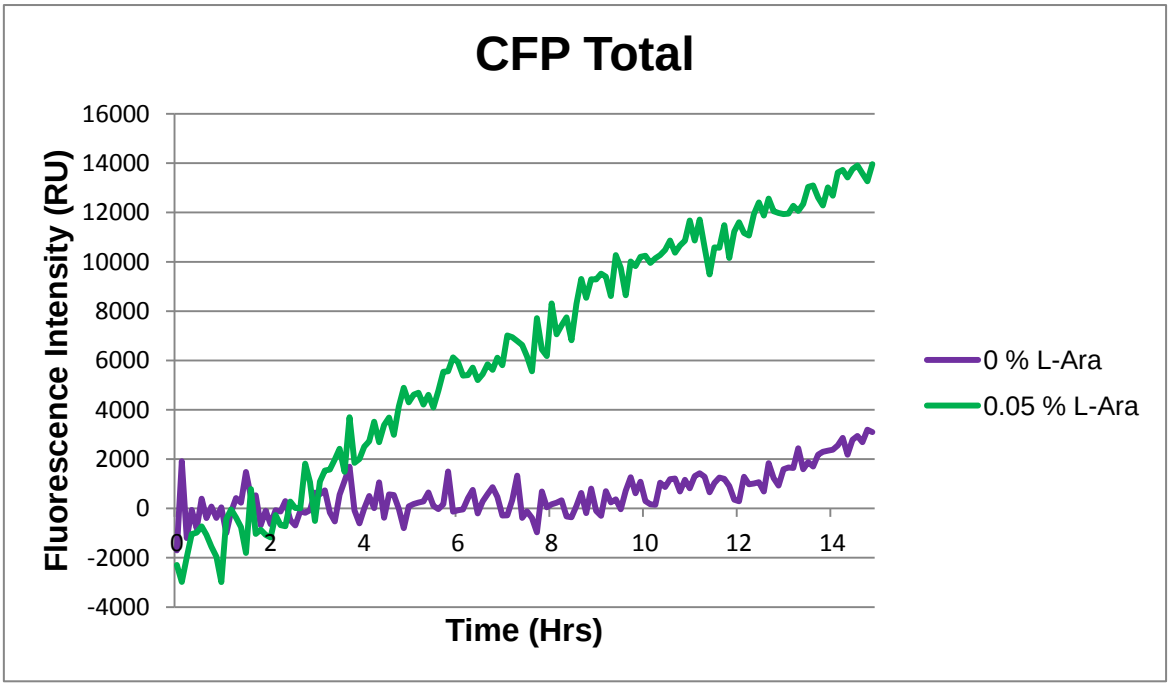

Figure 56: The total fluorescence response in the CFP channel in response to the presence and absence of the inducer L-arabinose. The results have been corrected for cell number by dividing the raw fluorescence data by the OD_{600} from

the same time point, followed by the subtraction of fluorescence produced by non-fluorescent control cells containing the pAraNtrC* plasmid.

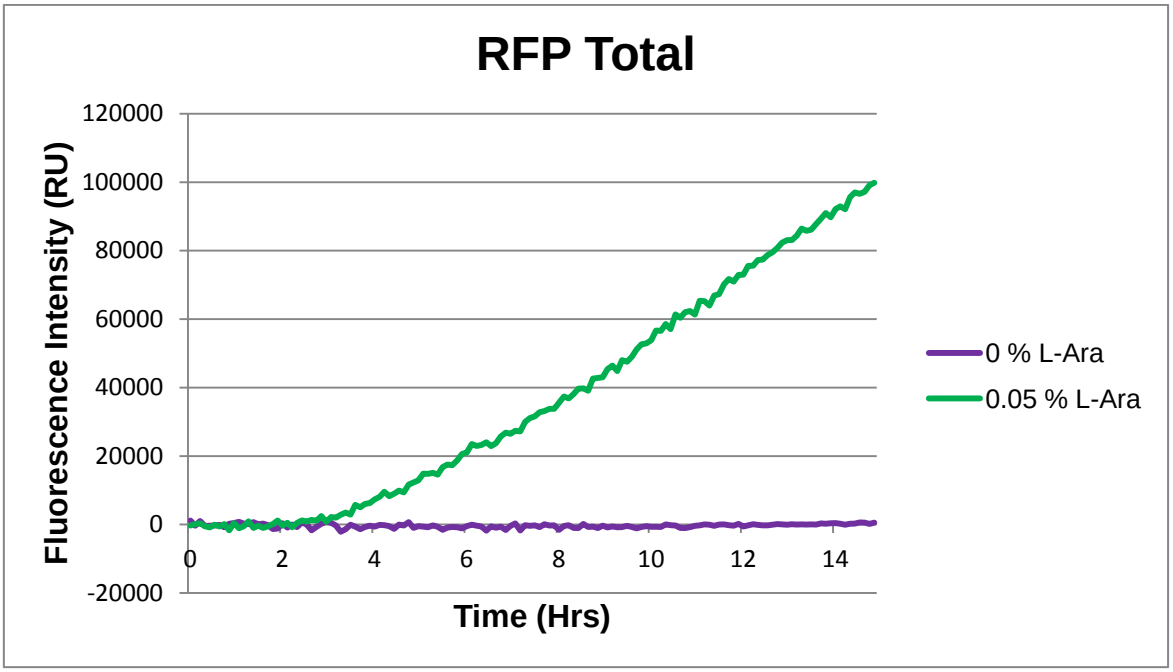

Figure 57: The total fluorescence response in the RFP channel in response to the presence and absence of the inducer L-arabinose. The results have been corrected for cell number by dividing the raw fluorescence data by the OD_{600} from the same time point, followed by the subtraction of fluorescence produced by non-fluorescent control cells containing the pAraNtrC* plasmid.

The results show that the increase in L-arabinose from 0% (no induction) to 0.05% (high induction), gives a large increase in fluorescence signal from the reporter plasmid in all three of the reporter channels.

5.5 IPTG induction of *ntrC**

The arabinose inducible promoter is known to act more as a switch in inducing protein expression in individual cells than as a graded inducer of protein synthesis (Megerle *et al.*, 2008;Siegele and Hu, 1997). Therefore, *ntrC** was transferred into

an IPTG inducible vector, pACYCDuet-1 (Novogen), for subsequent analysis. The IPTG induction of transcription acts as a graded inducer (Lutz and Bornscheuer, 2012), which will allow us to create a calibration curve for IPTG using our biosensor.

The overlap-extension PCR product, NtrC* (Section 5.3), was digested with *Nc*oI and *Hin*dIII. In a similar reaction pACYCDuet-1 was also digested with *Nc*oI and *Hin*dIII. The digested PCR NtrC* was ligated into pACYCDuet-1 to create a second activator plasmid, pLacNtrC*.

The activator plasmid, pLacNtrC*, was transformed into competent *E. coli* C43 cells that already contained the reporter plasmid, pMFO-1. It was possible to use both plasmids in the same cell as the pMFO-1 plasmid contains the ColE1 origin of replication and confers resistance to ampicillin, whereas the pACYCDuet-1 plasmid contains the P15A origin of replication and confers resistance to chloramphenicol. This allows both plasmids to replicate and to be selected for using the two different antibiotics. Activation of transcription by NtrC* was tested by incubating the cells with different concentrations of IPTG and measuring the fluorescence output from the pMFO-1 reporter plasmid.

The *E. coli* strain C43 containing both pMFO-1 and pLacNtrC* plasmids, and as a control for background fluorescence the *E. coli* strain C43 containing only the pLacNtrC* plasmid, were grown overnight in LB containing appropriate antibiotics. The overnight cultures were then sub-cultured 1 in 50 into fresh LB containing

appropriate antibiotics and grown to an OD_{600} of 0.6. 1 ml of the culture was spun down in a bench top centrifuge and re-suspended in M9 minimal media (Appendix A2.3) containing appropriate antibiotics, 128 mM NH_4Cl to suppress phosphorylation of the natural NtrC, and IPTG ranging in concentration from 0 μM to 256 μM to induce expression of NtrC*. 150 μl of the cell culture was transferred to a 96-well plate and incubated at 30°C to allow induction of expression of NtrC*. The fluorescence output of the reporter plasmid was measured for each different concentration of IPTG in a plate reader. The total fluorescence output is shown below for the YFP channel (Figure 59), CFP channel (Figure 60) and RFP channel (Figure 61).

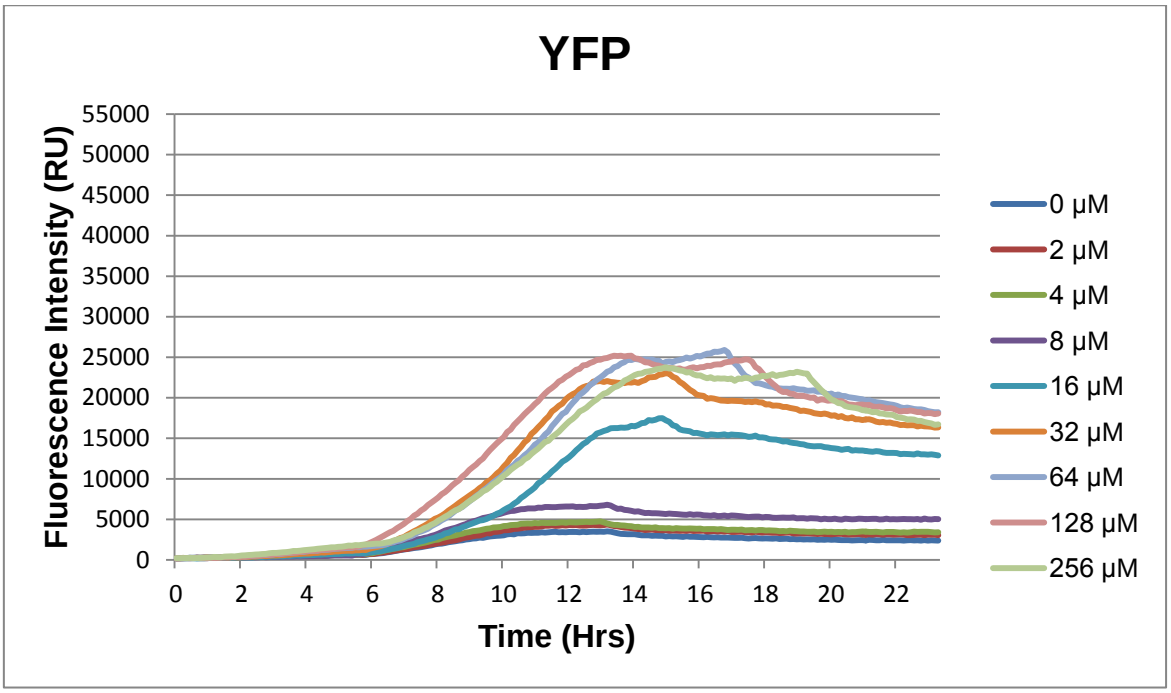

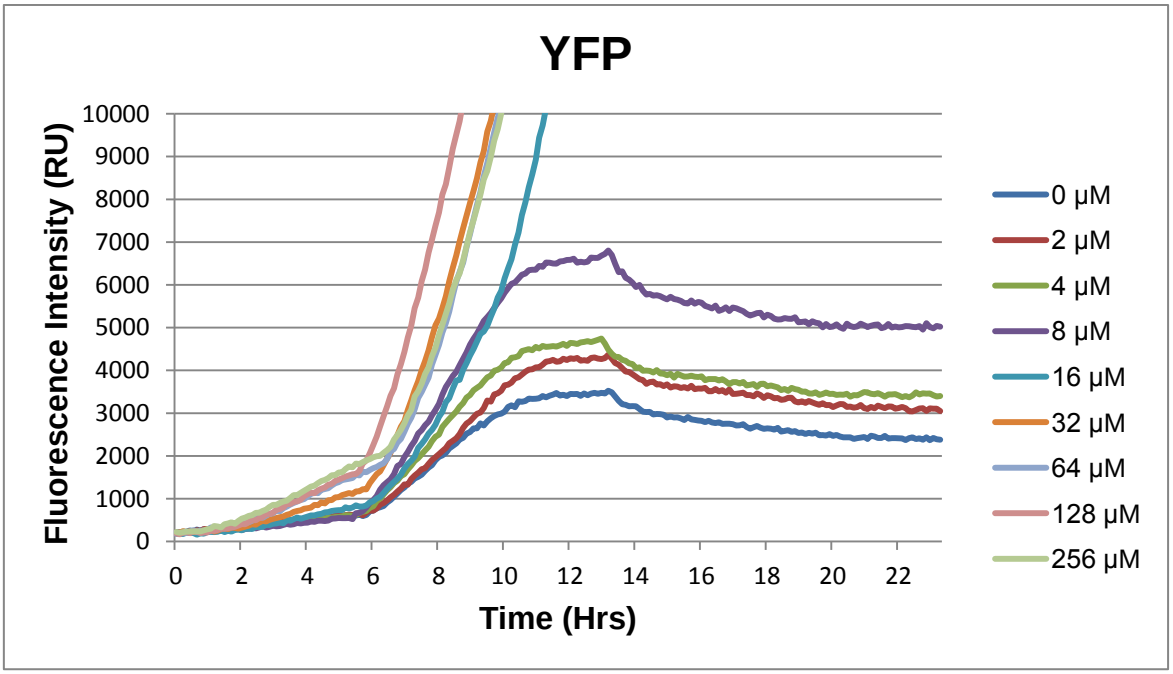

Figure 58: The total fluorescence response in the YFP channel to varying concentrations of IPTG. The results have been corrected for cell number by dividing the raw fluorescence data by the OD_{600} from the same time point, followed by the subtraction of fluorescence produced by non-fluorescent control cells containing the empty pACYCDeut-1 plasmid. The two graphs represent the same data, but the lower graph is zoomed in to show responses at low levels of induction.

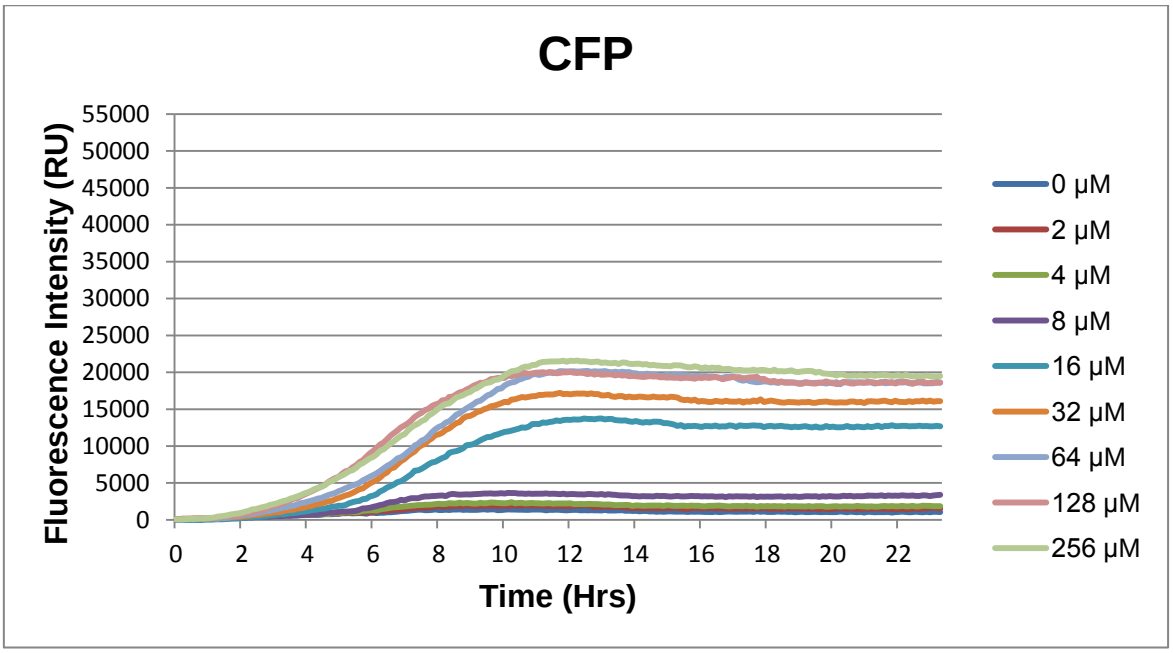

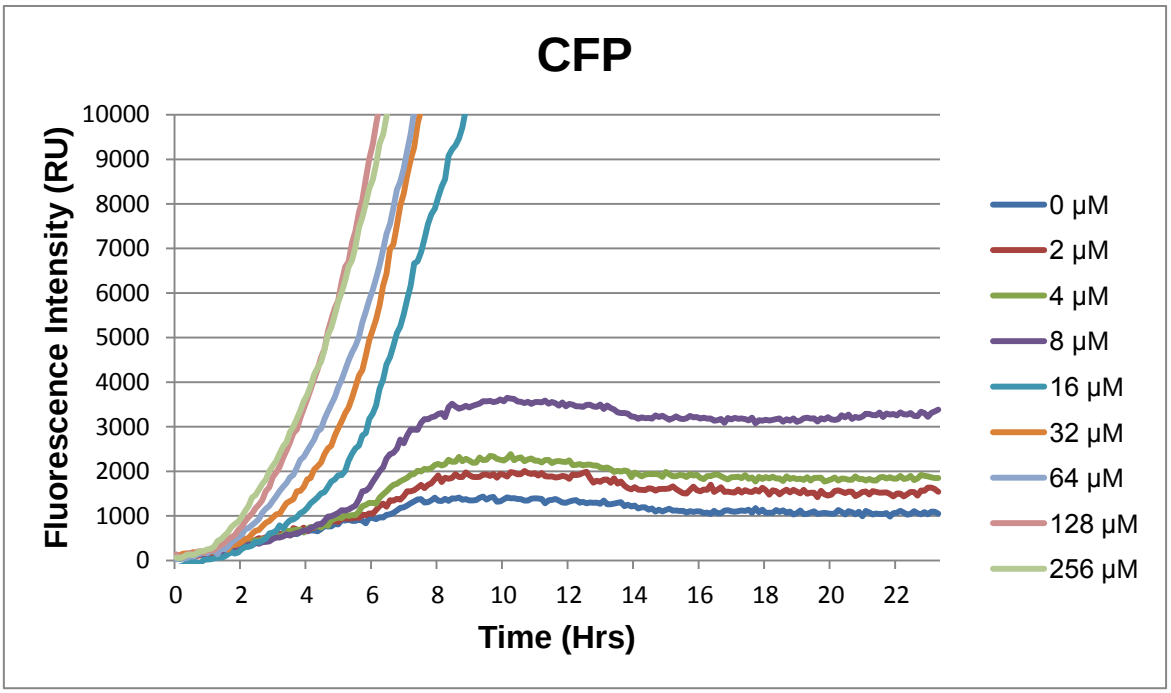

Figure 59: The total fluorescence response in the CFP channel to varying concentrations of IPTG. The results have been corrected for cell number by dividing the raw fluorescence data by the OD_{600} from the same time point, followed by the subtraction of fluorescence produced by non-fluorescent control cells containing the empty pACYCDeut-1 plasmid. The two graphs represent the same data, but the lower graph is zoomed in to show responses at low levels of induction.

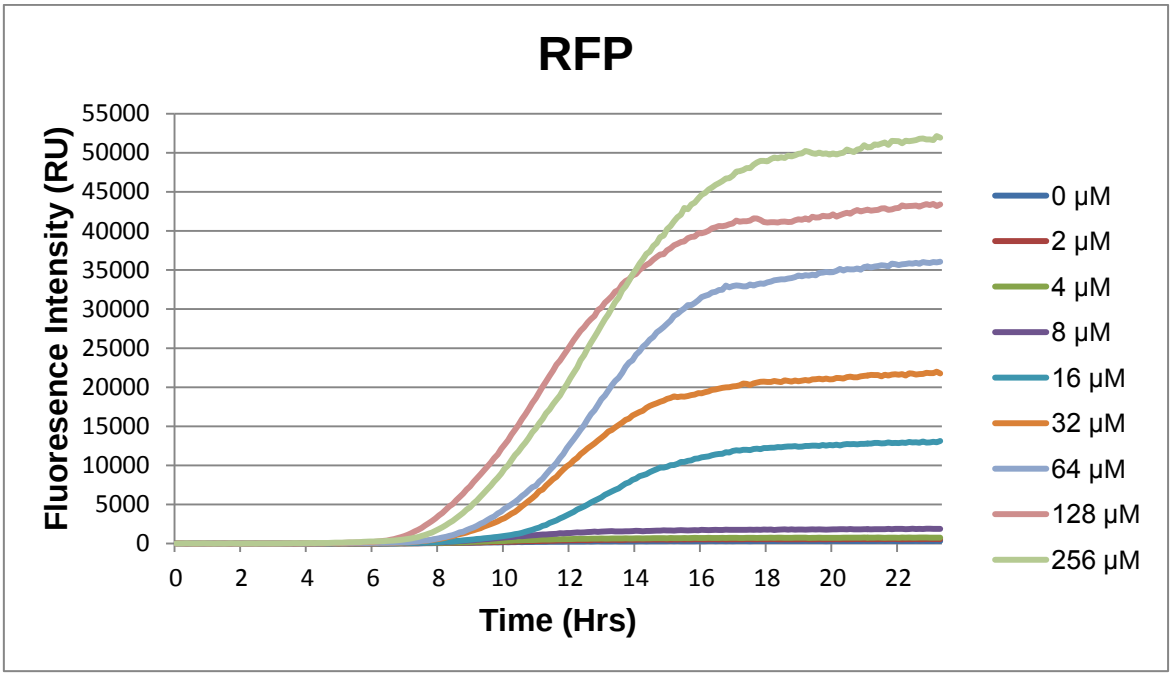

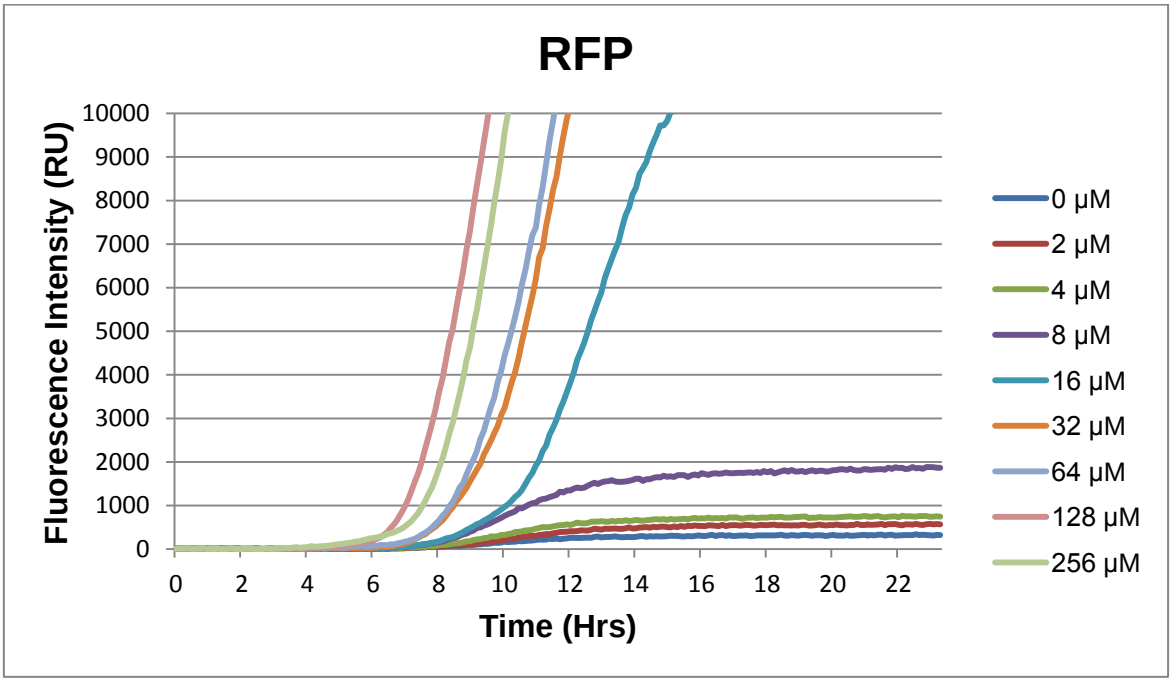

Figure 60: The total fluorescence response in the RFP channel to varying concentrations of IPTG. The results have been corrected for cell number by dividing the raw fluorescence data by the OD_{600} from the same time point, followed by the subtraction of fluorescence produced by non-fluorescent control cells containing the empty pACYCDeut-1 plasmid. The two graphs represent the same

data, but the lower graph is zoomed in to show responses at low levels of induction.

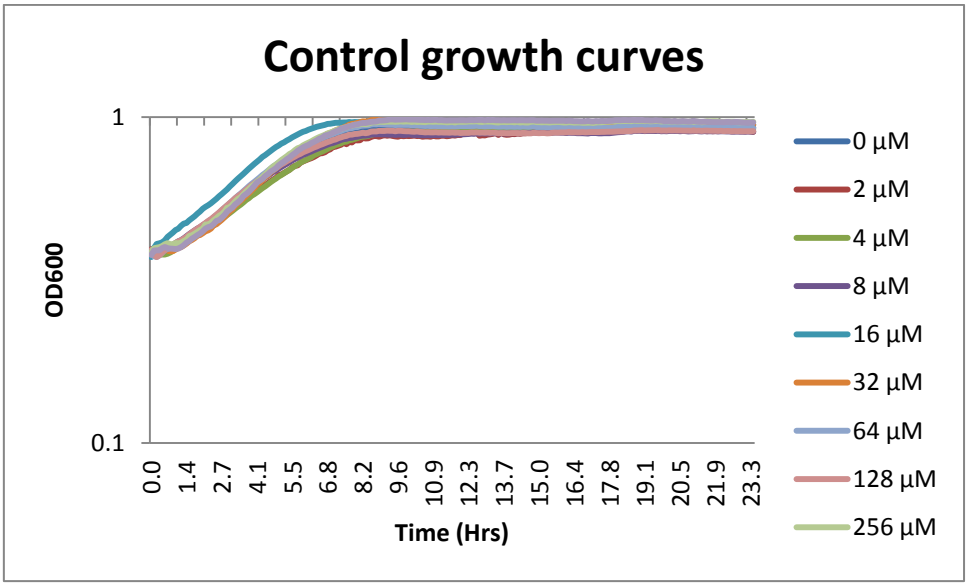

Figure 61: Growth curves of cells containing the pMFO-1 reporter plasmid and empty pACYCDeut-1 in the presence of increasing concentration of IPTG.

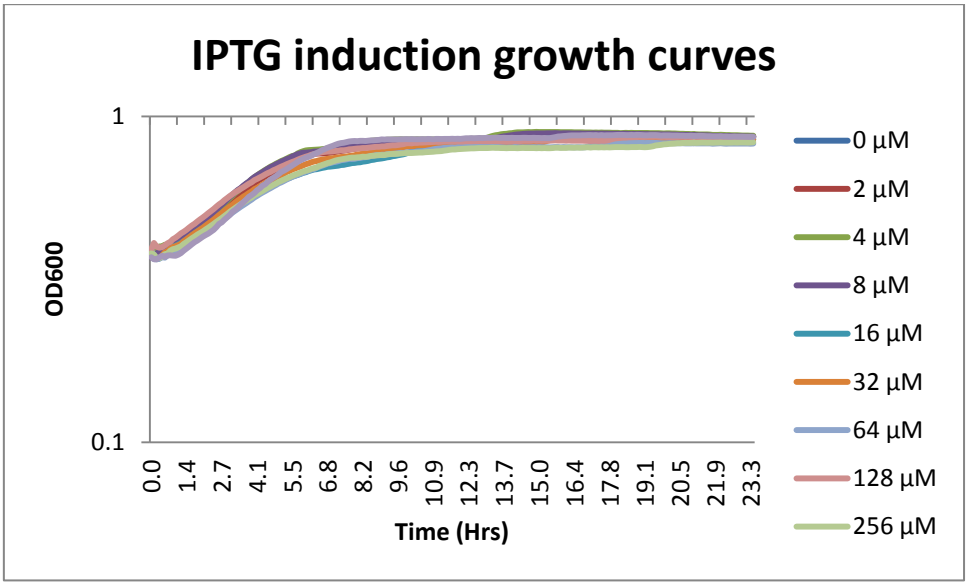

Figure 62: Growth curves of cells containing the pMFO-1 reporter plasmid and pLacNtrC* in the presence of increasing concentration of IPTG.

The increasing IPTG concentration induces production of more NtrC* from the activator plasmid, which goes on to activate transcription of the fluorescent proteins from the reporter plasmid. This shows that NtrC* is capable of activating transcription from the *E. coli ntr* promoters used in the reporter plasmid even when nitrogen levels are plentiful in the growth media, thus eliminating the requirement for the NtrB protein kinase.

The high affinity reporter, producing the YFP signal, is better at resolving differences in concentration of IPTG at low concentration levels (0 µM, 2 µM, 4 µM and 8 µM) than the medium and low affinity reporters. The Low affinity reporter, producing the RFP signal, is much better at resolving differences in concentrations of IPTG at high concentration levels (16 µM, 32 µM, 64 µM, 128 µM, and 256 µM) than the high and medium affinity reporters. The medium affinity reporter, producing the CFP signal, performs well in the mid-range concentrations of IPTG (8 µM, 16 µM, and 32 µM) but cannot resolve differences in concentrations at the upper and lower limits.

This means that with the MFO reporter it is possible to distinguish between the full range of concentrations of IPTG if you were to use this as a biosensor, however, if only one of the different affinity reporters were present in a biosensor then there would be information missing at either the upper or lower concentration limits. Growth of cells is not adversely affected by the production of NtrC* and the resulting fluorescent proteins (see Figure 62 & Figure 63).

5.6 Ratio of two fluorescent outputs

The MFO reporter can also be used to take a ratio of two of the fluorescent outputs instead of just looking at the information from the three individual fluorescence channels of the reporter. This should reduce the variation in fluorescence output of the reporter as it removes the errors associated with varying copy number of plasmids and proteins in the host cell. The absolute maximum fluorescence output in response to different concentrations of IPTG are shown below for the YFP channel (Figure 64), CFP channel (Figure 65) and RFP channel (Figure 66). The result of taking a ratio of the CFP and RFP reporter outputs are shown in Figure 67.

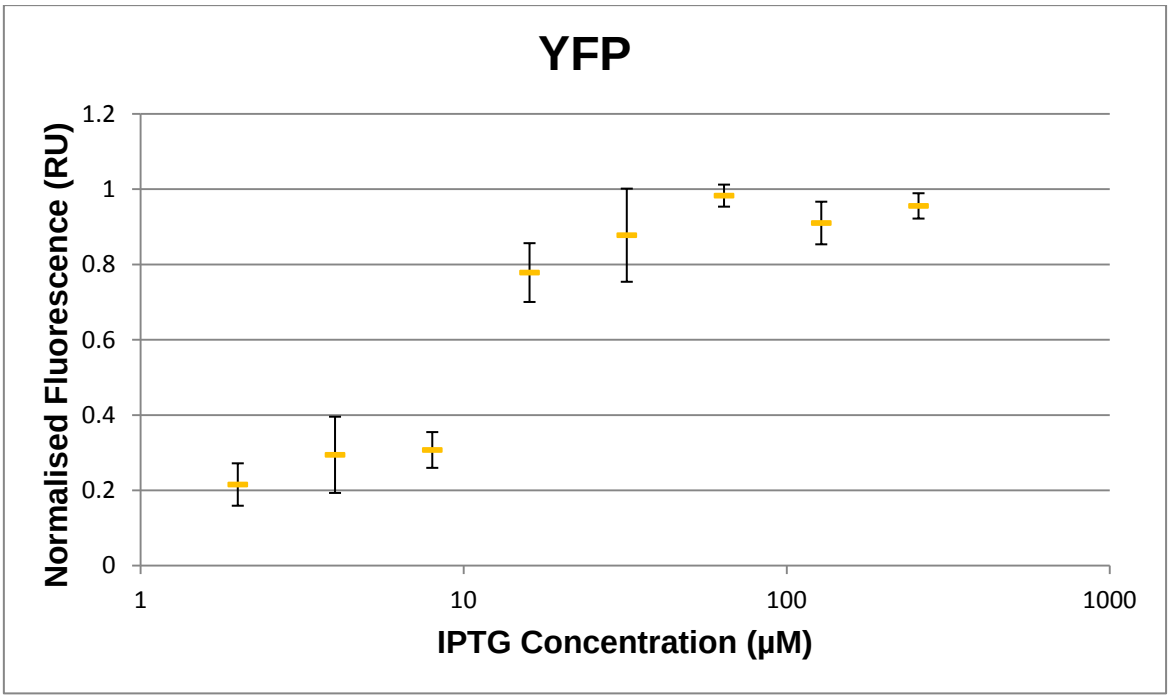

Figure 63: The maximum fluorescence output in the YFP channel in response to different concentrations of the inducer IPTG. The data has been normalised for cell number and fluorescence from control cells grown under the same conditions has been subtracted and displayed at a percentage of maximum fluorescence. The error bars represent the standard error of the mean for three biological repeats.

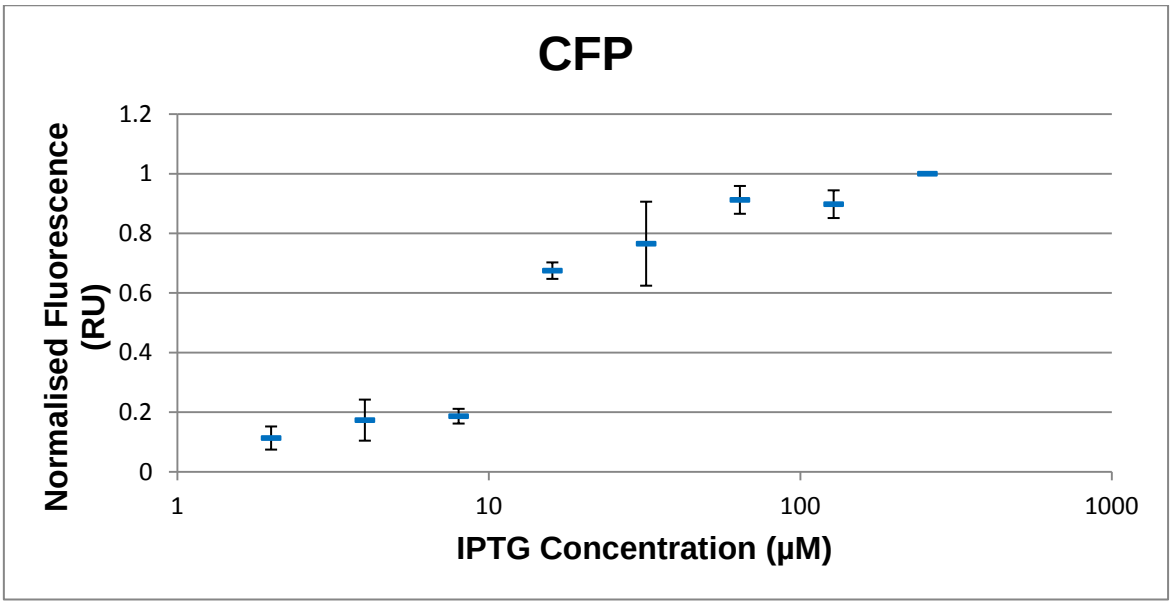

Figure 64: The maximum fluorescence output in the CFP channel in response to different concentrations of the inducer IPTG. The data has been normalised for cell number and fluorescence from control cells grown under the same conditions has been subtracted and displayed at a percentage of maximum fluorescence. The error bars represent the standard error of the mean for three biological repeats.

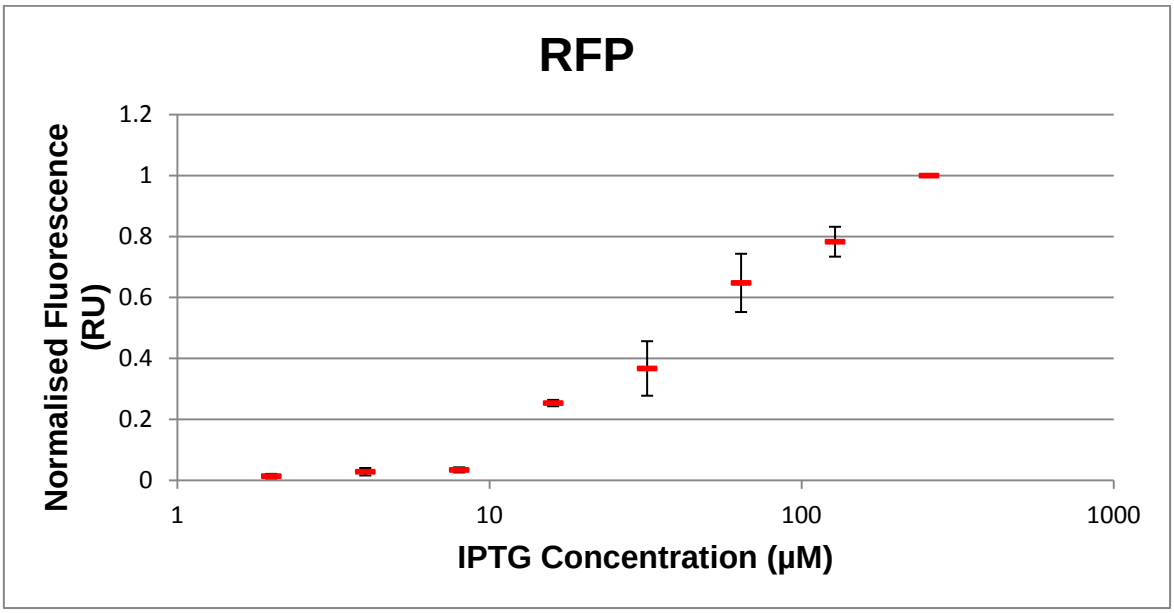

Figure 65: The maximum fluorescence output in the RFP channel in response to different concentrations of the inducer IPTG. The data has been normalised for cell number and fluorescence from control cells grown under the same conditions has been subtracted and displayed at a percentage of maximum fluorescence. The error bars represent the standard error of the mean for three biological repeats.

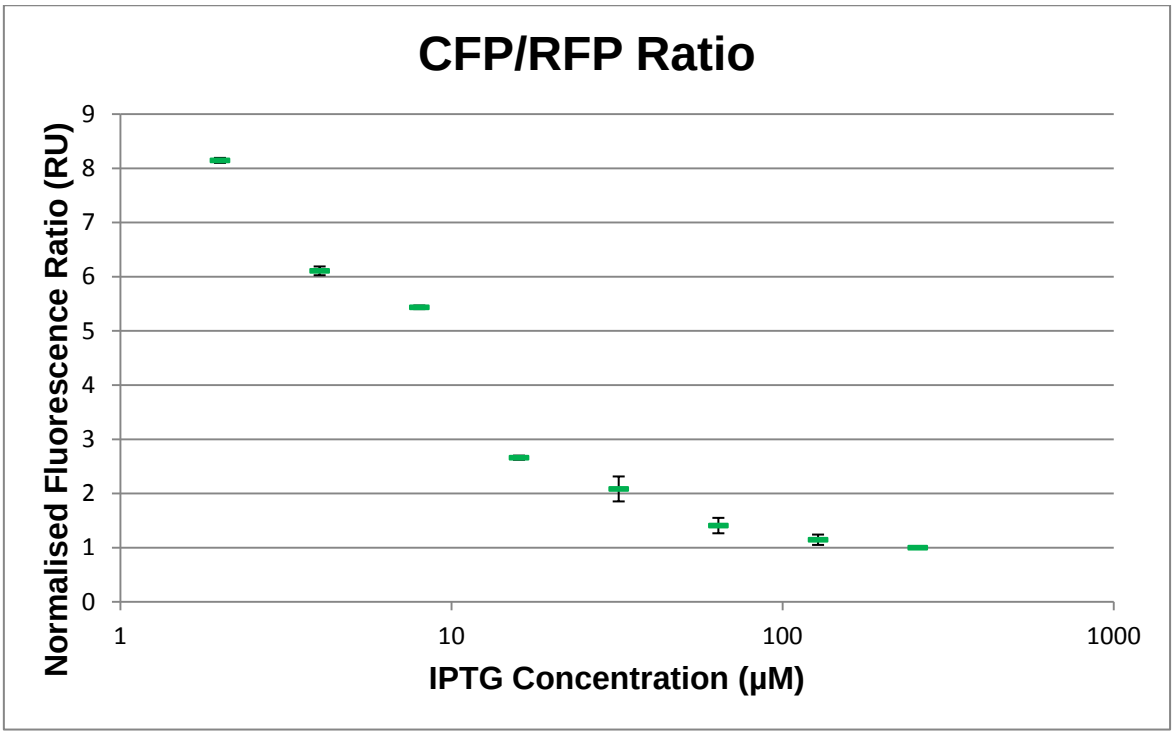

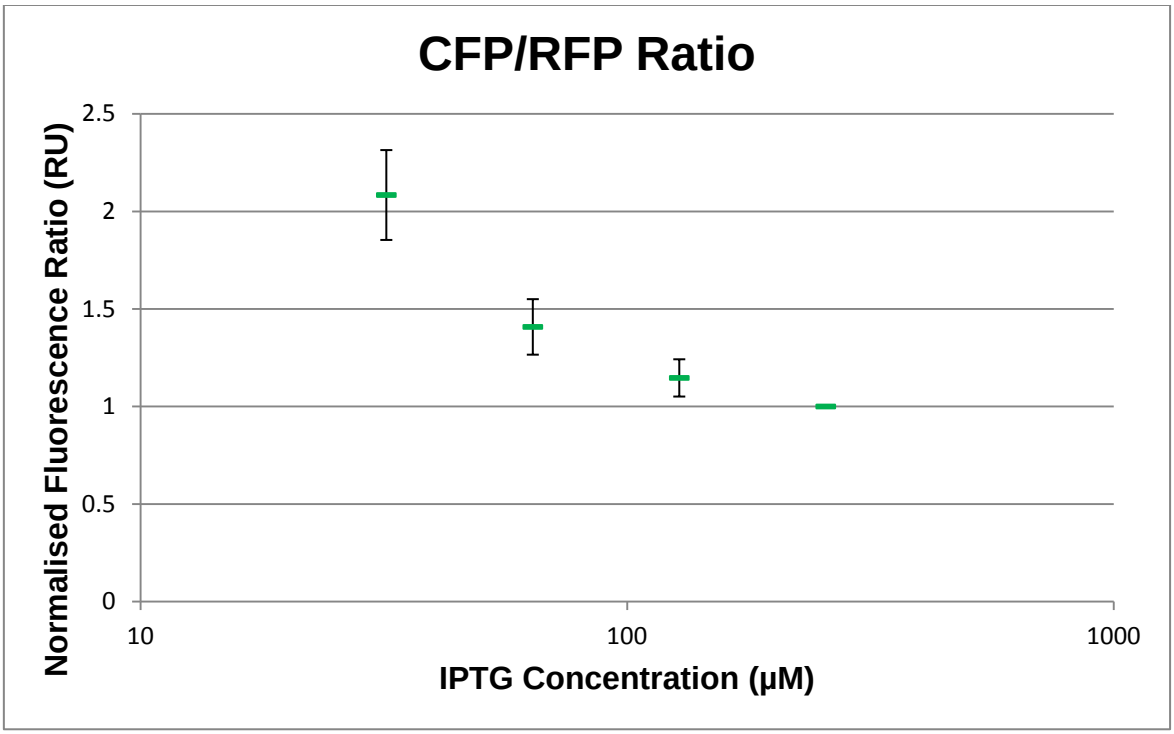

Figure 66: The CFP/RFP ratio in response to different concentrations of the inducer IPTG. The data has been normalised for cell number and fluorescence from control cells grown under the same conditions has been subtracted and displayed at a percentage of maximum fluorescence. The error bars represent the standard error of the mean for three biological repeats.

The results show that the YFP and CFP reporters quickly become saturated and do not allow us to differentiate well between high concentrations of IPTG. The RFP reporter show a linear response between 8 µM and 256 µM IPTG and gives good resolution between these concentrations, however it is not possible to resolve the difference between lower concentrations as the output for the lower IPTG concentrations between 2 µM and 8 µM is too similar.

If a ratio is taken of the output from the CFP and RFP reporters it is possible to resolve the differences in IPTG concentration across the whole range tested. This is due to the removal of errors associated with variation in copy number of the activator and reporter plasmids and also machine noise.

5.7 Identification of “unknown” samples

The *E. coli* strain C43 containing both pMFO-1 and pLacNtrC* plasmids and as a control for background fluorescence the *E. coli* strain C43 containing only the pLacNtrC* plasmid, were grown overnight in LB containing appropriate antibiotics. The overnight cultures were then sub-cultured 1 in 50 into fresh LB containing appropriate antibiotics and grown to an OD_{600} of 0.6. 1 ml of the culture was spun down in a bench top centrifuge and re-suspended in M9 minimal media containing appropriate antibiotics, 128 mM NH_4Cl to suppress phosphorylation of the natural NtrC, and IPTG ranging in concentration from 0 µM to 256 µM to induce expression of NtrC*. 150 µl of the cell culture was transferred to a Corning 3603 96-well black microplate and incubated at 30 °C with shaking in the plate reader to allow induction of expression of NtrC*. The fluorescence output was measured

over time in plate reader. Mean steady state values for each fluorescent channel were determined for 6 independent cultures and the mean and standard deviation of the raw fluorescence signal plotted against the IPTG concentration to generate the standard curves shown in Figure 68A. It should be noted that in this case absolute fluorescence was used, not corrected for cell number or auto fluorescence. These data shows that all three reporters respond in a dose dependent manner to the addition of different concentrations of IPTG by increasing fluorescence output. However, the shapes of the curves and degree of saturation of the output for any given IPTG concentration vary with promoter strength. The high and medium affinity promoters, activating YFP and CFP expression respectively, show good induction between 8-64μM IPTG but seem to saturate at higher levels. The low affinity promoter, activating RFP, shows good induction between 32-256μM IPTG but does not change significantly at lower concentrations. Due to the complex nature of NtrC-P binding to multiple sites at these promoters the best fits are obtained by a sigmoidal Hill plot with four parameters, in each case having an adjusted R^2 value of 0.999 (SigmaPlot). It should also be noted that the standard deviation on the mean raw fluorescence values obtained from the six independent cultures is very high.

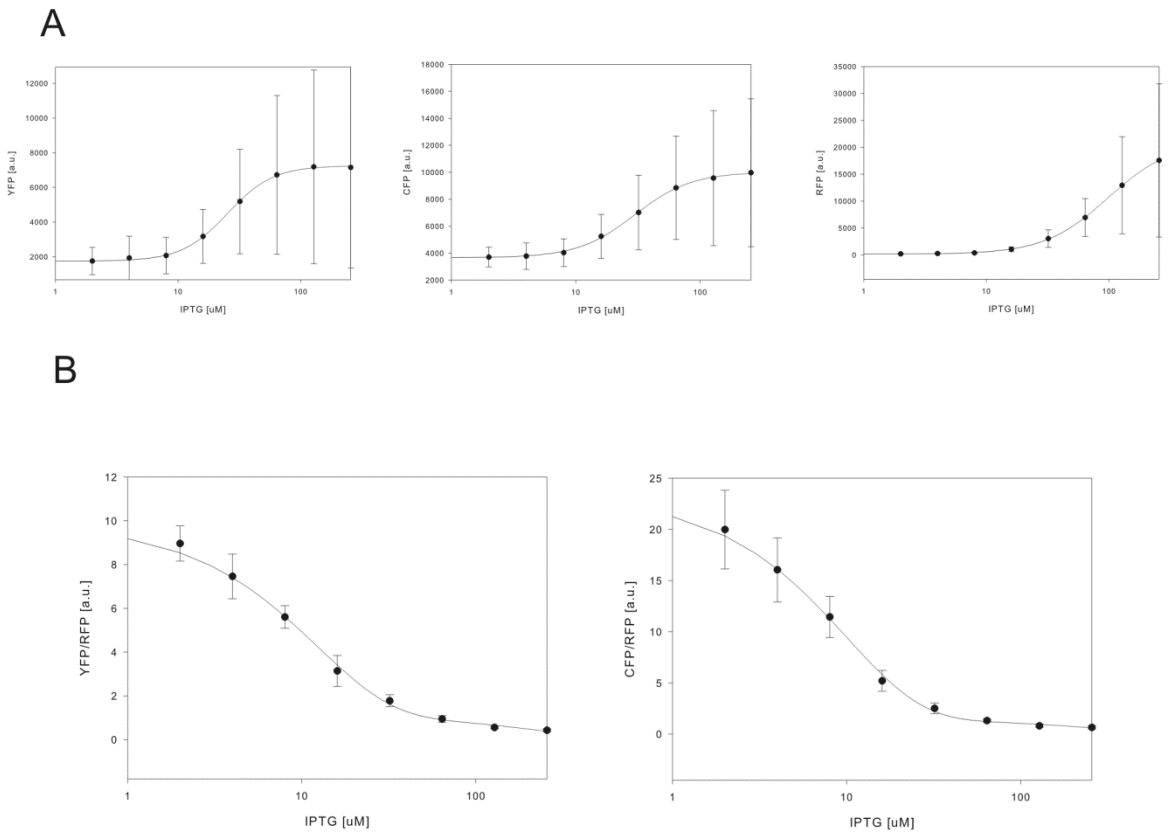

Figure 67: Mean raw data for fluorescence values obtained from six independent cultures at varying IPTG induction levels. (A) single channel data for the high (YFP), medium (CFP) and low (RFP) affinity promoter; (B) ratiometric data. Error bars represent 1 standard deviation for six biological repeats.

To determine whether the dynamic range and reproducibility of the raw standard curve data could be improved, the YFP/RFP and CFP/RFP ratios were calculated from the raw fluorescent signals and plotted against the IPTG concentration to generate the standard curves show in Figure 68B. In both cases the range of IPTG concentrations over which we see good separation of reporter output is greater than for either single channel alone. The standard deviation of the mean from the six independent cultures is also significantly smaller than for the single channel raw fluorescence data as well. In these cases, the best fit curves are obtained with an exponential decay double fit with four parameters and adjusted

R^2 values of 0.994 and 0.997 respectively (SigmaPlot). The use of ratios of fluorescence automatically adjusts for differences in cell number in the wells and for some autofluorescence as well removing the requirement for OD measurements and separate non-fluorescent negative control samples.

In order to test the accuracy of our reporter plasmid we repeated our experiments but with a selection of IPTG concentrations which were different to those used to generate the standard curves. We then used the raw fluorescent values obtained from these “unknown” samples to read off the apparent IPTG concentration from our standard curves. Figure 69A shows the mean calculated IPTG concentration compared to the real IPTG concentration when using each single channel raw fluorescence value alone. Surprisingly, the high and medium affinity promoters provide a very poor estimate of the actual IPTG concentration across the whole range of “unknowns”, although it should be remembered that the standard curves only showed good differences in induction between 8-64μM and so it is possible that only the “unknown” samples of 10 and 50μM are really within the range of detection for these reporters. The low affinity RFP reporter fares much better, although this still appears to underestimate the real values at higher concentrations of IPTG.

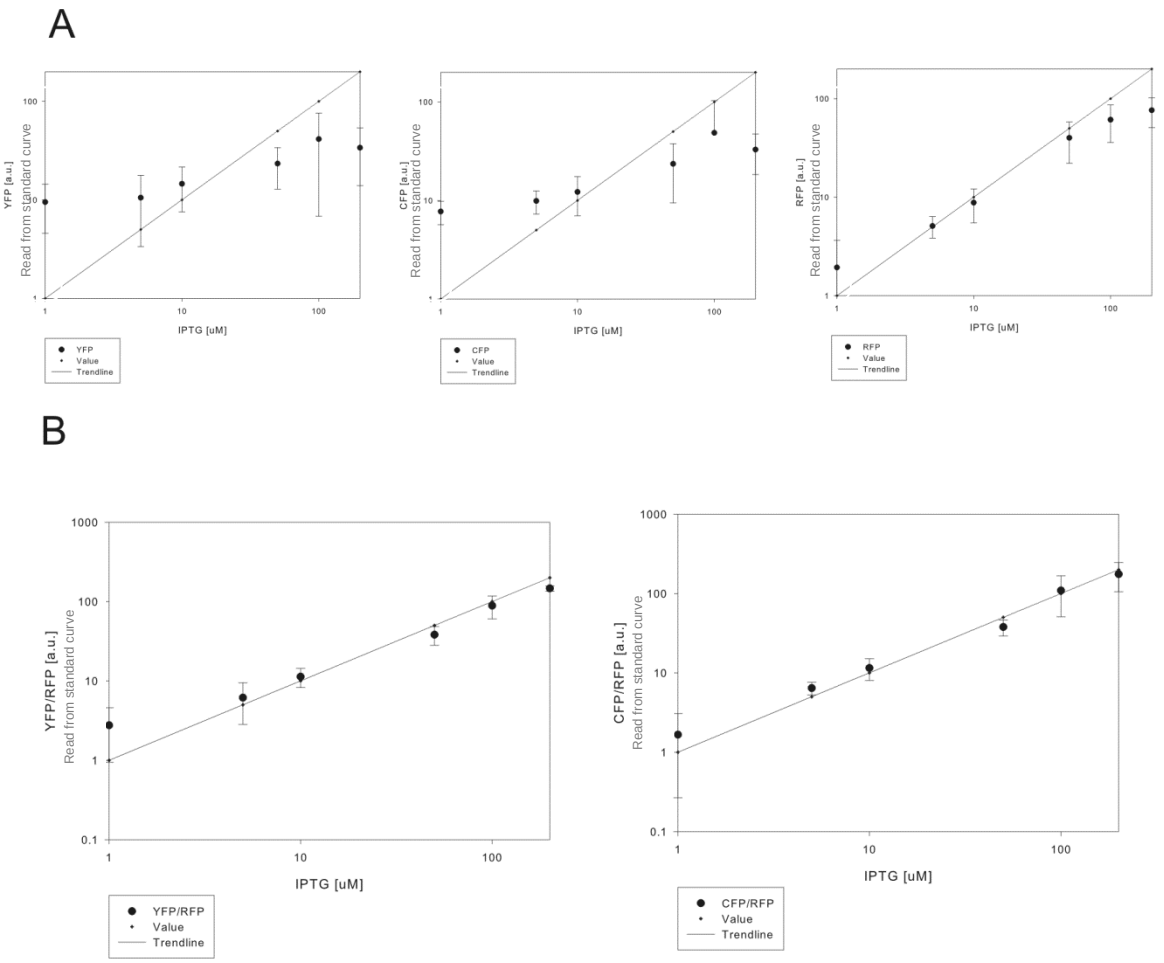

Figure 68: Mean read from the standard curves generated in figure 68 versus real IPTG concentrations added to the biosensor. The trend line shows the ideal 1:1 relationship between real and calculated values. (A) single channel data for the high (YFP), medium (CFP) and low (RFP) affinity promoter; (B) ratiometric data (YFP/RFP) and (CFP/RFP). Error bars represent 1 standard deviation for six biological repeats.

We then used the YFP/RFP and CFP/RFP ratios to calculate the IPTG concentrations in our “unknown” samples, Figure 69B. In both cases, the mean values from the six independent repeats were much closer to the “real” IPTG concentrations for the whole dynamic range of inputs. We are no longer underestimating the highest IPTG concentrations and are less likely to overestimate the lowest concentrations either. It should also be noted that the

standard deviation of the six samples is also much smaller than for the values calculated from single channel data alone due to the ratios correcting for differences in cell numbers in each well as described previously.

5.8 Discussion

The equivalent NtrC mutation that was shown to activate transcription at *ntr* promoters without the need for activation by NtrB in *S. typhimurium* has been shown to be successful in creating a constitutively active form of the *E. coli* NtrC protein. The highest level of activation seen in *S. typhimurium* was with a double mutant of NtrC containing the changes S160F and D54E; however, the D54E mutation proved to be toxic to *E. coli* cells. Despite this, the single S160F *E. coli* mutant has been shown to produce a good level of activation of transcription from the *ntr* promoters on the reporter plasmid.

The NtrC* transcriptional activator has been put under the control of two different promoters, one induced by L-arabinose and the other by IPTG. The two activator plasmids that have been tested have both produced high levels of signal in all three fluorescent channels demonstrating that when nutrients are plentiful in the growth media the *E. coli* C43 host cells are capable of sustaining the high levels of fluorescent protein production required for this biosensor. This supports the idea that under nitrogen limiting conditions the cells simply did not have enough nutrients available to give a strong output in all of the different reporter channels.

As the concentration of the inducer is increased the production of NtrC* from the activator is increased and the higher the level of NtrC* in the cell, the higher the fluorescence output from the reporter plasmid. The high affinity reporter performs best at low concentrations and the low affinity reporter performs best at high concentrations. So the MFO reporter would provide a better response over a wider range of concentrations if used as a biosensor than any of the single reporters on their own. However if we look at different biological repeats, where the copy numbers of the activator and reporter plasmid may differ, the repeats of this experiment show variation in the absolute maximum output between repeats.

This issue can be addressed with the MFO reporter by using a ratio of two of the fluorescent channels instead of just looking at the individual reporters. The CFP and RFP channels were selected for the ratio from the IPTG experiment as these two give the best combined range of detection under these particular conditions. Using the ratio gives better resolution of different concentrations of IPTG and allows detection over the full range of IPTG concentrations tested even when taking into account the differences in absolute fluorescent output from three biological repeats. The improved accuracy of the measurements is likely to be a result of the removal of machine noise and any error caused by variation between cells in copy number of either reporter plasmid or activator plasmid. Both using CFP/RFP and YFP/RFP ratios allowed the concentration of “unknown” IPTG samples to be more accurately read from a standard curve of “known” samples than any individual channel. The use of ratios also removes the need to make separate OD measurements for cell number or to have non-fluorescent cell

negative controls making its implementation as a biosensor less technically difficult.

The benefit of using ratios over individual measurements is evident in the identification of unknown concentrations of IPTG (see section 5.7).

6. General Discussion

6.1 A multi-fluorescent reporter plasmid

The majority of commercially available biosensors utilise host cell stress responses to respond to a broad range of toxic compounds that can affect the host cell. The compound-specific biosensors that are available have been engineered is to be as sensitive as possible and to detect very low concentrations of chemicals. The aim of this study was to create a generic reporter that can sensitively report on the concentration of a specific compound in the environment over a wide dynamic range. It also aimed to reduce the problems associated with most biosensors which is that the output is directly proportional to the number of viable cells in the test (a value that is not easily quantifiable).

In order to achieve these aims, the MFO reporter was designed to respond to a wider range of chemical concentrations than a single output biosensor by utilising three different coloured fluorescent proteins fused to three different strength *E. coli* Ntr system promoters; all of which are regulated naturally by NtrC-P. The reporter plasmid was tested extensively in *E. coli* and in other species to investigate optimum conditions for maximum signal to noise ratio in the output of the reporter plasmid.

This study also highlighted important factors in fine tuning of a reporter system to optimise the performance of a biosensor. These include the growth media used for

cell growth, copy number of the reporter plasmid and amount of transcriptional activator produced in the host cell.

It is important to minimise the level of auto-fluorescence from the media that the host cells are grown in, to give a good signal to noise ratio from the reporter when low concentrations of a compound are detected. It has been shown that M9 is better than LB for this property, however the cells must also have enough carbon and nitrogen sources to synthesise the high levels of reporter proteins required in a response when high concentrations of a compound are detected. Therefore, a balance must be reached by supplementing the M9 media with sufficient ammonium and glucose to sustain a high level of protein synthesis and produce a strong response from the reporter.

The copy number of the reporter plasmid also plays a key role in producing a good signal to noise ratio. We observed that a high copy number reporter plasmid provided better signal to noise ratio, but only if the transcriptional activator can reach high enough levels in the host cell to activate all promoters. If a lower copy number reporter plasmid is used then there is less chance of sequestering all of the transcriptional activators with the high affinity promoters but the lower level of signal produced results in problems with the signal to noise ratio when detecting low concentrations of a compound.

The copy number of the reporter plasmid also plays a role in the problem of variation in the absolute reporter output between different biological repeats. This

variability is a result of a number of factors, including variation in copy number of the reporter plasmid in the cell, the number of viable cells in the test well and the nutrient availability to produce the output. This problem was addressed by using the ratio of two reporter outputs on the same plasmid, in the same celll to eliminate the variation due to copy number differences, cell density and nutrient fluctuations. This results in more accurate measurements giving greater sensitivity and increased dynamic range from the response of the biosensor.

To get the maximum potential output from the MFO reporter, it was necessary to decouple the output from the nitrogen availability in the environment. The constitutively active response regulator, NtrC* was engineered to achieve this. The production of NtrC* from a separate plasmid allows the level of the transcriptional activator to be increased above the normal level of NtrC-P found in the cell, this solves the problem of high affinity binding sites sequestering the transcriptional activator and means that a high copy reporter can be used in the biosensor to give a high signal to noise ratio from the output.

The use of the YFP/RFP and CFP/RFP ratios to calculate the IPTG concentrations in our “unknown” samples were much closer to the “real” IPTG concentrations for the whole dynamic range of inputs than any of the individual channels. We are no longer underestimating the highest IPTG concentrations and are less likely to overestimate the lowest concentrations either. It should also be noted that the standard deviation of the six samples is also much smaller than for the values calculated from single channel data alone due to the ratios correcting for

differences in cell numbers in each well, copy number of plasmids and viable cells as described previously.

6.2 Future application for MFO reporter

It has been shown that it is possible to switch the chemical being detected by the MFO reporter by changing the activator plasmid in the host cell so that the production of NtrC* is activated by the presence of L-Arabinose in one case and by IPTG in the other case. This principle can be applied to switch the output of the reporter to respond to other inputs by altering the promoter that controls the expression of NtrC*. The production of NtrC* could easily be linked to other environmental sensing promoters such as those that detect arsenic and other pollutants to produce a dynamic and sensitive response to the presence of these compound in a sample.

We have also shown that the reporter plasmid can function in other species of bacteria, so the reporter could be transferred to a different host such as *P. putida* to make use of other sensory proteins and the more robust nature of the host when exposed to environmental pollutants (Chang *et al.*, 2008b).

The proof of concept demonstrated with the Ntr-C based multi-fluorescent reporter system could be reapplied in the future to an engineered promoter system that has less interaction with the metabolic state of the host microbe. Methods such as BD inframe fusions or TOPO cloning could be applied in future to remove the need for complex ligations, however, with advances in artificial DNA synthesis it would be

possible to design a reporter plasmid based on any promoter system with naturally occurring variable strength promoters or introduce mutations in the regulator binding regions to create multiple strength promoters. A promoter system could be designed with no interference with the host cell regulatory pathways and the plasmid artificially synthesised ready for application in a biosensor. The same strategy could be applied to the NtrC* activator plasmid to allow any promoter to control the production of NtrC*. The plasmid already has a multiple cloning site, but polylinkers could be added to increase the options for regulation of NtrC* production.

The use of NtrC* could also be changed as there are potential issues in using a global transcriptional regulator to activate the reporter plasmid in that its over expression is going to have other effects on the host cells' transcriptional activity; altering expression of other genes and even controlling the expression of the native NtrC that is still present in the host cell genome. There are options to look for hosts without an endogenous Ntr system or to identify other regulators that can be mutated to be constitutively active to control the aforementioned artificial reporter plasmid. When adding high numbers of promoter regions to a cell like on the reporter plasmid, there will always be issues with titrating out proteins that bind to them, for example RpoN is required for transcription from Ntr promoters and may therefore not be available to bind to other genes under its control when we are expressing high levels of proteins. We did not observe any issues with growth, but did not look at other gene expression in any detail, if this became an issue, additional RpoN could be provided on the activator plasmid to increase the intracellular amount.

6.3 Summary and final conclusions

For applications from biosensor generation to synthetic biology, the ability to accurately and quantitatively generate input-output data from biological systems over a wide dynamic range is becoming increasingly important. This study has demonstrated that a simple approach utilising multiple promoters, recognising the same transcriptional activator but with differing affinities, linked to compatible reporter genes can achieve this goal. This simple system highlights that even for complex promoters with multiple binding sites we can use the ratio of two reporters to obtain accurate and reproducible input-output data for reporters contained on a high copy number plasmid without the need for any background subtraction, accurate determination of cell number and despite the fact that the numerical fits to the ratiometric standard curves had lower adjusted R^2 values than those to any single channel data (Figure 67). It has also demonstrated that the precise promoter strengths are not too crucial to the design, provided they are significantly different, as the ratio of either the high affinity/low affinity (YFP/RFP) or medium affinity/low affinity (CFP/RFP) channels give similar improvements over any single channel alone.

The modularity of this system means that it would be possible to exchange the IPTG inducible promoter and hence place the *ntrC** gene under the regulation of any environmentally important promoter. Potential examples include the *urcA* (Hillson *et al.*, 2007) Uranium responsive promoter , the *tod* (Dawson et al., 2008) or *Pu* (Li *et al.*, 2008b) BTEX responsive promoters and the *arsR (Fernandez et al., 2014)*, arsenite responsive promoter. In these cases the promoters can be either activated by the binding of a transcriptional activator or repression relieved

by the removal of the repressor from the promoter, either of which would result in NtrC* production and subsequent production of fluorescent proteins from the reporter plasmid.

One of the major features of this study is its general applicability. There is a wealth of data on promoter architectures and a large number of different strength promoters are currently being biologically characterised by the synthetic biology community. It should therefore be possible to simply construct different strength promoters for the same transcriptional activator by standard DNA synthesis techniques, therefore allowing direct ratiometric detection of specific active transcription factors. Similarly, the choice of reporters is not limited by the technique so long as they can be adequately distinguished from each other in the final assays. Finally, there is considerable interest in the biosensor field in the use of immobilised cells for field based applications. In these cases, determining the exact number of viable cells present at the time of use may be problematic and obtaining high signal levels may also be essential. In this regard, the use of ratiometric reporters from constructs on high copy number plasmids could alleviate many of these potential problems and significantly simplify the required biosensor detection equipment.

7. Bibliography

Alpat, S., Alpat, S. K., Cadirci, B. H., Yasa, I., and Telefoncu, A. (2008) A novel microbial biosensor based on *Circinella sp.* modified carbon paste electrode and its voltammetric application. *Sensors and Actuators B: Chemical* **134:** 175-181.

Ames, B. N., Durston, W. E., Yamasaki, E., and Lee, F. D. (1973) Carcinogens are mutagens: a simple test system combining liver homogenates for activation and bacteria for detection. *Proc Natl Acad Sci U S A* **70:** 2281-2285.

Atkinson, M. R., Blauwkamp, T. A., Bondarenko, V., Studitsky, V., and Ninfa, A. J. (2002) Activation of the *glnA, glnK,* and *nac* promoters as *Escherichia coli* undergoes the transition from nitrogen excess growth to nitrogen starvation. *J Bacteriol* **184:** 5358-5363.

Bagdasarian, M., Lurz, R., Ruckert, B., Franklin, F. C., Bagdasarian, M. M., Frey, J. *et al.* (1981) Specific-purpose plasmid cloning vectors. II. Broad host range, high copy number, RSF1010-derived vectors, and a host-vector system for gene cloning in *Pseudomonas*. *Gene* **16:** 237-247.

Beaulieu, E. D., Ionescu, M., Chatterjee, S., Yokota, K., Trauner, D., and Lindow, S. (2013) Characterization of a Diffusible Signaling Factor from *Xylella fastidiosa*. *mBio* **4**.

Benson, D. E., Conrad, D. W., de Lorimier, R. M., Trammell, S. A., and Hellinga, H. W. (2001) Design of bioelectronic interfaces by exploiting hinge-bending motions in proteins. *Science* **293:** 1641-1644.

Bobacka, J., Ivaska, A., and Lewenstam, A. (2008) Potentiometric Ion Sensors. *Chemical Reviews* **108:** 329-351.

Borisov, S. M. and Wolfbeis, O. S. (2008) Optical biosensors. *Chem Rev* **108:** 423-461.

Bourgeois, W., Burgess, J. E., and Stuetz, R. M. (2001) On-line monitoring of wastewater quality: a review. *J Chem Technol Biotechnol* **76:** 337-348.

Chang, J. S., Kim, Y. H., and Kim, K. W. (2008) The ars genotype characterization of arsenic-resistant bacteria from arsenic-contaminated gold-silver mines in the Republic of Korea. *Appl Microbiol Biotechnol* **80:** 155-165.

Chen, L. Q., Hou, B. H., Lalonde, S., Takanaga, H., Hartung, M. L., Qu, X. Q. *et al.* (2010) Sugar transporters for intercellular exchange and nutrition of pathogens. *Nature* **468:** 527-532.

Chouteau, C., Dzyadevych, S., Durrieu, C., and Chovelon, J. M. (2005) A bi-enzymatic whole cell conductometric biosensor for heavy metal ions and pesticides detection in water samples. *Biosensors and Bioelectronics* **21:** 273-281.

Claverie-Martin, F. and Magasanik, B. (1991) Role of integration host factor in the regulation of the *glnHp2* promoter of *Escherichia coli*. *Proc Natl Acad Sci U S A* **88:** 1631-1635.

D'Souza, S. F. (2001) Microbial biosensors. *Biosens Bioelectron* **16:** 337-353.

Daunert, S., Barrett, G., Feliciano, J. S., Shetty, R. S., Shrestha, S., and Smith-Spencer, W. (2000) Genetically engineered whole-cell sensing systems: coupling biological recognition with reporter genes. *Chem Rev* **100:** 2705-2738.

Dawson, J. J. C., Iroegbu, C. O., Maciel, H., and Paton, G. I. (2008) Application of luminescent biosensors for monitoring the degradation and toxicity of BTEX compounds in soils. *Journal of Applied Microbiology* **104:** 141-151.

Day, R. N. and Davidson, M. W. (2009) The fluorescent protein palette: tools for cellular imaging. *Chem Soc Rev* **38:** 2887-2921.

de Ruijter, N. C. A., Verhees, J., van Leeuwen, W., and van der Krol, A. R. (2003) Evaluation and Comparison of the GUS, LUC and GFP Reporter System for Gene Expression Studies in Plants. *Plant Biology* **5:** 103-115.

Ding, L., Du, D., Zhang, X., and Ju, H. (2008) Trends in cell-based electrochemical biosensors. *Curr Med Chem* **15:** 3160-3170.

Eaton, A. D., Franson, M. A. H., American Public Health Association, American Water Works Association, and Water, E. F. (2005) *Standard Methods for the Examination of Water & Wastewater*. American Public Health Association.

Fehr, M., Lalonde, S., Ehrhardt, D. W., and Frommer, W. B. (2004) Live imaging of glucose homeostasis in nuclei of COS-7 cells. *J Fluoresc* **14:** 603-609.

Fehr, M., Lalonde, S., Lager, I., Wolff, M. W., and Frommer, W. B. (2003a) In vivo imaging of the dynamics of glucose uptake in the cytosol of COS-7 cells by fluorescent nanosensors. *J Biol Chem* **278:** 19127-19133.

Fent, K. (2003) Ecotoxicological problems associated with contaminated sites. *Toxicol Lett* **140-141:** 353-365.

Fernandez, M., Niqui-Arroyo, J. L., Conde, S., Ramos, J. L., and Duque, E. (2012) Enhanced tolerance to naphthalene and enhanced rhizoremediation performance for *Pseudomonas putida* KT2440 via the NAH7 catabolic plasmid. *Applied and Environmental Microbiology* **78:** 5104-5110.

Fernandez, M., Udaondo, Z., Niqui, J. L., Duque, E., and Ramos, J. L. (2014) Synergic role of the two *ars* operons in arsenic tolerance in *Pseudomonas putida* KT2440. *Environmental Microbiology Reports* n/a.

Flashner, Y., Weiss, D. S., Keener, J., and Kustu, S. (1995) Constitutive forms of the enhancer-binding protein NtrC: evidence that essential oligomerization determinants lie in the central activation domain. *J Mol Biol* **249:** 700-713.

Frigault, M. M., Lacoste, J., Swift, J. L., and Brown, C. M. (2009) Live-cell microscopy - tips and tools. *Journal of Cell Science* **122:** 753-767.

Gerstein, M., Lesk, A. M., and Chothia, C. (1994) Structural Mechanisms for Domain Movements in Proteins. *Biochemistry* **33:** 6739-6749.

Gregor, J., Zeller, T., Balzer, A., Haberzettl, K., and Klug, G. (2007) Bacterial regulatory networks include direct contact of response regulator proteins: interaction of RegA and NtrX in *Rhodobacter capsulatus*. *J Mol Microbiol Biotechnol* **13:** 126-139.

Harms, H., Wells, M. C., and van, d. M., Jr. (2006) Whole-cell living biosensors--are they ready for environmental application? *Appl Microbiol Biotechnol* **70:** 273-280.

Harris, D. C. (2010) *Quantitative Chemical Analysis*. W. H. Freeman.

Heeb, S., Itoh, Y., Nishijyo, T., Schnider, U., Keel, C., Wade, J. *et al.* (2000) Small, stable shuttle vectors based on the minimal pVS1 replicon for use in gram-negative, plant-associated bacteria. *Mol Plant Microbe Interact* **13:** 232-237.

Hernando, M. D., Fernandez-Alba, A. R., Tauler, R., and Barcel I, D. (2005) Toxicity assays applied to wastewater treatment. *Talanta* **65:** 358-366.

Hervas, A. B., Canosa, I. s., Little, R., Dixon, R., and Santero, E. (2009) NtrC-Dependent Regulatory Network for Nitrogen Assimilation in *Pseudomonas putida*. *Journal of Bacteriology* **191:** 6123-6135.

Hervas, A. B., Canosa, I. s., and Santero, E. (2010) Regulation of glutamate dehydrogenase expression in *Pseudomonas putida* results from its direct repression by NtrC under nitrogen-limiting conditions. *Molecular Microbiology* **78:** 305-319.

Higashitani, A., Ishii, Y., Kato, Y., and Koriuchi, K. (1997) Functional dissection of a cell-division inhibitor, SulA, of *Escherichia coli* and its negative regulation by Lon. *Mol Gen Genet* **254:** 351-357.

Hillson, N. J., Hu, P., Andersen, G. L., and Shapiro, L. (2007) *Caulobacter crescentus* as a whole-cell uranium biosensor. *Appl Environ Microbiol* **73:** 7615-7621.

Hou, B. H., Takanaga, H., Grossmann, G., Chen, L. Q., Qu, X. Q., Jones, A. M. *et al.* (2011) Optical sensors for monitoring dynamic changes of intracellular metabolite levels in mammalian cells. *Nat Protoc* **6:** 1818-1833.

Huisman, O. and D'Ari, R. (1981a) An inducible DNA replication-cell division coupling mechanism in *E. coli*. *Nature* **290:** 797-799.

Ind, A. C., Porter, S. L., Brown, M. T., Byles, E. D., de Beyer, J. A., Godfrey, S. A. *et al.* (2009) Inducible-expression plasmid for *Rhodobacter sphaeroides* and *Paracoccus denitrificans*. *Appl Environ Microbiol* **75:** 6613-6615.

Jiang, P., Peliska, J. A., and Ninfa, A. J. (1998) Enzymological characterization of the signal-transducing uridylyltransferase/uridylyl-removing enzyme (EC 2.7.7.59) of *Escherichia coli* and its interaction with the PII protein. *Biochemistry* **37:** 12782-12794.

Jishage, M., Iwata, A., Ueda, S., and Ishihama, A. (1996) Regulation of RNA polymerase sigma subunit synthesis in *Escherichia coli*: intracellular levels of four species of sigma subunit under various growth conditions. *Journal of Bacteriology* **178:** 5447-5451.

Kara, S., Keskinler, B. +., and Erhan, E. (2009) A novel microbial BOD biosensor developed by the immobilization of *P. Syringae* in micro-cellular polymers. *J Chem Technol Biotechnol* **84:** 511-518.

Kaur, A., Kim, J. R., Michie, I., Dinsdale, R. M., Guwy, A. J., and Premier, G. C. (2013) Microbial fuel cell type biosensor for specific volatile fatty acids using acclimated bacterial communities. *Biosensors and Bioelectronics* **47:** 50-55.

King, J. M., Digrazia, P. M., Applegate, B., Burlage, R., Sanseverino, J., Dunbar, P. *et al.* (1990) Rapid, sensitive bioluminescent reporter technology for naphthalene exposure and biodegradation. *Science* **249:** 778-781.

Kirgoz, A., Timur, S., Odaci, D., Prez, B., Alegret, S., and Merko I, A. (2007) Carbon Nanotube Composite as Novel Platform for Microbial Biosensor. *Electroanalysis* **19:** 893-898.

Klose, K. E., Weiss, D. S., and Kustu, S. (1993) Glutamate at the site of phosphorylation of nitrogen-regulatory protein NtrC mimics aspartyl-phosphate and activates the protein. *J Mol Biol* **232:** 67-78.

Knudsen, J. D., Carlquist, M., and Gorwa-Grauslund, M. (2014) NADH-dependent biosensor in *Saccharomyces cerevisiae*: principle and validation at the single cell level. *AMB Express* **4:** 81.

Kolb, A., Busby, S., Buc, H., Garges, S., and Adhya, S. (1993) Transcriptional regulation by cAMP and its receptor protein. *Annu Rev Biochem* **62:** 749-795.

Krell, T., Lacal, J., Busch, A., Silva-Jimenez, H., Guazzaroni, M. E., and Ramos, J. L. (2010) Bacterial sensor kinases: diversity in the recognition of environmental signals. *Annu Rev Microbiol* **64:** 539-559.

Kuo, J. T., Chang, Y. J., and Tseng, C. P. (2003) Growth rate regulation of *lac* operon expression in *Escherichia coli* is cyclic AMP dependent. *FEBS Letters* **553:** 397-402.

Laub, M. T. and Goulian, M. (2007) Specificity in two-component signal transduction pathways. *Annu Rev Genet* **41:** 121-145.

Lei, Y., Chen, W., and Mulchandani, A. (2006) Microbial biosensors. *Analytica Chimica Acta* **568:** 200-210.

Leigh, J. A. and Dodsworth, J. A. (2007) Nitrogen regulation in bacteria and archaea. *Annu Rev Microbiol* **61:** 349-377.

Leveau, J. H. and Lindow, S. E. (2002) Bioreporters in microbial ecology. *Curr Opin Microbiol* **5:** 259-265.

Lewis, M., Chang, G., Horton, N. C., Kercher, M. A., Pace, H. C., Schumacher, M. A. *et al.* (1996) Crystal structure of the lactose operon repressor and its complexes with DNA and inducer. *Science* **271:** 1247-1254.

Li, Y. F., Li, F. Y., Ho, C. L., and Liao, V. H. (2008c) Construction and comparison of fluorescence and bioluminescence bacterial biosensors for the detection of bioavailable toluene and related compounds. *Environ Pollut* **152:** 123-129.

Lin, L., Xiao, L. L., Huang, S., Zhao, L., Cui, J. S., Wang, X. H. *et al.* (2006a) Novel BOD optical fiber biosensor based on co-immobilized microorganisms in ormosils matrix. *Biosens Bioelectron* **21:** 1703-1709.

Lin, L., Xiao, L. L., Xin, L. L., Zhao, L., and Chen, X. (2006b) [Fluorescence characterization of oxygen sensing film for BOD determination]. *Guang Pu Xue Yu Guang Pu Fen Xi* **26:** 15-18.

Lutz, S. and Bornscheuer, U. T. (2012) *Protein Engineering Handbook*. Wiley.

Magasanik, B. (1989) Regulation of transcription of the *glnALG* operon of *Escherichia coli* by protein phosphorylation. *Biochimie* **71:** 1005-1012.

McDaniels, A. E., Reyes, A. L., Wymer, L. J., Rankin, C. C., and Stelma, G. N. (1990) Comparison of the *Salmonella* (Ames) test, Umu tests, and the sos chromotests for detecting genotoxins. *Environ Mol Mutagen* **16:** 204-215.

Megerle, J. A., Fritz, G., Gerland, U., Jung, K., and Radler, J. O. (2008) Timing and dynamics of single cell gene expression in the arabinose utilization system. *Biophys J* **95:** 2103-2115.

Melamed, S., Naftaly, S., and Belkin, S. (2014) Improved detection of antibiotic compounds by bacterial reporter strains achieved by manipulations of membrane permeability and efflux capacity. *Appl Microbiol Biotechnol* **98:** 2267-2277.

Merrick, M. J. and Edwards, R. A. (1995) Nitrogen control in bacteria. *Microbiol Rev* **59:** 604-622.

Miroux, B. and Walker, J. E. (1996) Over-production of proteins in *Escherichia coli*: mutant hosts that allow synthesis of some membrane proteins and globular proteins at high levels. *J Mol Biol* **260:** 289-298.

Miyawaki, A., Sawano, A., and Kogure, T. (2003) Lighting up cells: labelling proteins with fluorophores. *Nat Cell Biol* **Suppl:** S1-S7.

Muller-Taubenberger, A. and Anderson, K. I. (2007) Recent advances using green and red fluorescent protein variants. *Appl Microbiol Biotechnol* **77:** 1-12.

Ninfa, A. J. and Jiang, P. (2005) PII signal transduction proteins: sensors of alpha-ketoglutarate that regulate nitrogen metabolism. *Curr Opin Microbiol* **8:** 168-173.

Ninfa, A. J., Reitzer, L. J., and Magasanik, B. (1987) Initiation of transcription at the bacterial *glnAp2* promoter by purified *E. coli* components is facilitated by enhancers. *Cell* **50:** 1039-1046.

Nojima, T., Lin, A. C., Fujii, T., and Endo, I. (2005) Determination of the termination efficiency of the transcription terminator using different fluorescent profiles in green fluorescent protein mutants. *Anal Sci* **21:** 1479-1481.

Nomura, Y., Chee, G. J., and Karube, I. (1998) Biosensor technology for determination of BOD. *Field Analyt Chem Technol* **2:** 333-340.

Oda, Y., Nakamura, S., Oki, I., Kato, T., and Shinagawa, H. (1985) Evaluation of the new system (Umu-test) for the detection of environmental mutagens and carcinogens. *Mutat Res* **147:** 219-229.

Olaniran, A. O., Hiralal, L., and Pillay, B. (2011) Whole-cell bacterial biosensors for rapid and effective monitoring of heavy metals and inorganic pollutants in wastewater. *J Environ Monit* **13:** 2914-2920.

Operations, C. (2004) Clone Manager Suite. *Cloning* **1**.

Orosz, A., Boros, I., and Venetianer, P. (1991) Analysis of the complex transcription termination region of the *Escherichia coli rrnB* gene. *Eur J Biochem* **201:** 653-659.

Parkinson, J. S. and Houts, S. E. (1982) Isolation and behavior of *Escherichia coli* deletion mutants lacking chemotaxis functions. *J Bacteriol* **151:** 106-113.

Patterson, G., Day, R. N., and Piston, D. (2001) Fluorescent protein spectra. *J Cell Sci* **114:** 837-838.

Peijnenburg, W. J. and Jager, T. (2003) Monitoring approaches to assess bioaccessibility and bioavailability of metals: matrix issues. *Ecotoxicol Environ Saf* **56:** 63-77.

Penfold, R. J. and Pemberton, J. M. (1992) An improved suicide vector for construction of chromosomal insertion mutations in bacteria. *Gene* **118:** 145-146.

Ponraj, P., Shankar, M., Ilakkiam, D., and Gunasekaran, P. (2012) Influence of siderophore pyoverdine synthesis and iron-uptake on abiotic and biotic surface colonization of *Pseudomonas putida* S11. *Biometals* **25:** 1113-1128.

Prior, J. E., Lynch, M. D., and Gill, R. T. (2010) Broad-host-range vectors for protein expression across gram negative hosts. *Biotechnol Bioeng* **106:** 326-332.

Quillardet, P., Huisman, O., D'Ari, R., and Hofnung, M. (1982) SOS chromotest, a direct assay of induction of an SOS function in *Escherichia coli* K-12 to measure genotoxicity. *Proc Natl Acad Sci U S A* **79:** 5971-5975.

Rabaey, K. and Verstraete, W. (2005) Microbial fuel cells: novel biotechnology for energy generation. *Trends in Biotechnology* **23:** 291-298.

Reid, B. G. and Flynn, G. C. (1997) Chromophore formation in green fluorescent protein. *Biochemistry* **36:** 6786-6791.

Reitzer, L. (2003) Nitrogen assimilation and global regulation in *Escherichia coli*. *Annu Rev Microbiol* **57:** 155-176.

Reitzer, L. and Schneider, B. L. (2001) Metabolic context and possible physiological themes of sigma(54)-dependent genes in *Escherichia coli*. *Microbiol Mol Biol Rev* **65:** 422-44, table.

Reitzer, L. J. and Magasanik, B. (1983) Isolation of the nitrogen assimilation regulator NR(I), the product of the *glnG* gene of *Escherichia coli*. *Proc Natl Acad Sci U S A* **80:** 5554-5558.

Reitzer, L. J., Movsas, B., and Magasanik, B. (1989) Activation of glnA transcription by nitrogen regulator I (NRI)-phosphate in *Escherichia coli*: evidence for a long-range physical interaction between NRI-phosphate and RNA polymerase. *J Bacteriol* **171:** 5512-5522.

Renggli, S., Keck, W., Jenal, U., and Ritz, D. (2013) Role of autofluorescence in flow cytometric analysis of *Escherichia coli* treated with bactericidal antibiotics. *J Bacteriol* **195**: 4067-4073.

Rotariu, L., Bala, C., and Magearu, V. (2004) New potentiometric microbial biosensor for ethanol determination in alcoholic beverages. *Analytica Chimica Acta* **513:** 119-123.

Rothstein, D. M., Pahel, G., Tyler, B., and Magasanik, B. (1980) Regulation of expression from the *glnA* promoter of *Escherichia coli* in the absence of glutamine synthetase. *Proc Natl Acad Sci U S A* **77:** 7372-7376.

Sambrook, J. and Russell, D. W. (2001) *Molecular cloning: a laboratory manual, 3rd ed.* Cold Spring Harbour Laboratory Press, Cold Spring Harbour, N.Y.

Sezonov, G., Joseleau-Petit, D. l., and D'Ari, R. (2007) Escherichia coli Physiology in Luria-Bertani Broth. *Journal of Bacteriology* **189:** 8746-8749.

Shinagawa, H., Kato, T., Ise, T., Makino, K., and Nakata, A. (1983) Cloning and characterization of the *umu* operon responsible for inducible mutagenesis in Escherichia coli. *Gene* **23:** 167-174.

Shul'ga, A. A., Soldatkin, A. P., El'skaya, A. V., Dzyadevich, S. V., Patskovsky, S. V., and Strikha, V. I. (1994) Thin-film conductometric biosensors for glucose and urea determination. *Biosensors and Bioelectronics* **9:** 217-223.

Siegele, D. A. and Hu, J. C. (1997) Gene expression from plasmids containing the *araBAD* promoter at subsaturating inducer concentrations represents mixed populations. *Proc Natl Acad Sci U S A* **94:** 8168-8172.

Skerker, J. M., Prasol, M. S., Perchuk, B. S., Biondi, E. G., and Laub, M. T. (2005) Two-component signal transduction pathways regulating growth and cell cycle progression in a bacterium: a system-level analysis. *PLoS Biol* **3:** e334.

Sniegowski, J. A., Lappe, J. W., Patel, H. N., Huffman, H. A., and Wachter, R. M. (2005a) Base catalysis of chromophore formation in Arg96 and Glu222 variants of green fluorescent protein. *J Biol Chem* **280:** 26248-26255.

Sniegowski, J. A., Phail, M. E., and Wachter, R. M. (2005b) Maturation efficiency, trypsin sensitivity, and optical properties of Arg96, Glu222, and Gly67 variants of green fluorescent protein. *Biochem Biophys Res Commun* **332:** 657-663.

Snoeijers, S., Perez-Garcia, A., Joosten, M., and De Wit, P. (2000) The effect of nitrogen on disease development and gene expression in bacterial and fungal plant pathogens. *European Journal of Plant Pathology* **106:** 493-506.

Sockett, R. E. and Armitage, J. P. (1991) Isolation, characterization, and complementation of a paralyzed flagellar mutant of *Rhodobacter sphaeroides* WS8. *J Bacteriol* **173:** 2786-2790.

Staden, R., Beal, K. F., and Bonfield, J. K. (2000) The Staden package, 1998. *Methods in molecular biology (Clifton, N J)* **132:** 115-130.

Stock, A. M., Robinson, V. L., and Goudreau, P. N. (2000) Two-component signal transduction. *Annu Rev Biochem* **69:** 183-215.

Su, L., Jia, W., Hou, C., and Lei, Y. (2011) Microbial biosensors: a review. *Biosens Bioelectron* **26:** 1788-1799.

Takanaga, H. and Frommer, W. B. (2010) Facilitative plasma membrane transporters function during ER transit. *FASEB J* **24:** 2849-2858.

Tam, R. and Saier, M. H., Jr. (1993) Structural, functional, and evolutionary relationships among extracellular solute-binding receptors of bacteria. *Microbiol Rev* **57:** 320-346.

Ulrich, L. E., Koonin, E. V., and Zhulin, I. B. (2005) One-component systems dominate signal transduction in prokaryotes. *Trends Microbiol* **13:** 52-56.

Utsumi, R., Brissette, R. E., Rampersaud, A., Forst, S. A., Oosawa, K., and Inouye, M. (1989) Activation of bacterial porin gene expression by a chimeric signal transducer in response to aspartate. *Science* **245:** 1246-1249.

van der Meer, Jr. and Belkin, S. (2010) Where microbiology meets microengineering: design and applications of reporter bacteria. *Nat Rev Microbiol* **8:** 511-522.

Wadhams, G. H. and Armitage, J. P. (2004) Making sense of it all: bacterial chemotaxis. *Nat Rev Mol Cell Biol* **5:** 1024-1037.

Wang, J. (2007) Stripping Analysis. *Encyclopedia of Electrochemistry*. Wiley-VCH Verlag GmbH & Co. KGaA.

Wang, Y. M., Tegenfeldt, J. O., Reisner, W., Riehn, R., Guan, X. J., Guo, L. *et al.* (2005) Single-molecule studies of repressor–DNA interactions show long-range interactions. *Proceedings of the National Academy of Sciences of the United States of America* **102:** 9796-9801.

White, D., Drummond, J. T., and Fuqua, C. (2012) *The Physiology and Biochemistry of Prokaryotes*. Oxford University Press.

Willner, I. (2001) Protein hinges for bioelectronics. *Nat Biotechnol* **19:** 1023-1024.

Wuichet, K., Cantwell, B. J., and Zhulin, I. B. (2010) Evolution and phyletic distribution of two-component signal transduction systems. *Curr Opin Microbiol* **13:** 219-225.

Yagi, K. (2007) Applications of whole-cell bacterial sensors in biotechnology and environmental science. *Appl Microbiol Biotechnol* **73:** 1251-1258.

Yang, F., Moss, L. G., and Phillips, G. N., Jr. (1996) The molecular structure of green fluorescent protein. *Nat Biotechnol* **14:** 1246-1251.

Yoshida, T., Phadtare, S., and Inouye, M. (2007a) Functional and structural characterization of EnvZ, an osmosensing histidine kinase of *E. coli*. *Methods Enzymol* **423:** 184-202.

Yoshida, T., Phadtare, S., and Inouye, M. (2007b) The design and development of Tar-EnvZ chimeric receptors. *Methods Enzymol* **423:** 166-183.

Zhao, L., Xiao, L. L., Lin, L., Chen, X., and Wang, X. R. (2005) Fluorescent characters of optical BOD sensing film. *Guang Pu Xue Yu Guang Pu Fen Xi* **25:** 2039-2043.

A1. Appendix 1 PCR Primers

A1.1 Reporter plasmid primers

Primer Name	Primer Sequence (5'-3')
fmdA	GGATCTAGAGTCCCTTTGTGATCGCTTTC
fmdB	CTCGCCCTTGCTCACCATACTTTAACTCTCCTG
fmdC	CAGGAGAGTTAAAGTATGGTGAGCAAGGGCGAG
fmdD	GATGCCTGGCAGTTCCCTACTTGTACAGCTCGTC
fmdE	GACGAGCTGTACAAGTAAGGAACTGCCAGGCATC
fmdF	GGATGAAGCTTGTTTGTAGAAACGC
fmdG	GGAGGTACCCTGTGTTGAGTGCACAATTTTAG
fmdH	CCTCGCCCTTGCTCACCATAGCATTTCCTTTTTTCTATC
fmdI	GGATAGAAAAAAGGAAATGCTATGGTGAGCAAGGGCGAG
fmdJ	CGACTCTAGAGGATCCTTACTTGTACAGCTCGTC
fmdK	GACGAGCTGTACAAGTAAGGATCCTCTAGAGTCG
fmdL	GGATCTAGAGTTTGTAGAAACGC
fmdM	GGAGAATTCTTTCAACAAAGTGGTGAG
fmdN	CTCTTCGCCCTTAGACACCATGTTGCCTCCGGTTTTTAAG
fmdO	CTTAAAAACCGGAGGCAACATGGTGTCTAAGGGCGAAGAG
fmdP	GATGCCTGGCAGTTCCCTAATTAAGTTTGTGC
fmdQ	GCACAAACTTAATTGAGGAACTGCCAGGCATC
fmdR	GGAGGTACCGTTTGTAGAAACGC

A1.2 NtrC* primers

Primer Name	Primer Sequence (5'-3')
S160FA	GGACCATGGAACGAGGGATAGTCTGGGTAG
S160FB	GCACGCTAATAGAAAAACGCGAAAGCCGAC
S160FC	GTCGGCTTTCGCGTTTTTCTATTAGCGTGC
S160FD	GGAGGAAAGCTTTCACTCCATCCCCAGCTC
D54EA	GGACCATGGAACGAGGGATAGTCTGGGTAG
D54EB	CCGGCATACGGATTTCTGAAAGCAGCAC
D54EC	GTGCTGCTTTCAGAAATCCGTATGCCGG
D54ED	GGAGGAAAGCTTTCACTCCATCCCCAGCTC

A2. Reagent recipes

A2.1 LB (Luria Bertani) broth

Ingredient	Quantity
Bacto-tryptone	10 g
Yeast extract	5 g
Sodium Chloride	5 g

Made up to 1 l with distilled water, adjusted to pH 7.0 (with NaOH), and autoclaved.

A2.2 Succinate medium

Ingredient	Quantity
1M Phosphate buffer pH 7.0	20 ml
Concentrated base (Appendix A2.5)	20 ml
Growth factors (Appendix A2.7)	2 ml
Ammonium sulphate $(NH_4)_2SO_4$	0.5 g
Sodium succinate	2 g
Sodium Chloride	0.5 g
Casamino acids	1 g

Made up to 1 l with distilled water, adjusted to pH 7.0 (with KOH), and autoclaved.

A2.3 M9 minimal medium (-NH_4^+)

Ingredient	Quantity
M9 salts (10x) (Appendix A2.9)	100 ml
1M Magnesium sulphate $MgSO_4$	2 ml
20% glucose	20 ml
1M Calcium chloride $CaCl_2$	0.1 ml

Made up to 1 l with distilled water, adjusted to pH 7.2 (with KOH), and autoclaved.

A2.4 Succinate medium (-NH_4^+)

Ingredient	Quantity
1M Phosphate buffer pH 7.0	20 ml
Concentrated base (Appendix A2.5)	20 ml
Growth factors (Appendix A2.7)	2 ml
Sodium succinate	2 g
Sodium Chloride	0.5 g

Made up to 1 l with distilled water, adjusted to pH 7.2 (with KOH), and autoclaved.

A2.5 Concentrated base

Ingredient	Quantity
Nitrilotriacetic acid (Na salt)	5.94 g
Metals 44 solution (A2.6)	25 ml
Magnesium sulphate $MgSO_4.7H_2O$	14.5 g
Calcium chloride $CaCl_2.6H_2O$	2.5 g
Iron sulphate $FeSO_4.7H_2O$	0.05 g
Ammonium molybdate ($.4H_2O$)	0.0046 g

Made up to 1 l with distilled water and adjusted to pH 6.8.

A2.6 Metals 44 solution

Ingredient	Quantity
Tetrasodium versenate (EDTA)	2.5 g
Zinc sulphate $ZnSO_4.7H_2O$	11 g
Iron sulphate $FeSO_4.7H_2O$	5 g
Manganese sulphate $MnSO_4.7H_2O$	2 g
Copper sulphate $CuSO_4.5H_2O$	0.39 g
Boric acid H_3BO_3	0.12 g
Cobalt chloride $CoCl_2.6H_2$	0.2 g
3M sulphuric acid	1.5 ml

Made up to 1 l with distilled water and filter sterilised.

A2.7 Growth factors

Ingredient	Quantity
Biotin	20 mg
Sodium hydrogen carbonate $NaHCO_3$	500 mg
Niacin (Nicotinic acid)	1 g
Thiamine HCl	500 mg

Made up to 1 l with distilled water and autoclaved.

A2.8 SOC medium

Ingredient	Quantity
Bacto-tryptone	20 g
Yeast extract	5 g
Sodium chloride	0.59 g
Potassium chloride KCl	0.186 g
Magnesium chloride $MgCl_2$	2.03g
Magnesium sulphate $MgSO_4$	1.2 g

Made up to 820 ml with distilled water and autoclaved, then 180 ml sterile glucose (20 % w/v) was added.

A2.9 10X M9 salts (-NH_4^+)

Ingredient	Quantity
Sodium phosphate $NaHPO_4$ (anhydrous)	60 g
Potassium phosphate KH_2PO_4	30 g
Sodium chloride NaCl	5 g

Dissolved in 1 l with distilled water and autoclaved. Add chemicals in this order and dissolve each one before adding the next.

A2.10 TFBI

Ingredient	Quantity
Potassium Acetate	2.945 g
Rubidium Chloride	12.09 g
Calcium chloride $CaCL_2.2H_2O$	1.79 g
Manganese chloride $MnCL_2.4H_2O$	9.895 g
Glycerol	150 ml

Made up to 1 l with distilled water and adjusted to pH 5.8 with 0.2 M acetic acid then filter sterilised.

A2.11 TFBII

Ingredient	Quantity
PIPES (or MOPS)	302 mg (231 mg)
Rubidium Chloride	1221 mg
Calcium chloride $CACl_2.2H_2O$	1.1 g
Glycerol	15 ml

Made up to 100 ml in distilled water and adjusted to pH 6.8 with 0.1 M HCl (with 0.1 M NaOH if using MOPS) then filter sterilised.

A2.12 5X DNA loading dye (for agarose gel electrophoresis (2.2.2))

Ingredient	Quantity
Glycerol	7 ml
TE (A2.13)	3 ml
Bromophenol blue	25 mg
Xylene cyanol	25 mg

A2.13 TE buffer

Ingredient	Quantity
Tris base	1.21 g
EDTA (di-sodium salt)	373 mg

Made up to 1 l with distilled water and adjusted to pH 8.0 then autoclaved

A2.14 1 Kb plus DNA ladder

Ingredient	Quantity
1 Kb plus ladder (Invitrogen)	37.5 µl
TE (A2.13)	362.5 µl
5X DNA loading dye (A2.12)	100 µl

A2.15 ½X TBE

Ingredient	Quantity
Tris base	108 g
Boric acid	55 g
EDTA	7.4 g

Dissolved in 1 l of MilliQ. Made up to 20 l in MilliQ.